Journal of Consciousness Exploration & Research

Volume 6 Issue 9

Experimental Production of Excess Brain Correlation Across the Atlantic Ocean & Other Important Results

Focus Issue Featuring Michael A. Persinger Group's Latest Breakthroughs

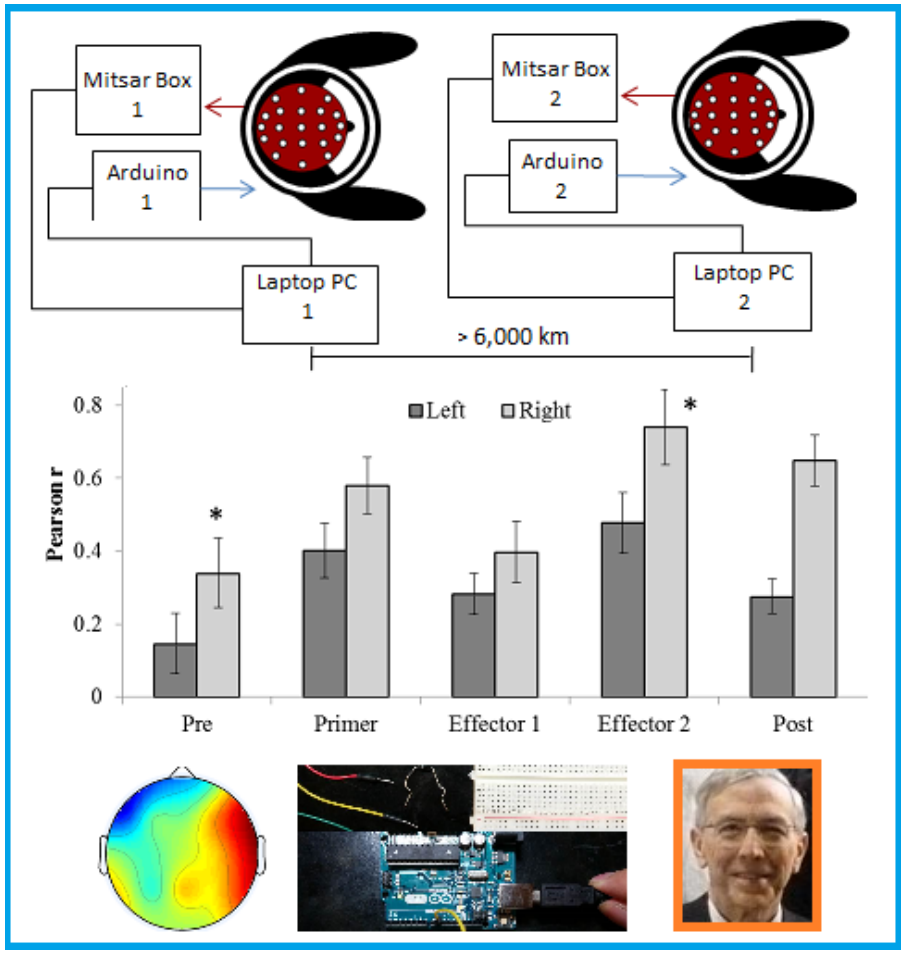

Experiment Producing Excess Brain Correlation across the Atlantic Ocean; Potential Experimental Demonstration of the Entanglement Velocity of 10^{23} m·s^{-1}; Enhanced Spectral Power Densities of Schumann Resonance in Microtubule; Demonstration of Excess Correlation in Non-Local Random Number Generators; Quantitative Support for Water as the Conduit for Universal Entanglement; & News: Transatlantic Excess Brain Correlations Are Experimentally Produced.

Editors:
Huping Hu, Ph.D., J.D.
Maoxin Wu, M.D., Ph.D.

Advisory Board

Dainis Zeps, Ph.D., Science and Religion Dialogue Interdisciplinary Group, University of Latvia, Latvia
Matti Pitkanen, Ph.D., Independent Researcher, Finland
Arkadiusz Jadczyk, Professor (guest), Center CAIROS, IMT, Univ. Paul Sabatier, Toulouse, France
Gregory M. Nixon, Ph.D., University of Northern British Columbia, Canada
Sultan Tarlacı, M.D., Neurology Specialist, NeuroQuantologist, Turkey
Stephen P. Smith, Ph.D., Visiting Scientist, Physics Dept., UC Davis, United States
Michael A. Persinger, Professor, Laurentian University, Canada
Elio Conte, Professor, Dept. of Neurological and Psychiatric Sciences, Univ. of Bari, Italy, Italy
Andrei Khrennikov, Professor, In'tl Center for Mathematical Modeling, Linnaeus Univ., Sweden
Chris King, Independent Researcher, New Zealand
Graham P. Smetham, Independent Researcher, United Kingdom
Steven E. Kaufman, Independent Researcher, United States
Christopher Holvenstot, Independent Researcher in Consciousness Studies
Pradeep B. Deshpande, Professor Emeritus of Chemical Engineering, University of Louisville, United States
Iona Miller, Independent Researcher, United States
Massimo Pregnolato, Quantumbiolab, Dept. of Drug Sciences, Univ. of Pavia, Italy

Table of Contents

Articles

Experimental Production of Excess Correlation across the Atlantic Ocean of Right Hemispheric Theta-Gamma Power between Subject Pairs Sharing Circumcerebral Rotating Magnetic Fields (Part I)
Mandy A. Scott, Nicolas Rouleau, Brendan S. Lehman, Lucas W. E. Tessaro, Lyndon M. Juden-Kelly, Kevin S. Saroka, and Michael A. Persinger 658-684

Experimental Production of Excess Correlation across the Atlantic Ocean of Right Hemispheric Theta-Gamma Power between Subject Pairs Sharing Circumcerebral Rotating Magnetic Fields (Part II)
Mandy A. Scott, Nicolas Rouleau, Brendan S. Lehman, Lucas W. E. Tessaro, Lyndon M. Juden-Kelly, Kevin S. Saroka, and Michael A. Persinger 685-707

Potential Experimental Demonstration of the Entanglement Velocity of 10^{23} m·s^{-1} During Trans-Atlantic Excess Correlation of Paired Brain Activity
Nicolas Rouleau, Stanley A. Koren & Michael A. Persinger 708-715

Spectral Power Densities of the Fundamental Schumann Resonance Are Enhanced in Microtubule Preparations Exposed to Temporally Patterned Weak Magnetic Fields: Implications for Entanglement
Blake T. Dotta, David A. E. Vares & Michael A. Persinger 716-727

Demonstration of Excess Correlation in Non-Local Random Number Generators Sharing Circular, Changing Angular Velocity Magnetic Fields
Lyndon M. Juden-Kelly, Blake T. Dotta, David A. E. Vares & Michael A. Persinger 728-737

Quantitative Support for Water as the Conduit of Interaction for Universal Entanglement
Trevor N. Carniello, David A. E. Vares & Michael A. Persinger 738-749

News

Transatlantic Excess Brain Correlations Are Experimentally Produced by Persinger's Group
Huping Hu & Maoxin Wu 750-755

Article

Experimental Production of Excess Correlation across the Atlantic Ocean of Right Hemispheric Theta-Gamma Power between Subject Pairs Sharing Circumcerebral Rotating Magnetic Fields (Part I)

Mandy A. Scott, Nicolas Rouleau, Brendan S. Lehman, Lucas W. E. Tessaro, Lyndon M. Juden-Kelly, Kevin S. Saroka & Michael A. Persinger*

Neuroscience Research Group, Human Studies and Biomolecular Sciences Programs, Laurentian University, Sudbury, Ontario, Canada P3E 2C6

ABSTRACT

There have been multiple historical and cross-cultural reports of excess correlation of specific experiences between individuals separated by thousands of kilometers. Recently there have been experimental demonstrations of excess correlations between measurable cerebral events for small percentages of test subjects. More reliable effects can be elicited when electromagnetic fields and photons are involved. In this experiment completed during the summer of 2015, 5 pairs of volunteers separated by more than 6,000 km wore identical cerebral toroids through which patterns of phase shifting, 30 nT magnetic fields that diminished the local magnetic field in both loci by 1-5 nT were exposed to the sequences that produced excess correlation in chemiluminescent reactions and shifts in pH. Compared to the various baselines and control procedures enhanced power between the right hemispheres of pairs of participants occurred during the interval documented to produce excess correlation. Specific analyses indicated diminished coherence within the theta band only within the right temporal lobes of the pairs. Sequential block analyses revealed that the paired brains' responses to pulsed tones at 6.5 Hz occurred within the 30-40 Hz band over the caudal temporal lobes during the exposures to the effector field. Primary independent component analyses verified these patterns. During the 6.5 Hz tones there was a peak in the spectral power density (SPD) at that frequency over the right temporal lobe of the person listening but a trough in (SPD) over this region for the person who was not. Even subjective experiences, as measured by the Profile of Mood States (POMS), indicated significantly increased excess correlation for scales by which increased anger and decreased vigour are inferred. This experiment, based upon physical principles, suggests there is a technology that can generate reliable excess correlation of brain activity (and potentially consciousness and specific experiences) between two people separated by thousands of kilometers.

Part I of this two-part article includes: 1. Introduction; 2. Method; 3. Equipment; and 4. Results and Discussion.

Keywords: Excess correlations, entanglement, transatlantic effects, theta frequency, right temporal lobe, toroidal magnetic fields, brain coherence.

*Corresponding author: Dr. M. A. Persinger, mpersinger@laurentian.ca

1. Introduction

Consciousness has been strongly correlated with a single brain's structure and electromagnetic activity most typically measured by electroencephalography (EEG). The interaction between two loci associated with consciousness has assumed that distance is limited because locality is required. It is mediated by proximal physical stimuli such as visual or auditory events. However from an operational perspective as long as reliable, specific excess correlation for measureable events occurs between person A and person B, distance is not limited. Even from a classical behaviorist perspective the reciprocal interactions between two people are simply the manifestations of alternating stimulus-response sequences. We have developed a paradigm to evoke powerful excess correlations between chemilumiscent reactions (Dotta and Persinger, 2012; Dotta et al, 2013a) shifts in pH within spring water (Dotta et al, 2013b), and alterations in malignant cell growth (Karbowski et al, 2015) within two loci separated at distances between 10 m and 3 km. Here we present experimental evidence for the first known trans-Atlantic excess correlations in the type of brain activity associated with consciousness when the brains of pairs of people, each separated by thousands of kilometers, share toroidal, rotating magnetic fields with changing angular velocities.

The Nature of Locality and Causality

The definition of a causal relationship between a stimulus and response depends upon their space-time contiguity and whether or not the display of the responses systematically follows the occurrence of the stimuli. Examples are bright light flashes that elicit eye blinks or the verbal behavior of one person that elicits the verbal behavior of another. The usual perspective is: 1) there is some proximity between the locus of the stimulus and the locus of the response, and, 2) the correlation approaches 1 such that for every stimulus there is always a specified response. This would be an example of the maximum limit or "asymptote" for excess correlation which is often described as causality. However near thresholds or limens for perceptual phenomena such as detecting the presence or absence of a tone the elicitation of a response to a stimulus is not one-to-one but becomes a weaker and weaker correlation until there is some point where the "excess correlation" does not vary from random variation. As aptly demonstrated by decades of research in psychophysics signal detection around thresholds is a multivariate process where even chaotic distributions or stochastic components can enhance the capacity to discern the signal.

When the two loci that are attributed to the stimulus and response are separated by distances that do not appear to involve proximity or locality, the mechanisms for any excess correlation may be different. Dozens of theoretical approaches and experiments have shown that non-local effects are easily reproduced for quantum systems. The measurement involves photons (Vaziri, et al, 2002). Experimental free-space quantum teleportation involving photons has been measured at distances of up to 600 m according to Jin et al (2010). However Hotta et al (2014) has indicated that quantum energy teleportation does not necessarily display a limit of distance. Megidish et al (2013) showed that entanglement can occur between photons that never coexisted in traditional space-time, which suggests that specific modifications of the electromagnetic-gravitational features of spaces could induce excess correlation. This interpretation is consistent

with the theory developed by Hu and Wu (2006a, b; 2013) that the primary source of the macroscopic manifestation of quantum entanglement originates from primordial spin processes in non-spatial and non-temporal pre-space-time and involves gravity. When one considers the measurement by Fickler et al (2013) that single photons (even though they differ by 600 in quantum number as long as they exhibit quantized orbital angular momentum from helical wave structures) can exhibit excess correlation, then the potential for remote sensing become feasible.

Entanglement is defined as "when the quantum system contains more than one particle, the superposition principle gives rise to the phenomenon of entanglement" (Aczel, 2002). The superposition principle, or more specifically the principle of superposition of states, indicates that a new state of a system may be composed of two or more states such that a new state emerges that shares some of the properties of each of the composite states. If X and Y are two different properties of a particle, for example existing in two different loci, then superposition indicates a condition X+Y arises which has properties of both entities. Thus there would be a non-zero probability that the particle could be in both loci simultaneously. The application to a "multi-particle" system or one that involves more than one photon has been shown experimentally. Macroscopic manifestations of "excess correlation" have also been shown. Julsgaard et al (2001) demonstrated excess correlation in two macroscopic objects (gas molecules). Dotta and Persinger (2012) measured this effect with millions of photons each generated by separated reactions of hypochlorite and hydrogen peroxide.

Development of the Theory and the Technology

Excess correlation at spaces greater than quantum levels may appear to require physical conditions that allow the superposition of two loci such that they display the behavior of a single space. Based upon the conceptual approaches of Ernst Mach (1988), Sir Arthur Eddington (1981), Niehls Bohr (1958), and Hu and Wu (2006a, b; 2013), we had reasoned that the circular momentum of a quantized electromagnetic field could create the condition to facilitate entanglement between two loci (and the state of matter within those loci) separated by non-traditional distances (Persinger and Koren, 2013; 2014). The essential premise is that the physical mechanisms that serve as the substrate for entanglement reflect the properties of the entire universe as a unit within which differences in space and time may be less critical. It would be similar to Hu and Wu's (2013) concept that it is a feature of the universe before space and time emerged as properties with which they are now recognized.

Our initial methodology employed bursts of weak magnetic fields rotating within a circular array of 8 solenoids. The angular velocity of these rotating magnetic fields either increased or decreased. The pattern of the magnetic fields that were produced within each solenoid in the circular array of solenoids was produced by a computer program that generated pulsed or punctate 1 ms or 3 ms fields that composed either an accelerating or decelerating frequency-modulated and phase-modulated magnetic field. The durations of ~1 ms and ~3 ms were derived from our (Persinger and Koren, 2007) calculations that these two values reflected the time for an electron and a proton to expand one Planck's Length. Since those initial quantifications, several experimental results have supported this interpretation (Persinger, 2013a; Koren et al, 2014).

Inspired by the importance of the difference in phase and group velocities of photons in order to produce a non-zero rest mass (Tu et al, 2005) Dotta and Persinger (2012) compared the effects of different combinations of accelerating and decelerating group velocities (the changing angular velocities of the whole field rotating around the array of solenoids) and accelerating and decelerating frequency-modulation or phase-modulation of the patterns of magnetic fields that were being generated by the computer to each solenoid. The change in velocity was accomplished by adding +2 or -2 ms to the base duration of 20 ms as the field rotated around the ring of solenoids. They found that only one combination produced excess correlation. The group angular velocities were equivalent to frequencies between 5 and 20 Hz with specific locations around the array where the acceleration was convergent with g: 9.8 $m \cdot s^{-2}$.

If an initially accelerating group velocity embedded with a decelerating frequency-modulation field was presented first (**the primer field**), the subsequent presentation of a decelerating group velocity embedded with an accelerating frequency-modulated field (**the effector field**) produced excess correlation of photon emissions between two loci separated by either 10 m or 3 km for about 8 minutes. These were the only two distances tested. During the approximately 8 min interval the power density of the photons emitted from the chemical reactions in one location was double that of the typical measures. In fact it was equivalent to injecting twice the reactant into a single reaction when there was no excess correlation. This was consistent with our assumption that the structure of the two loci separated by non-traditional distances behaved as if they had been superimposed into a single space. In other words, the states exhibit superposition.

The Electroencephalogram and Brain Imaging

The most frequent tool employed to study consciousness is electroencephalographic activity. These measurements obtained from sensors located more or less equally over the surface of the scalp measure the variations in the averaged, distant electric fields from the approximately 20±5 billion neurons that compose the human cerebral cortices (Pakkenberg and Gundesen, 1997). We have employed the 10-20 international system. Although other researchers who prefer denser sensor arrays we have found this matrix is sufficient to discern the phenomena we are investigating. The measurements are within the microvolt range. The corresponding magnetic field component exhibits picoTesla values and is consistent with the product of magnetic permeability of a vacuum and the current density from these voltages within the resistivity of extracellular fluid across the length of the human brain (Persinger and Saroka, 2015; Saroka and Persinger, 2014).

Quantitative electroencephalography (QEEG) was a major development that permitted the quantized perspective to be applied to brain activity. The decomposition of fluctuations from scalp sensors into quantized microvolt increments markedly increased the complexity and numbers of measurements and permitted the consideration of QEEG activity as a field potentially composed of "infinite, infinitesimal points". When real-time brain activity from 19 sensors is sampled between 250 to 1000 times per second the density of the potential data arrays is sufficient to discern very subtle changes from the environment yet manageable for routine analyses. Such complexity could be sufficient to demonstrate the subtle changes in two locations

displayed by two human brains that could meet the criteria for "excess correlation" or entanglement.

QEEG has the potential to manifest excess correlation because the data can be considered as representative (or by inference) of a "state" composed of a more or less reliable field or pattern of frequencies and intensities. There are reliable microstates first described by Lehmann et al (1998) and standardized by Koenig et al (2001) that remain relatively consistent across a person's life time. There are primarily four states of whole cerebrum organization with polarities arranged in left frontal to right caudal, right frontal to left caudal, frontal to caudal and central frontal to caudal patterns. They accommodate more than 70% of cerebral activity. Each state exists for about 80 to 120 ms, the duration of a "percept," and is remarkably similar across human beings. The median value is conspicuously equivalent to 10 Hz.

The concept of a field involving billions of neurons would appear to contain considerable momentum that would oppose alteration by a single, small source energy. There is clear experimental evidence that very small energies can alter states composed of millions or billions of units. Houwelling and Brecht (2008) found that the activity of only one neuron could affect the direction of a rat's motor behaviour. Within a single barrel cortical column containing about 8,500 excitatory neurons, detection required 2,500 action potentials above the 1,500 action potentials (a difference of 1,000) per 200 ms period. This means that the initiatory detection and the whole-organism effect required only about 5 action potentials per 1 ms. Later Li et al (2009) reported that repetitive high frequency spiking of only a *single* rat cortical neuron could trigger a shift between two cortical states that resembled rapid-eye-movement (REM) and slow wave sleep.

In other words the energies required to produce significant alterations in brain states and overt behaviour are in the order of 10^{-20} J. This is the energy from the effect of the net change of an action potential upon a unit charge (Persinger, 2010). It is also a likely increment of energy that might integrate the distribution of energy at the level of Planck's Length throughout the universe. The total force within the universe based upon its mass, length and squared "Zitterbewegung" frequency divided by the total number of Planck's voxels in the universal volume distributed across the wavelength of the hydrogen line results in 10^{-20} J (Persinger, et al, 2008; Persinger, 2015). Thus very small increments of energy transmitted through non-local space could alter the entire pattern of global brain activity.

Previous Experiments of EEG-Related Excess Correlation

Hans Berger, the pioneer who developed the concept and original tools that now define modern electroencephalography, was interested in explaining a personal experience that would now be identified as a potential example of excess correlation between his exposure to a trauma that could have been deadly and the cerebral ideation of his sister who was living in different city of that country. The first major high profile experiment showing that two (2) of 15 pairs of twin infants separated by non-traditional distances displayed excess correlation in elicitation of alpha rhythms was published by Duane and Behrendt in *Science* in the year 1965. Although there were many interesting preliminary studies involved with "extrasensory perceptual" research, including that of a martial arts master who was instructed to emit "qi" force and the concurrent increase in

strip-chart alpha wave moving in a rostral direction from the occipital region of the student recipient sitting in another room (Kawano, et al, 2000), direct experimental manipulation of the process has been more rare.

Standish et al (2004) reviewed about a dozen experiments involving "remote transfer of signals" from the previous 40 years. Standish and her colleagues found that 5 of the 60 subjects displayed reliable visually evoked potentials when their "senders" were viewing flickering but not static light displays. In a previous experiment Standish et al (2003) had demonstrated excess correlation between the MRI signals of two brains separated by non-traditional distances. Although there have been many reports of specific or exceptional individuals who report "spontaneous" experiences consistent with excess correlations at greater distances (Dotta et al, 2009; Scott and Persinger, 2013), without experimental manipulation or simulation of these conditions within the laboratory, the mechanisms cannot be isolated. In addition both the Duane and Behrendt (1965) and Standish et al (2004) experiments indicated that the effects were not demonstrable in all pairs of "senders" and "receivers". The relative portion is in the order of about 10%.

We have assumed that the spontaneous occurrences of excess correlations between the activities of two different brains separated by non-traditional distances suggest an aggregate phenomenon within which one component is essential. The analogy would be the remarkable analgesic and antipyretic effects of white willow bark. The clinical effects were often variable. However when late 19th century methods for organic chemistry were developed that allowed the extraction and later synthetic reproduction of the specific component (acetyl salicylic acid) that was responsible for the analgesia and antipyresis, the effects could be more reliably replicated between individuals. We have assumed spontaneous excess correlations between human brains separated by thousands of kilometers are natural phenomena that, like the white willow bark's correlation with analgesia, can be reliably elicited once the critical variables are isolated and experimentally manipulated.

Persinger et al (2003) first reported that the stimulation of one of a pair of siblings with a circular array of 8 solenoids placed around the head at the level of the temporal lobes produced a specific change in theta power (5 to 5.9 Hz) in the right temporal lobe of the other sibling (not wearing an array of field-generating solenoids) sitting blindfolded with earplugs in a separate room. The rates of rotation of the magnetic that were most effective involved 20 ms reference intervals. Additions or subtractions of unit times, such as 2 ms, as the field moved to each successive solenoid produced a changing angular velocity. This interval which is more likely a range between 15 and 25 ms is the classic "refresh" rate of consciousness (~40 Hz) which has been described as the rate of "re-entry" of continuous processes (Edelman, 1989). It can be considered a second derivative. A magnetic field moving within a circle might be considered as in a state of continuous acceleration. Changing that rate would result in a second derivative.

Because one of the features of excess correlation or entanglement is a history of shared space-time, Persinger et al (2008) paid pairs of random strangers to meet each other for one hour twice per week for four weeks and simply remain within a meter of each other. When one of the pair who had been randomly assigned to the entanglement process was stimulated with the same effective field parameters (20 ms intervals) while wearing the circular array of 8 solenoids and

the other member's QEEG was recorded there was an increase in power within the 5.0 to 5.9 Hz band over the temporal lobes but no other lobes. Pairs of people randomly selected on the days of the experiment who had no previous shared space-time history did not display this effect.

In that experiment the stimulus person (the one receiving the angular accelerating magnetic fields) was instructed to imagine walking to the other room and standing on the left side of the response person whose QEEG was being recorded. The response persons, during the period associated with the enhanced theta activity over the temporal lobes, reported (as indicated by post-experimental questionnaire responses) an increased incidence of sensed presences, anger, and sexual arousal. These effects were not reported by the other members of the pair who were exposed to the rotating magnetic fields or by the response persons who composed the random pairs of subjects for the reference (control) group.

These studies were predicated on the concept that the magnetic field condition for one person was a type of stimulus while the response in the EEG for the other person (no field) was the consequence of this effect. Subsequent experiments, which were similar to the excess correlation experiments for photon-chemical reactions (Dotta and Persinger, 2012) and shifts in pH (Dotta et al, 2014), involved both loci or the brains of both participants in a pair being exposed to the same rotating magnetic fields around each of their heads. The demonstration of proof of principle involved a reliable shift in the intercorrelations of QEEG sensor data over the scalp for the "receiver" person sitting blind folded and wearing ear plugs in one room while the "stimulus" person sitting in a closed, acoustic chamber was exposed to a series of different frequency lights (Persinger et al, 2010). The changes in the intercorrelations in the response person's brain when the stimulus person's brain was being exposed to the light flashes occurred over the *right* posterior hemisphere.

Dotta et al (2011) extended this study by measuring the photon emissions from the right hemisphere of the response person who was sitting in complete darkness while wearing one of the circular arrays of solenoids. When the stimulus person (also wearing the array of solenoids, was sitting in a closed acoustic chamber) was stimulated with light flashes the response person's right hemisphere displayed an increase in photon flux density when measured at a distance of about 15 cm. The reversible increases and decreases of these ultraweak biophoton emissions from one person as a function of the light exposure to a second (stimulus) person in another room was within the range of 10^{-11} to 10^{-12} $W \cdot m^{-2}$. This effect only occurred if both the stimulus and response persons were wearing the solenoid arrays and were simultaneously exposed to rotational fields with changing angular velocities. The results suggested that when both loci, or both person A and B, were exposed to the specific parameter of circular rotating weak (microTesla) magnetic fields with changing angular velocities changes consistent with excess correlation were stronger and more likely to occur reliably.

Estimated Magnitude of Energies

Any mechanism that is involved with excess correlations between two brain loci separated by non-local distances should involve energies that reflect those that involve the processes that mediate the effect. Saroka and Persinger (2014) and Persinger and Saroka (2015) have shown that the basic frequency and the harmonics of the Schumann Resonance (7-8 Hz, 14

Hz, 20-21, 26-27, 33-34, 39-40 Hz, etc) can be discerned within the spectral profiles of most human brain activity. Most all terrestrial organisms are immersed in these fields or their variants. The manifestation of the Schumann Resonances and the harmonics are more evident within the caudal portions of cerebral activity than more rostrally.

The magnitudes of both the electric field and the magnetic field of human cerebral electroencephalographic activity are similar to those of the fundamental Schumann resonance. These values are in the range of mV per meter for the electric field and 1 to 2 picoTesla for the magnetic field. The Schumann resonance is primarily generated by global lightning strikes whose average incidence is about 44±5 Hz (Christian, et al, 2003) which is the median interval of the gamma frequency frequently associated with consciousness. The propagating field from a single lightning discharge returns to the source over the spherical guide in about 20 to 25 ms with a phase shift of 13 ms within this 7 to 9 Hz interval. As shown by Llinas and his colleagues (e. g., 1993) the recurrent 20 to 25 ms propagating waves that integrate large areas of the human cerebral cortices occurs between the rostral and caudal cerebrum. This particular pattern occurs predominately during waking and dream sleep but not during slow wave sleep. The phase modulation is about 12.5 ms.

Even from a conservative electrophysiological perspective brain tissue displays a resonance frequency with a medium value in the 7 to 8 Hz range. According to traditional empirical measurements the permeability (inductance, L, per meter) of cortical grey matter at frequencies around 1 kHz is about 10^{-2} Henrys. This frequency (1 kHz) is equivalent to 1 ms which is the effective duration of the action potential of most neurons. The energy of a single action potential with this duration produced by the product of the shift in voltage and the unit charge is about 10^{-20} J which reflects both the magnitude and duration required to stack a base nucleotide upon the type of RNA sequence the produces the proteins that some neuroscientists consider the substrate of memory (Persinger, 2010). The permittivity value, C (capacitance), for grey matter is $2 \cdot 10^{-1}$ $F \cdot m^{-1}$. Application of the classic formula:

$$f=[\sqrt{2\pi \cdot (LC)^{-1/2}}]^{-1} \quad (1),$$

results in about 7 Hz.

The immersion of human brains within an electromagnetic pattern that shares peak spectral frequencies and electric and magnetic field intensities produces the condition for a pervasive diffusivity. The resistivity of the whole brain's primary constituent (physiological water) is about 2 $\Omega \cdot m$. When multiplied by magnetic susceptibility ($4\pi \cdot 10^{-7}$ $N \cdot A^{-2}$) the resulting diffusivity is $1.7 \cdot 10^{6}$ $m^2 \cdot s^{-1}$. The median potential difference for QEEG activity per Hz is ~$2 \cdot 10^{-6}$ V (2 μV). When this value is divided by $1.7 \cdot 10^{6}$ m^2 s^{-1} the equivalent magnetic field strength is about 10^{-12} T (pT). This is the value of the magnetic component of the Schumann Resonances. The convergence does not prove a variable that produces diffusivity is necessary for the similar strength magnetic field. However it suggests that a fundamental feature of space, magnetic permeability, with the exact conditions (extracellular fluid conductivity) within which a collection of neurons (a brain) interact could produce a conduit for this global interaction.

The functional duration for all human brains immersed within a common medium to be potentially interconnected has been calculated to occur within about 8 to 9 min (Dotta and Persinger, 2012). Assuming the conductivity of physiological saline within each brain to be σ=0.5 $S \cdot m^{-1}$, the magnetic diffusivity would be $0.63 \cdot 10^{6}$ $m^2 \cdot s^{-1}$. If the surface area of each human cerebrum is assumed to be $\sim\pi \cdot 10^{2}$ m^2 the total surface area for 7 billion human brains would be $22 \cdot 10^{7}$ m^2. When this value is divided by the magnetic diffusivity term the resulting value is 349 s or about 6 min (Persinger, 2013b). One interpretation is that if there was some factor that simultaneously integrated or "connected" all brains because they shared the same medium, such as the earth's static magnetic field within which the Schumann patterns are embedded, then the time required for a change in one brain to affect any one or all of the other 7 billion brains would be about 6 min.

This latency does not reveal the quantity of the effect being mediated. If $\sim 10^{-20}$ J is associated with the excess correlation as a basic unit about 10^{7} neurons each discharging around 10 Hz would be required to achieve the threshold for a percept where the person might be aware of the effect (Rouleau and Dotta, 2014). However if the demonstration by Houwelling and Brecht (2008) is applied and this magnitude of energy is sufficient to affect the overt response of an animal, an effect could occur without necessarily the awareness or perception of the effect. The phenomenon of "blind sight", for example, involves adaptive responses during ambulation of technically blind people. fMRI data indicate that small numbers of occipital cortical neurons respond to the optic stimuli but the numbers are not sufficient to meet the threshold at which "conscious awareness" occurs.

The conditions for the two similarities, from a signaling perspective, could be consistent with Lorentz's Lemma which relates any two electromagnetic fields if: a) they are the same frequency, b) outside of the source, and c) in a linear isotropic medium. If we assume: 1) the two fields are the Schumann resonance generated between the surface of the earth and ionosphere by lightning and the cerebral resonance generated between the corona of the cortices and the multiform layer of the cerebrum by action potentials (Persinger, 2012), and, 2) the Schumann Resonance and cortical fields are harmonic in time, then:

$$\text{del} \cdot (\mathbf{E}_b \times \mathbf{H}_s) = \text{del} \cdot (\mathbf{E}_s \times \mathbf{H}_b) \quad (1),$$

where **E** refers to the electric field vector component, **H** is the magnetic field ($A \cdot m^{-1}$) vector component and the subscripts refer to b (brain) and s (Schumann) sources. The aggregate is Watts per meter squared. For both the human and the Schumann Resonances, this value is $\sim 10^{-12}$ $W \cdot m^{-2}$. This is also the power density emitted from the right hemisphere of subjects imagining white light while sitting in a hyper-dark environment (Dotta and Persinger, 2011; Dotta et al, 2012).

As predicted by the Lorentz Lemma, Persinger and Saroka (2015) demonstrated *real time* intermittent coherence between the spectral power within the Schumann frequencies associated with the brain activity of 41 men and women and ionosphere measures. Transient coherence of spectral power densities with the first three modes (7-8 Hz, 13-14 Hz, 19-20 Hz) of the Schumann Resonance in real time were measured from local (measured in Sudbury) and distal (measured in Italy) stations. The duration of the coherence was for about 300 ms about twice per

min. This suggested that the "interface" interval between the global Schumann field within the spherical wave guide and each brain was once every ~30 s.

Topographical map clusters indicated the domain of maximum coherence was within the *right* caudal hemisphere within the volume occupied by the parahippocampal gyrus. These clusters, associated with shifts of about 2 μV, became stable about 35 to 45 ms after the onset of the synchronizing event. During the first 10 to 20 ms the isoelectric lines shifted from clockwise to counterclockwise rotation. Persinger and Saroka (2015) concluded that the results were consistent with the congruence of the frequency, magnetic field intensity, voltage gradient, and phase shifts that are shared by the human brain and the earth-ionospheric spherical wave guide. The observation that the intermittent coherence for brain measures was similar for measurements of the Schumann values in Italy and within a few meters (locally) of where the brain activity was being measured suggested that coherence might occur *any where on the planet* for some individuals. This capacity might be considered a major antecedent variable for phenomena represented as "non-local".

There are multiple examples of measurements demonstrating the magnetic fields of the cognitive correlates of brain function and of the Schumann Resonance at the fundamental (7-8 Hz) are about 10^{-12} T and the electric field components are about 1 $\mu V \cdot m^{-1}$ to 1 $mV \cdot m^{-1}$. The Lorentz Lemma adds the dimension of radiant flux density. For the human brain with an average of 1 μV per 10 cm per Hz or 10^{-5} $V \cdot m^{-1}$ and current gradient of $1 \cdot 10^{-6}$ V divided 2 Ω·m or $0.5 \cdot 10^{-6}$ $A \cdot m^{-1}$, the flux power density would be about $5 \cdot 10^{-12}$ $W \cdot m^{-2}$. This is the same order of magnitude as the photon flux density emitted from the earth and during human cognitions associated with imagination and thinking of white light when sitting in hyperdark settings (Dotta et al, 2012). The involvement of photons within a "macro-entanglement process" is expected from both theory and measurement because quantum phenomena manifested as discrete shifts of change in energy between electron shells is considered the bases of "entanglement". A similar concept, employing a different perspective, has been developed by the extraordinary original thinker Pitkanen (2012; 2013; 2014).

The Present Experiment

The major limit of our DAC (Digital-to-Analogue Convertors) technology is that is not readily accessible to the population. We (St-Pierre and Persinger, 2006) have found that when a technology is too complex its application by others (Persinger and Koren 2005) is often erroneous because of the numbers of requirements for function. This leads to results that can be misinterpreted. What was required was equipment that: 1) could be easily constructed by the average person and 2) imitated or replicated the excess correlation effects we have found in the laboratory. Burke et al (2013) found that when a toroid was placed over the head (level of the temporal lobes) of each individual in a pair separated by about 400 km while each subject's QEEG was being measured, LORETA profiles indicated excess correlation in the activity within the temporal lobes of both subjects when one of the pair was exposed to sound patterns. The effect was not observed with visual stimuli.

The excess correlation also occurred *only* during the component of the experiment when the rotating magnetic fields were functioning in a decelerating manner that simulated the

conditions in which double photon emissions were measured by Dotta and Persinger (2012). However in the Burke et al (2013) experiments the fields were generated from the programs within laptop computers to Arduino circuits that could be easily constructed. This meant that there was the potential for any person to construct the equipment with readily available components to replicate and extend this research.

Rouleau et al (2014) employed the same double toroid and Ardueno system within which two containers of spring water were placed in order to verify that the arrangement produced the excess correlation in the pH shift that was reported for the DAC system by Dotta et al (2013b). Rouleau and his colleagues (2014) found that the excess correlation effect was discernable within the component of the presentation of the field that was most similar to the "entanglement" phase of the DAC studies. In addition Rouleau and Persinger (2015) later found that the intensity required to produce the effect associated with the activation of these counterclockwise, experimental rotating fields (0.3 mG) was a small decrease in intensity of the ambient geomagnetic field between 1 and 5 nT. This small diminishment occurred primarily in **the east-west direction** or within the direction of the axial rotation of the earth**.**

This small shift of 1 to 5 nT is not trivial. The change in magnetic energy for a shift of 5 nT within a cerebral volume of 10^{-3} m^3 would be about 10^{-14} J, or, the mass equivalent of an electron. The convergence with the energy-mass relationship for an electron could be considered essential given the intricate connections between quantum photon emissions and absorptions and electron shells. In addition, the product of 1 to $5 \cdot 10^{-9}$ $kg \cdot A^{-1} \cdot s^{-2}$ (T) and the rotational velocity ($\sim 4.5 \cdot 10^{2}$ $m \cdot s^{-1}$) at the latitudes in which our experiments were completed is in the order of 10^{-6} $V \cdot m^{-1}$. In other words a potential difference that occurs in the cerebral cortical fields of the human brain is coupled to the angular velocity of the earth itself for the same magnetic field intensities that characterize both the dynamic activity associated with the Schumann and human brain harmonics.

The present experiment was designed to discern if excess correlation between pairs of two brains separated by the Atlantic Ocean would occur specifically during the effector component of the paired toroid design. In order to integrate all of the major themes and procedures that have been involved with previous experiments that pursued excess correlations over long distances without the participation of traditional senses, the design involved multiple operations for different types of cognitions, such as eyes open or closed, imagining sending or imaging receiving light, listening to either pulsed (6.5 Hz) or continuous tones, and field on or field off conditions.

We appreciated that the demonstration for excess correlation between brain activities of two individuals separated by thousands of kilometers but who shared the "entanglement" magnetic fields would be embedded within the normal activity of the brain that reflected the behavioural contingencies and cognitive structuring of the experiment. These conditions were employed as reference points or comparator functions so that the effect size and strength of any evidence of excess correlation could be quantified. We also realized that an elegant, simple design would appeal to parsimony. However if consciousness is a complex, emergent phenomenon, then the opportunity for interactions of processes to occur was considered preferable. This required a more multivariate design.

2. Method

Participants

The participants (N=10) were 4 female and 6 male adults aged 23 to 57 years (mean age=33.5 years). During the experiment they were located in Sudbury, Ontario, Canada; Berlin, Germany; and Madrid, Spain. They were divided into Groups A and B and then paired by trial (e.g. A1 with B1, see Table 1). Group A (n=5, 3 female, 2 male, mean age= 30.4 yr) was the first to be cued to "send" while simultaneously Group B (n=5, 1 female, 4 male, mean age= 36.6 yr) was the first to be cued to "receive" white light, the active engagement conditions. Group A was also the first to receive the burst tone while Group B was first exposed to the single tone + silence, the passive engagement and "rest" conditions.

Table 1. Designation of Participants in the TransAtlantic Entanglement Experiments

	Group A				**Group B**			
Pair	**ID**	**Sex**	**Age**	**Location**	**ID**	**Sex**	**Age**	**Location**
1	A1	1	31	Sudbury	B1	1	39	Berlin
2	A2	1	30	Sudbury	B2	2	40	Berlin
3	A3	2	24	Sudbury	B3	2	57	Madrid
5	A5	2	42	Berlin	B5	2	23	Sudbury
6	A6	1	25	Berlin	B6	2	24	Sudbury

Procedure: TransAtlantic Entanglement

Each pair of participants from Groups A and B completed a single trial of the paradigm in June 2015 between 16:00 to 19:00 UTC. Timing was precise (within 1 s) in order to facilitate synchronous measurements at distances exceeding 6000 km. At agreed upon times based on UTC, experimenters in the NRG Consciousness Research Laboratory located in Canada coordinated with out-bound experimenters located in Berlin, Germany and Madrid, Spain to complete the TransAtlantic measurements of Non-Local Entanglement. The orientation (facing) of the pairs (A and B, respectively) were: N-N, E-E, S-E, N-SE, and N-NW.

The participants completed a demographics questionnaire and pre-test profile of mood states (POMS-SF) after which the experimenters applied the 19 channel (Mitsar EEG-201) quantitative electroencephalogram (QEEG) for continuous measurement during the 42 minute paradigm, as well as the toroid systems for the field application, to each participant in the pairing. Stop watches for pairs of Group A and B measures were synchronized by the experimenters (to the second) via video-teleconferencing (Skype). Once watches were synchronized and a start time was determined (~5 min from synchronization), communication between experimenters was ended and the participants were each read verbatim a script describing cuing instructions for the paradigm (see Appendix A). The participants were informed that the entire experiment, except for baseline measures, would be completed with eyes closed, and that verbal cues to send-receive would be followed by rest conditions cued by audible tones.

Table 2. Flow diagram of the temporal components of QEEG data extracted for analyses and the operations within each component.

#	1	2	3	4	5	6	7	8	9	10	11
Condition	EO-pre	EC-pre	Rest	S-R	R-S	Rest	S-R	R-S	Rest	S-R	R-S
Field	No field					Primer Field				Effector Field (I)	

#	12	13	14	15	16	17	18	19	20	21	22
Condition	Rest	S-R	R-S	Rest	S-R	R-S	Rest	S-R	R-S	EC-post	EO-post
Field			Effector Field (II)				No Field				

The experiment began with a 6 min baseline (3 min eyes opened then 3 min eyes closed) followed by a 1 min "rest" period, the onset of which was signaled by an audio cue (either burst tone or single tone + silence, for Groups A and B respectively). The carrier tone was 220 Hz while the pulsation of that tone was 6.5 Hz. Next Group A was cued to "send" while simultaneously Group B was cued to "receive" (condition S-R) for a duration of 2 min, after which the pairs switched (Group A receives while Group B sends, condition R-S) for another 2 min. Following this first block of send/receive conditions, the second 1 min "rest" period was cued and Group A received the single tone + silence while Group B receives the burst tone. The conditions alternated for a set of 6 send/receive + rest repetitions.

The magnetic field application was initiated through the Toroid + Arduino system at the start of the second rest period, 11 min into the paradigm, following one full trial of both passive and active engagement conditions (Rest, S-R, R-S), for a total duration of 20 min, involving 2 different magnetic field patterns. The second trial of entanglement conditions was completed during exposure to the first pattern, a counter-clockwise decelerating magnetic field pattern (minutes 11 to 17, for 6 min total).

At the end of the third rest period (min 17) the second field pattern was initiated. It was a counter-clockwise accelerating magnetic field. Send/Receive trials 3-5 were completed during the accelerating field exposure, from minute 17 to 31 in the full paradigm and minutes 6 to 20 within the magnetic field exposure time. The fields were turned off at the start of the 6^{th} and final rest period, at minute 31. The participants completed trial 6 of the send/receive paradigm post-field exposure before completing a 6 min post-experimental baseline measure (3 min eyes closed and 3 min eyes open). The participants completed the POMS (Profile of Mood States) before the beginning and at the end of the 22 sequences (42 min).

Table 3. Locations of the pairs of subjects and the estimated distances of separation.

City	Longitude	Latitude	UTC	Distance (km) to Sudbury
Sudbury, Canada	46.49° N	81.01° W	UTC-5	0
Berlin, Germany	52.52° N	13.38° E	UTC+1	6341
Madrid, Spain	40.40° N	3.68° E	UTC+1	6019

Quantitative EEG Data

The continuous data, spanning a total of 2520 sec, from each of the 19 channels for each of the pairs were extracted from WINEEG Software and imported into MATLAB for synchronization by pair. This allowed for artifact removal from paired data without compromising the synchrony of the measurements. The continuous synchronized data were then segmented into the 22 conditions (Table 2), from pre to post baseline. Segmented data were then spectral analyzed into 8 band ranges from delta to gamma (1.5-4.5, 4.5-7.5, 7.5-10, 10-13, 13-20, 20-25, 25-30, 30-44 Hz) and imported into SPSS Windows for further analyses. The segmented data were also entered into a series of coherence analyses within MATLAB comparing 19 x 19 channels within each pair, from A1 to B1, etc., across the 8 frequency bins.

3. Equipment

Toroid & Arduino

The devices consisted of identical torus-shaped coils coupled to identical microcontrollers receiving synchronized signal-generating procedures from separate laptop computers. Previous studies have shown that this configuration induced a stimulus-response pattern in human participants such that quantitative electroencephalographic (QEEG) activity associated with stimuli presented to an individual at location A was effectively displayed for a second, stimulus-naïve individual at location B where the paired participants were separated by over 300 km (Burke et al., 2013). Additionally, discrete pH shifts were recorded in coupled beakers of spring water such that the injection of a proton donor at location A (decrease in pH) was associated with reliable increases in pH (more alkaline) at location B where the paired beakers were separated by 1 meter (Rouleau, Carniello, & Persinger, 2014).

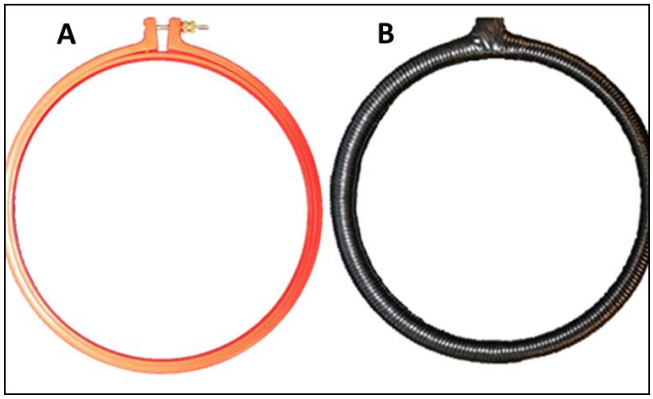

Figure 1. A plastic crotchet ring (A) before and after (B) copper wrapping. The coil is covered in black vinyl electrical tape.

Each coil consisted of a plastic ring with a diameter of 25.4 cm, wrapped in a single layer of 16 gauge insulated copper wire for a total of 225 turns around the 79.8 cm circumference (Figure 1). This toroid, fastened to the head by an elastic cap, was plugged into a solderless

breadboard equipped with the basic circuit seen in Figure 2. The details, including schematic representation, were specified by Rouleau & Persinger (2015).

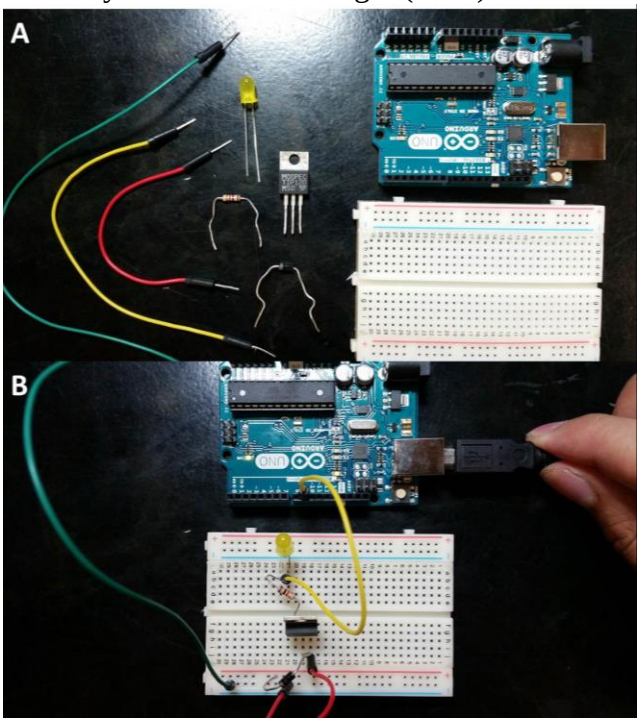

Figure 2. Components of the circuit disassembled (A) and assembled (B).

The solderless breadboard and coupled coil received pulsed current from an Arduino Uno R3 Microcontroller (as seen in Figure 2). Two pulse patterns were coded within the Arduino 1.0.6 software interface. The **Primer** pattern consisted of 7 all-or-none 3 ms point potentials which continuously looped, separated by incrementally longer inter-stimulus intervals beginning with 20 ms and increasing by 2 ms for every pulse, recycling back to 20 ms after the 7-pulse sequence. The 3 ms point duration was selected on the bases of calculations by Persinger and Koren (2007), derived from the Hubble parameter, for the time required for a proton to expand one Planck's Length. The **Effector** pattern involved the same all-or-none potentials. However, the inter-stimulus intervals between points starting with 20 ms decreased by 2 ms for every pulse. The code is partially displayed in Figure 3 whereas 2D representations of the pulse patterns are provided in Figure 4.

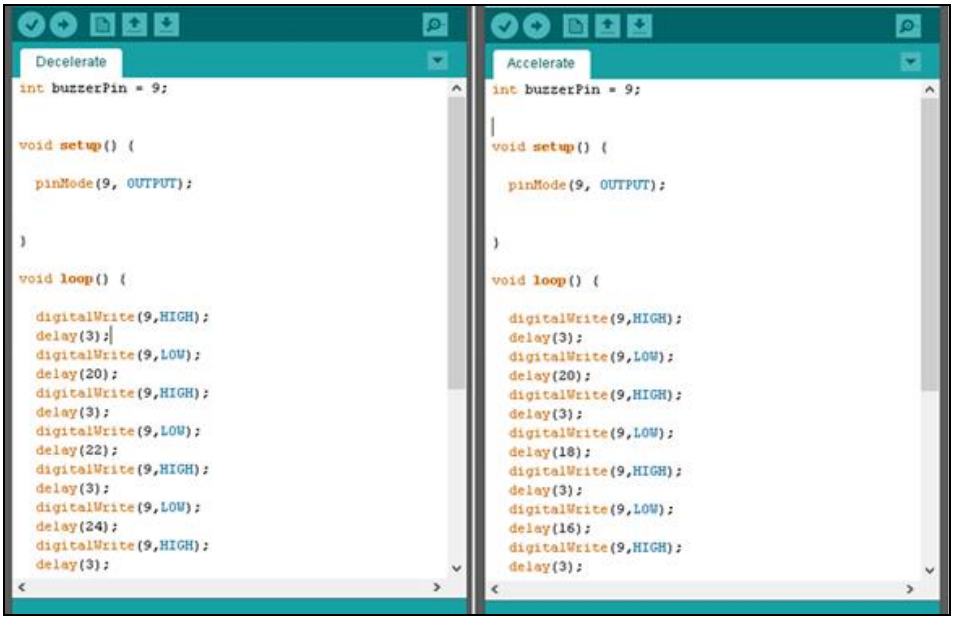

Figure 3. Arduino code for the Primer (left) and Effector (right) pulse patterns.

Once the fields were initiated, the duration of the whole exposure procedure was 20 minutes. The first field (Primer) was presented for 360 s and immediately followed by the second field (Effector), which was presented for 840 s. Rouleau and Persinger (2015) have reported that the electromagnetic fields generated within the center of the coils outputting these pulse patterns undergo 1-5 nT diminishments within the East-West horizontal axis referenced to Magnetic North as recorded by a MEDA FVM-400 Vector Magnetometer. A power frequency unit indicated that the strength of the pulsed magnetic fields rotating around the toroids averaged 30 nT (0.3 mG). This was the intensity that produced the largest excess correlation in the pH studies that employed this equipment.

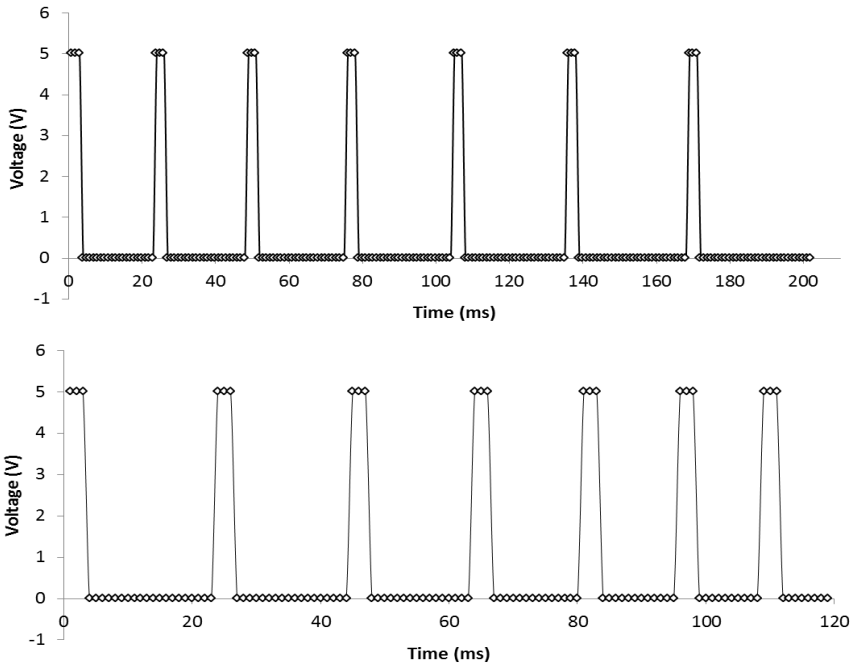

Figure 4. Primer (top) and Effector (bottom) pulse patterns as specified by the code. Each diamond represents a 1 ms point. Note that each pulse duration was 3 ms.

The field exposure procedure subsequent to cap application and antecedent psychometric data collection can be summarized succinctly. First, the participant was fitted with the toroid over the head (Figure 5). The participant then sat still in a comfortable chair while baseline QEEG recordings were obtained. The Primer pattern was initiated upon the 11th minute of the trial by plugging in the USB cord which connected the laptop to the microcontroller. Synchronization of this step across both locations was accomplished by strict adherence to pre-synchronized time keeping devices and the experimental schedules that accompanied them. Once connected by the USB cord, the microcontroller, breadboard, and coil drew power from the laptop. After 360 s had elapsed, the Effector pattern was initiated manually using the Arduino 1.0.6 software. Once uploaded, the Effector pattern cycled for 840 s. The field was terminated by unplugging the USB cord, thereby removing the power source of the device. QEEG recording continued until the 42nd minute of the experiment had elapsed.

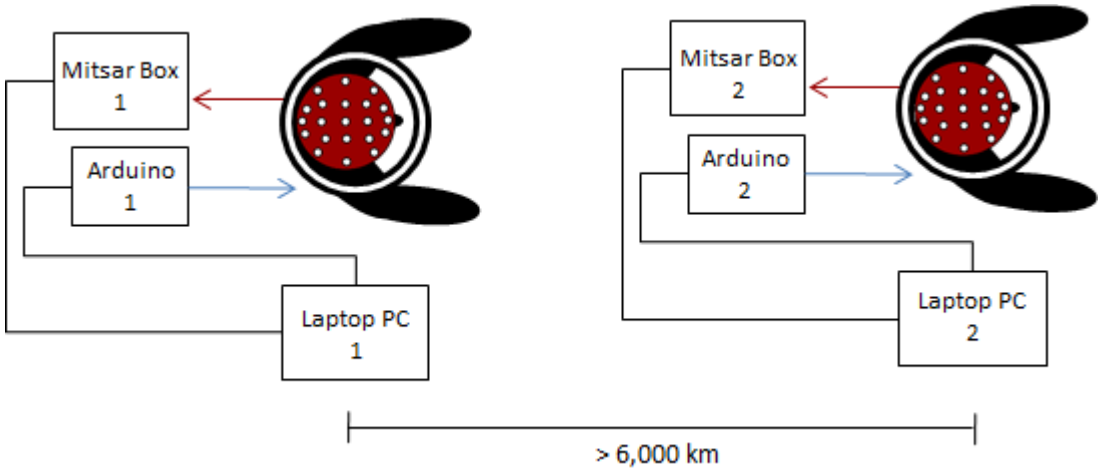

Figure 5. Schematic of the experimental equipment.

4. Results and Discussion

Expected Activities of Local Behaviours (Within Subject Brain Correlations)

In order to compare any statistically significant effects for the shared hemispheric correlations between subject (non-local) effects we measured the magnitude of intercorrelations between hemispheres **within** subjects, i.e., within the same brain. Table 4 shows the global power in µV for each person's left and right hemisphere as well as the net difference in power and the equivalent voltage when the eyes were opened. There were baseline differences in the two Mitsar boxes employed in the experiments. This is shown by yellow and grey color. However the net differences in voltage between the persons' left and right hemisphere were comparable for the two instruments.

Table 4. Global Power for the Left and Right Hemispheres of the 10 participants during eyes open conditions as well as the net difference in power and equivalent in microVolts. Yellow vs grey reflects the intrinsic characteristics of the two Mitsar devices.

			Eyes Open Global Power Converted to µV
Left Global Power	Right Global Power	Net Difference in Power	Net Difference in µV
49.22	50.58	1.36	7.236
24.57	23.44	1.13	6.595
19.8	21.95	2.15	9.098
25.55	28.53	2.98	10.711
30.53	37.44	6.91	16.310
8.64	6.9	1.74	8.184
4.44	4.6	0.16	2.481
3.07	3.32	0.25	3.102
12.28	8.48	3.8	12.095

6.49	8.29	1.8	8.324

Table 5 also shows the global power differences and net changes when the subject's eyes were closed. The net increase in μV global power when the eyes were closed was typical for the normal person and representative of what we have measured in the last approximately 500 subjects assessed with this technology. A separate analyses by another one of the authors showed that the average increase in global spectral power was about 5 to 10 μV higher during phases 2 through 21 of the experiment when the subjects' eyes were closed compared to the pre (phase 1) and post (phase 22) baselines whose average was 20 and 16 μV respectively.

Table 5. Global power for the left and right hemispheres for all 10 participants during the eyes closed conditions as well as the net differences in power between the hemispheres in microVolts. Yellow vs grey indicates the two Mitsar devices.

Eyes Closed Global Power Converted to μV			
Left Global Power	Right Global Power	Net Difference in Power	Net Difference in μV
5.6	6.05	0.45	4.162
5.51	4.31	1.2	6.797
3.22	3.69	0.47	4.253
11.44	8.96	2.48	9.771
7.36	7.17	0.19	2.704
38.62	40.6	1.98	8.730
50.7	44.26	6.44	15.741
29.28	34.97	5.69	14.800
36.31	41.66	5.35	14.351
81.42	99.65	18.23	26.493

The interhemispheric correlations for each subject across the phases of the experiment are shown in Figure 6. Because these measures reflected the intrasubject correlation of activity across hemispheres the expected near 1.00 values were expected. The coefficients for the 10 subjects per phase ranged between r=0.97 to r=0.99. From a neurofunctional perspective, the inter-correlations between the individuals' own lobes is significant. As seen in Figures 7 thorugh 10 the individual lobes are strongly intercorrelated. Although T3 (left) and T4 (right) sensors were least correlated and accommodated only 77% of the shared variance compared to the other examples (> 90% of shared variance), the effect is not statistically significant because of the sample size (n=10).

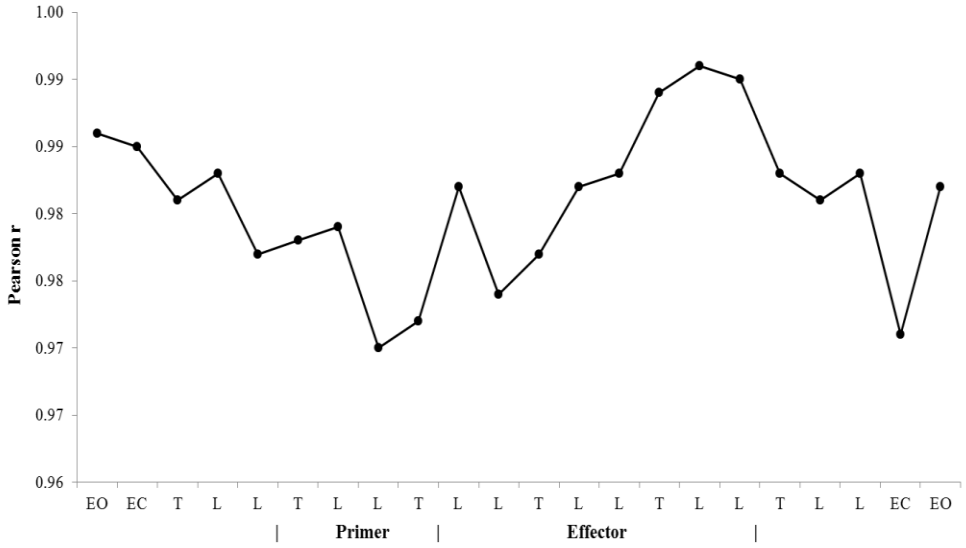

Figure 6. Within subject correlation between the magnitudes of the global power within the left and right hemisphere of the same brain for the 10 participants

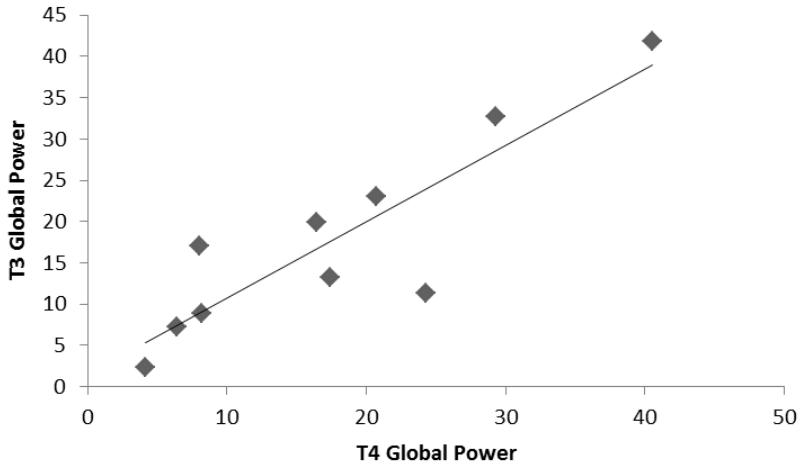

Figure 7. Correlation (r=0.88) between T3 and T4 global power for each person's brain (n=10) during eyes opened conditions.

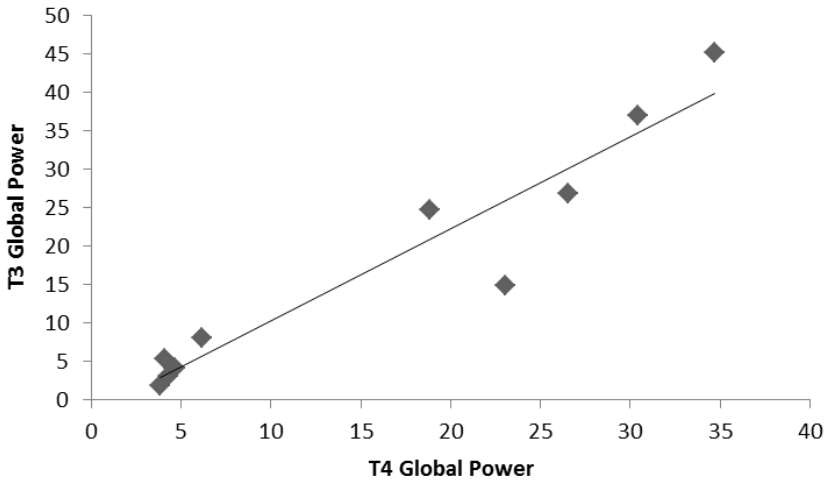

Figure 8. Correlation (r=0.95) between T3 and T4 global power for each person's brain (n=10) during eyes closed conditions

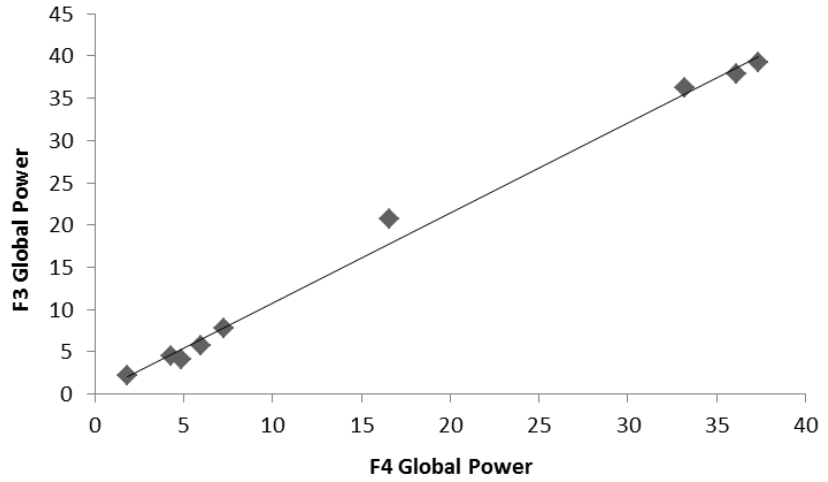

Figure 9. Correlation (r=0.99) between global power between the left and right frontal sensors for each person's brain during eyes closed condition.

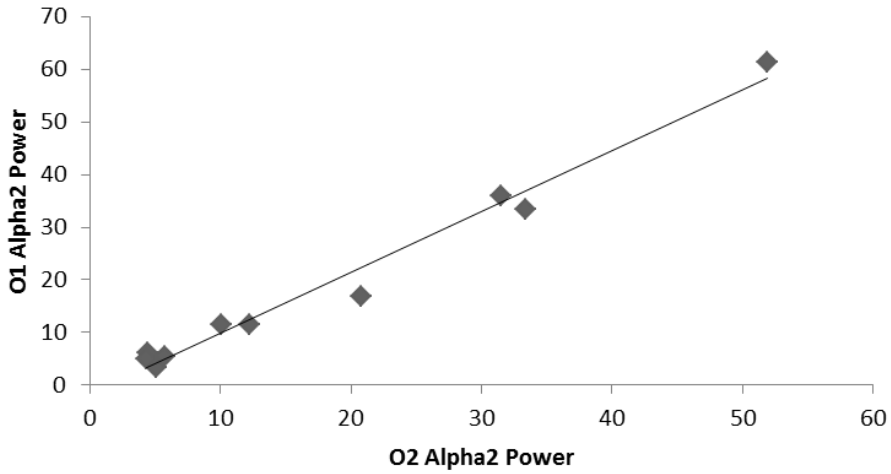

Figure 10. Correlation (0.99) between global power between the left and right occipital sensors within each person's brain during eyes closed condition.

*Excess Correlation Patterns **Between** Subjects at a Distance: Global Power*

The same methods of comparisons were completed for correlations of global power values between each pairs left hemisphere and right hemisphere even though they were separated by more than 6,000 km. During the Effector field sequence of the EMF exposure, statistically significant increased coherence of global spectral power density across **right** hemispheric sensors equivalent to a correlation coefficient of .88 could be discerned, explaining approximately 77% of the variance (Figure 11).

Spectral power densities were highly correlated over F4 ($r = .95$, $p<.05$; rho= .90, $p<.05$) and T4 ($r = .97$, $p<.01$; rho= .90, $p<.05$), which were the sensors located over the *right* frontal and *right* anterior temporal areas. Removing pairs systematically from the analysis revealed that a cluster of significant non-parametric correlation coefficients could be identified for right hemispheric global power during the second half of the Effector field sequence, continuing somewhat after the termination of the field ($p<.05$).

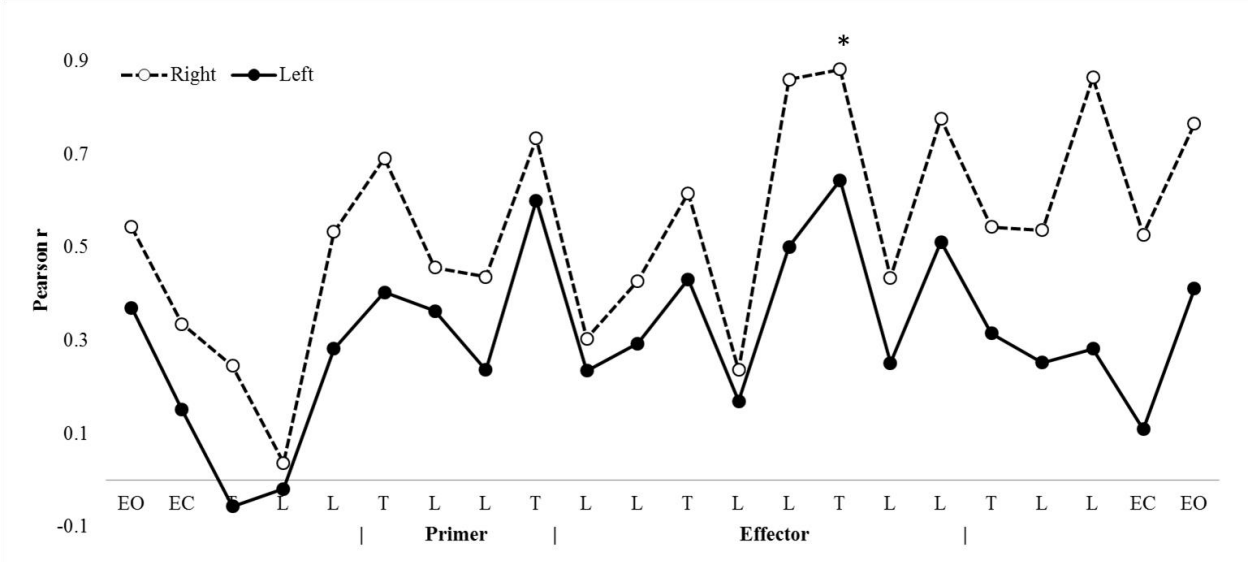

Figure 11. Correlation coefficients plotted overtime indicative of the strength of the association between paired right (light circle; dotted line) and paired left (dark circle; full line) hemispheric global spectral power densities. EO indicates baseline with eyes open, EC indicates baseline with eyes closed, L indicates white light visualization, and T indicates paired tone presentations.

Correlation coefficients presented in Figure 12 were loaded and chunked into 5 experimental sequences across time: Pre-Baseline (n=5), Primer (n=4), Effector 1 (n=4), Effector 2 (n=4), and Post-Baseline (n=5). An ANOVA revealed that correlation coefficients indicative of the strength of the association between global spectral power density over right hemispheric sensors of paired participants differed as a function of sequence, $F(4,21)= 3.83$, $p<.05$, $\eta^2= .47$. Left sensors did not demonstrate the effect after Bonferroni correction ($p<.05$). *Post-hoc* analyses revealed two homogenous subsets where the primary source of variance was accommodated by differences in the correlation coefficients during Effector 2 (M= .74, SE= .10) relative to Pre-Baseline (M= .34, SE= .09), $t(7)= 2.84$, $p<.05$, $r^2= .53$.

During the second half of the Effector field sequence (Effector 2), correlation coefficients indicative of the strength of the association between global spectral power density measures across QEEG channels for paired participants differed as a function of channel, $F(7,31)= 21.90$, $p<.001$, $\eta^2=.86$. As visualized in Figure 13, the weak association between paired right occipital sensors (O2) relative to all other sensor pairs was the major source of variance ($p<.001$). However, it should be noted that further differences among the remaining sensors were identified. Increased average correlation coefficients were noted for paired T6 sensors (M= .90, SE= .04) relative to paired C4 sensors (M= .74, SE= .05, $t(6)= 2.51$, $p<.05$, $r^2= .51$). Similarly, correlation coefficients were increased for paired F4 sensors (M= .92, SE= .03) relative to paired C4 sensors, $t(6)= 3.21$, $p<.05$, $r^2=.63$.

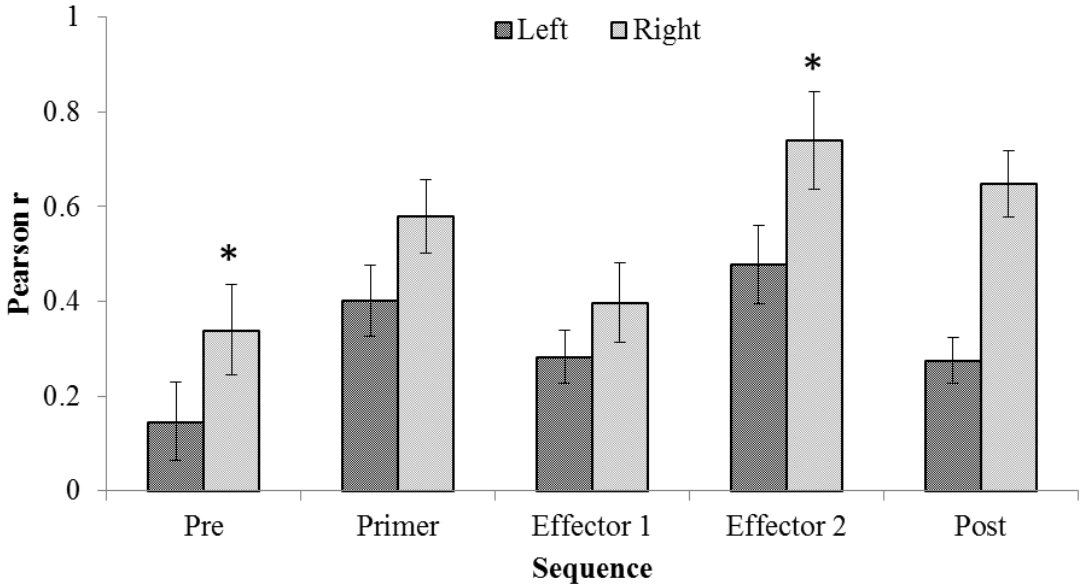

Figure 12. Average correlation coefficient indicative of the strength of the association between global spectral power density for sensors over the left (dark) and right (light) hemispheres for paired individuals.

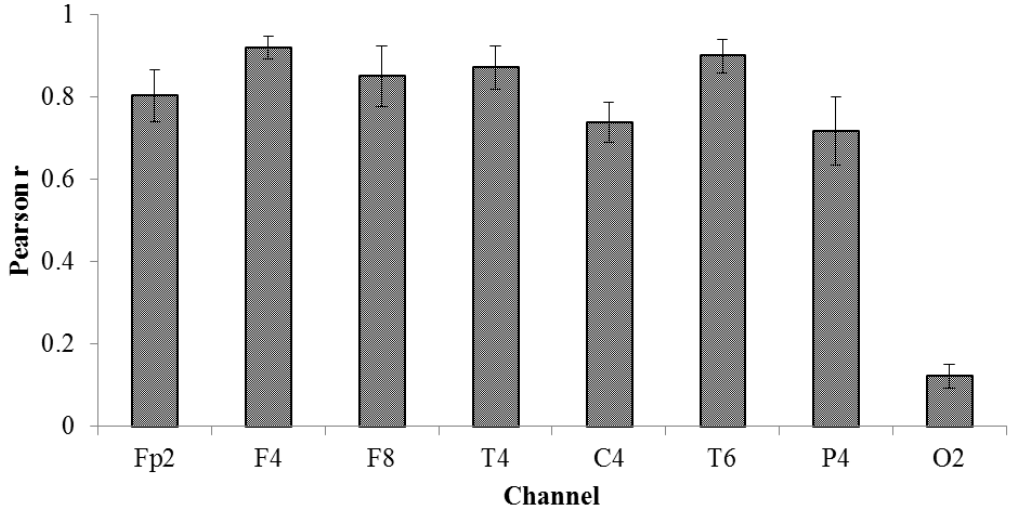

Figure 13. Average correlation coefficients indicative of the strength of the association between global spectral power densities displayed at sensors over the right hemisphere for paired individuals during the second half of the Effector sequence (Effector 2).

Figure 14 shows mean differences between correlation coefficients associated with μV from the left and right hemispheric sensors. These computed values, with their measures of dispersion, are indicative of the magnitude of the global spectral power density coherence disparity between the left and right hemispheres of the paired individuals over the course of the experiment. This was accomplished by subtracting left-hemisphere-associated correlation coefficients from right-hemisphere-associated correlation coefficients. An ANOVA revealed that

this measure differed as a function of the sequence of the experiment, $F(4,21)= 4.83$, $p<.01$, $\eta^2=.53$. The source of the variance associated was an increased value for this metric associated with the Post-Baseline (M= .37, SE= .06) relative to the Effector 1 sequence (M= .11, SE= .03) at the point of inflection, $t(7)= -3.52$, $p=.01$, $r^2= .64$.

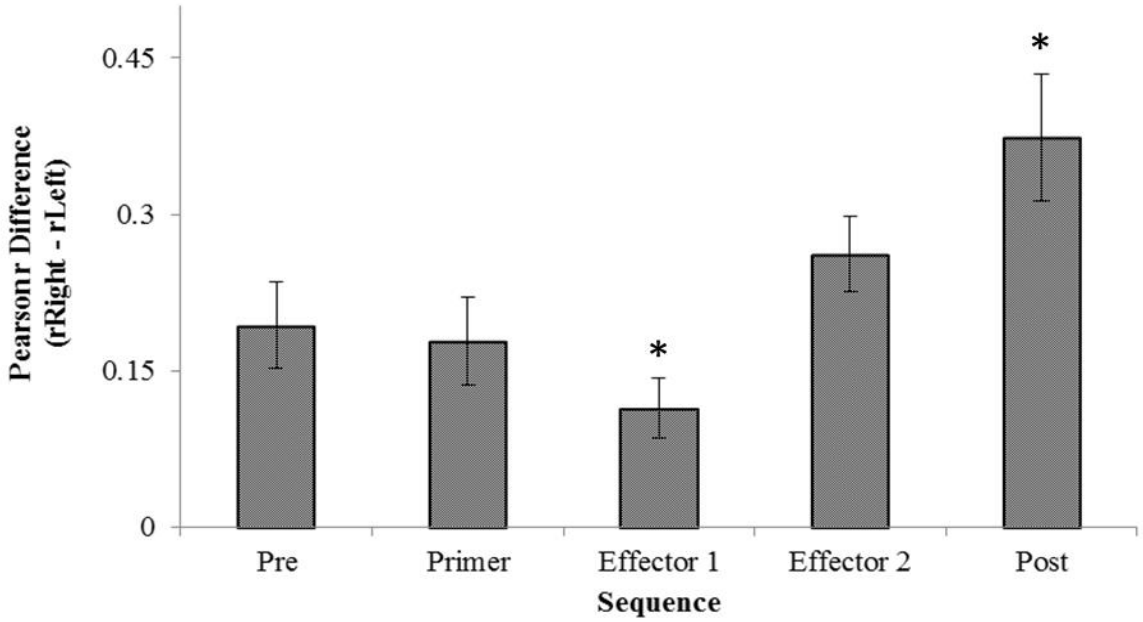

Figure 14. Difference scores obtained by subtracting correlation coefficients indicative of the strength of the association between global power spectral densities for sensors over the left hemisphere of paired individuals from those displayed over the right hemisphere as a function of the sequence of the experiment.

Excess Correlations Between Subjects at a Distance: Intrahemispheric and Interhemispheric Coherence

The mean coherence values for the five pairs of participants over the blocks of the protocol for power within the **theta** and **gamma** bands between the left and right hemisphere for each of the four lobes indicated that the only major significant and obvious effects involved the *temporal* lobes. These bands are the predominant interaction mode between the hippocampal formation and cerebral cortices (Bear, 1996; Whitman et al, 2013). The other frequency bands, delta, alpha-1, alpha-2, beta-1, and beta-2 did not exhibit any significant coherence differences across the phases of the experiment for the shared hemispheric activity for the pairs of participants. The parietal, occipital and frontal regions did not show this effect during the effector field period. There was a marginally significant increase in coherence over the right prefrontal regions for gamma activity during the beginning of the experiment when the instructions were given and individuals were concentrating accordingly.

The conspicuous effect of changed coherence between the more rostral left (T3) and right (T4) temporal lobes as a function of the phase of the experiment and type of magnetic field configuration is shown in Figure 15. During the effector field only there were statistically

significant (as inferred by the absence of overlap of the SEMs) and transient **diminishments** of the coherence of power within the *theta* bands between the *right* temporal lobes of the pairs of individuals separated by ~6000 km. This was not evident for the left temporal region for this frequency band or for the theta band for either temporal lobe.

The specificity of the (right) temporal lobe (and not other lobes) and the gamma band (compared to all other bands) strongly suggests the effect was not simply an artifact of direct exposure to the simultaneously applied toroidal fields. This effect was also not apparent during the primer fields, which also strongly indicates the effect was not due to simply shared magnetic fields. The diminishment was from a right temporal (person 1) to right temporal (person 2) value of 0.15 to 0.10 or a shift of 0.05. For comparison the typical correlations between spike counts from groups of individual neurons in cortical networks range between 0.1 to 0.3 (Ecker et al, 2010).

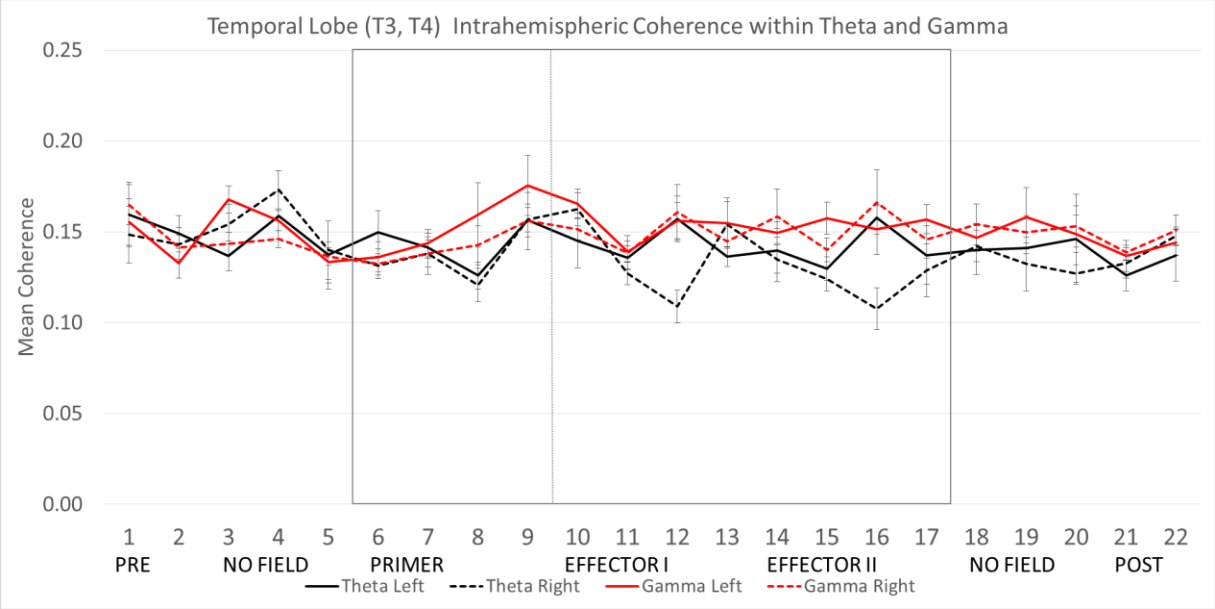

Figure 15. Mean coherence between the left temporal (T3) and right (T4) temporal sensors for the pairs for the theta and gamma band. The only statistically significant differences occurred during the entanglement (effector) stage associated with the depression for right theta coherence. Vertical bars indicate SEMs.

A similar effect was noted only during the effector field condition for the region of the more caudal portion of the temporal lobes (T5, T6). However in this region the diminishment of interbrain coherence during the latter portion of the effector phase occurred for both the left and right hemisphere. It is relevant that these two surface sensor positions are most strongly correlated with activity within the parahippocampal gyrus. The parahippocampal gyrus is the general region by which interactions between the two hippocampuses are mediated through the dorsal hippocampal commissure. It is located in the rostral portion of the splenium of the corpus

callosum. The dorsal hippocampal commissure in the human being mediates information between the hippocampal formations within the left and right hemisphere without processing through the neocortices. Consequently memory modifications can occur without self-awareness.

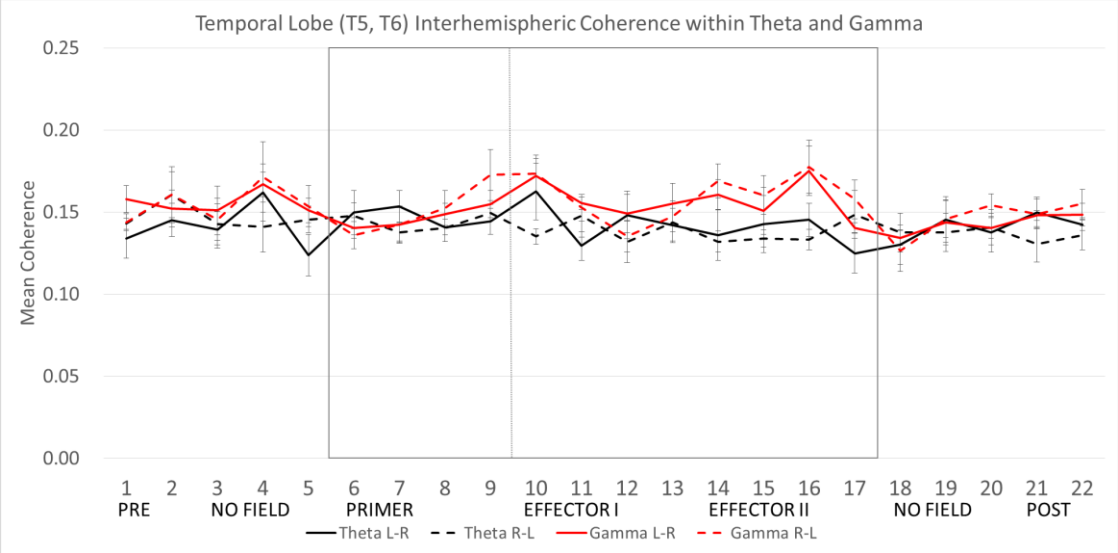

Figure 16. Mean coherence between the left temporal (T5) and right (T6) temporal lobes for each pair (separated by 6000 km) for the power within the gamma and theta band over the various conditions of the experiment. The only statistically significant differences occurred during the entanglement (Effector II) stage. Vertical bars indicate SEMs.

(Continued on Part II)

Article

Experimental Production of Excess Correlation across the Atlantic Ocean of Right Hemispheric Theta-Gamma Power Between Subject Pairs Sharing Circumcerebral Rotating Magnetic Fields (Part II)

Mandy A. Scott, Nicolas Rouleau, Brendan S. Lehman, Lucas W. E. Tessaro, Lyndon M. Juden-Kelly, Kevin S. Saroka & Michael A. Persinger*

Neuroscience Research Group, Human Studies and Biomolecular Sciences Programs, Laurentian University, Sudbury, Ontario, Canada P3E 2C6

ABSTRACT

There have been multiple historical and cross-cultural reports of excess correlation of specific experiences between individuals separated by thousands of kilometers. Recently there have been experimental demonstrations of excess correlations between measurable cerebral events for small percentages of test subjects. More reliable effects can be elicited when electromagnetic fields and photons are involved. In this experiment completed during the summer of 2015, 5 pairs of volunteers separated by more than 6,000 km wore identical cerebral toroids through which patterns of phase shifting, 30 nT magnetic fields that diminished the local magnetic field in both loci by 1-5 nT were exposed to the sequences that produced excess correlation in chemiluminescent reactions and shifts in pH. Compared to the various baselines and control procedures enhanced power between the right hemispheres of pairs of participants occurred during the interval documented to produce excess correlation. Specific analyses indicated diminished coherence within the theta band only within the right temporal lobes of the pairs. Sequential block analyses revealed that the paired brains' responses to pulsed tones at 6.5 Hz occurred within the 30-40 Hz band over the caudal temporal lobes during the exposures to the effector field. Primary independent component analyses verified these patterns. During the 6.5 Hz tones there was a peak in the spectral power density (SPD) at that frequency over the right temporal lobe of the person listening but a trough in (SPD) over this region for the person who was not. Even subjective experiences, as measured by the Profile of Mood States (POMS), indicated significantly increased excess correlation for scales by which increased anger and decreased vigour are inferred. This experiment, based upon physical principles, suggests there is a technology that can generate reliable excess correlation of brain activity (and potentially consciousness and specific experiences) between two people separated by thousands of kilometers.

Part II of this two-part article includes: 4. Results and Discussion (continued); 5. General Discussion; Appendix A; and References.

Keywords: Excess correlations, entanglement, transatlantic effects, theta frequency, right temporal lobe, toroidal magnetic fields, brain coherence.

*Corresponding author: Dr. M. A. Persinger, mpersinger@laurentian.ca

4. Results and Discussion (Continued from Part I)

Excess Correlation Between Subjects at a Distance: Independent Component Analyses

Emergent relationships or "fields" of activity patterns can be discerned by more advanced statistical analyses that extract shared sources of variance in voltage fluctuations. Independent component analysis is an aggregate form of factor analyses. The QEEG data for the individuals from each of the pairs that were formatted for EEGLAB and transformed to MATLAB were split into Local and Non-Local arrays and truncated to the shortest array length for clustering software (20,000 ms). A total of 100 datasets were imported into the EEGLAB to discern interactions between: 1) when during the procedure, 2) which of the two people in a pair, and, 3) which locality within the brain interacted.

Cluster analyses were employed to extract patterns in the combined data. The clustering results were structured to display the differences between the primer and effector fields relative to the person who was "first-to-send" and "first-to-receive." A total of 30 datasets were entered into each analysis. Although "first to send" and "first to receive" varied with each pair of subjects and was selected arbitrarily during the experiment, we reasoned that a specific effect would represent the significance of the intention and cognitive state in entanglement processes.

The regions of the cerebrums of the pairs that exhibited the most conspicuous clustering for the differences between the primer and effector fields were discernable by visual inspection. The most significant region for the strength of clustering was the right temporal lobe for both participants simultaneously during the primer and effector field conditions. This is shown in Figure 17 which represents a colorized distribution of where the greatest strength of clustering occurred. The **right** temporal lobe (red) was the region of strongest activation within the cluster while the left prefrontal region (blue) exhibited the weakest activation within the cluster. The other colors along the spectrum represent intermediate values.

The most visual cluster pattern indicated an increase in power within the right temporal lobe during the primer field for the person who was designated in that trial as the receiver but an increase in theta power within the right temporal lobe for the sender during the effector phase. The quantitative difference when $10^* \log_{10}(\mu V^2)$ was assessed indicated the shift was from 20 to 22 units. The actual values would have involved an increase of theta power from 10 μV to 12.6 μV or an increase of about 2.6 μV. As calculated previously this value across the cerebral length would be associated with a current of $\sim 10^{-7}$ A and when divided into the diffusivity based upon the permeability constant of the magnetic field in a vacuum and conductivity of the extracellular fluid of the brain results in an equivalent magnetic field strength of about 1 pT. This is the range of the immersive Schumann Resonance, particularly the fundamental of 7 to 8 Hz.

The power curve across the frequency band for the optimal cluster measured in log base 10 of μV^2 (quantity multiplied by 10) for the effector and primer fields for the receiver and the sender as well as the orthogonal combination the primer field for the sender and receiver and the effector field for the sender and receiver are shown in Figure 18 through 21. The portions of the band that displayed the statistically significant differences were primarily within the theta and

gamma ranges. This is indicated by the black bars along the horizontal axis. The reason that some separations are wider than others but were statistically significant reflects the nature of the variability of power measures for those comparisons.

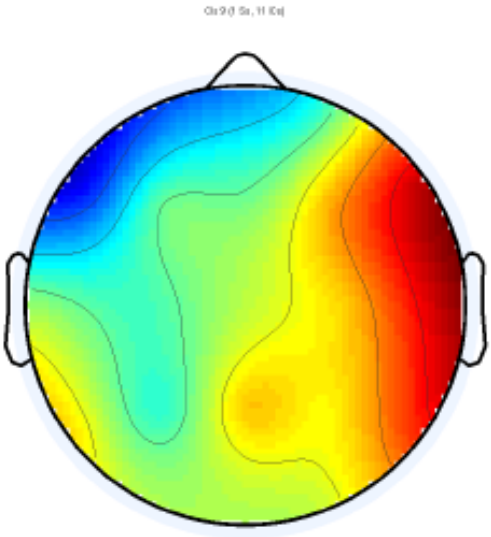

Figure 17. Colorized distribution of where according to independent component analyses the coherence in brain activity during the effector (entanglement) field the increased shared variance in the two brains separated by 6,000 km occurred. Red, the right temporal region, showed the marked enhancement. Blue refers to least power over the left prefrontal region.

For the receiver the theta power was less during the effector field than during the primer field. This difference was not statistically significant for the sender. During the primer field condition the senders' brains displayed a marked increase in power in the gamma range compared to the receivers' brains. However during the effector field condition, when "excess correlation" occurred during other experiments which involved chemiluminescent chemical reactions and shifts in pH (including a paradigm identical to the present procedure), there was decreased power within the receivers' brains within *both* the theta and gamma band. This would be consistent with an activation of the hippocampal formation-cortical pathway which is dominated by 40 Hz ripples superimposed upon a 7-8 Hz fundamental frequency. Because there is an "absolute reference" another interpretation is that the frequency bands that differed between the sender and receiver during the primer and effector fields were the theta and gamma frequencies.

Psychometric Test Results

Although psychometric tests are often considered crude indicators of brain activity their strength of association with actual EEG activity particularly over the temporal lobes is evident even with strip-chart comparisons (Makarec and Persinger, 1990). Recently, employing both

QEEG and sLORETA Collins and Persinger (2014) showed that the loosely clustered items by which egocentricism is inferred were visibly associated with increases in the cerebral cortices Default Mode Network and showed the expected hemispheric differences with respect to gender. Because we predicted a strong state of confluence between the moods of the two participants, (particular if one assumed the metaphor that the two shared circularly rotating magnetic fields at distant loci resulted in a juxtaposition of space and superposition of states) such that they behaved as if they were the *same* space this condition should be evident even by psychometric reflection.

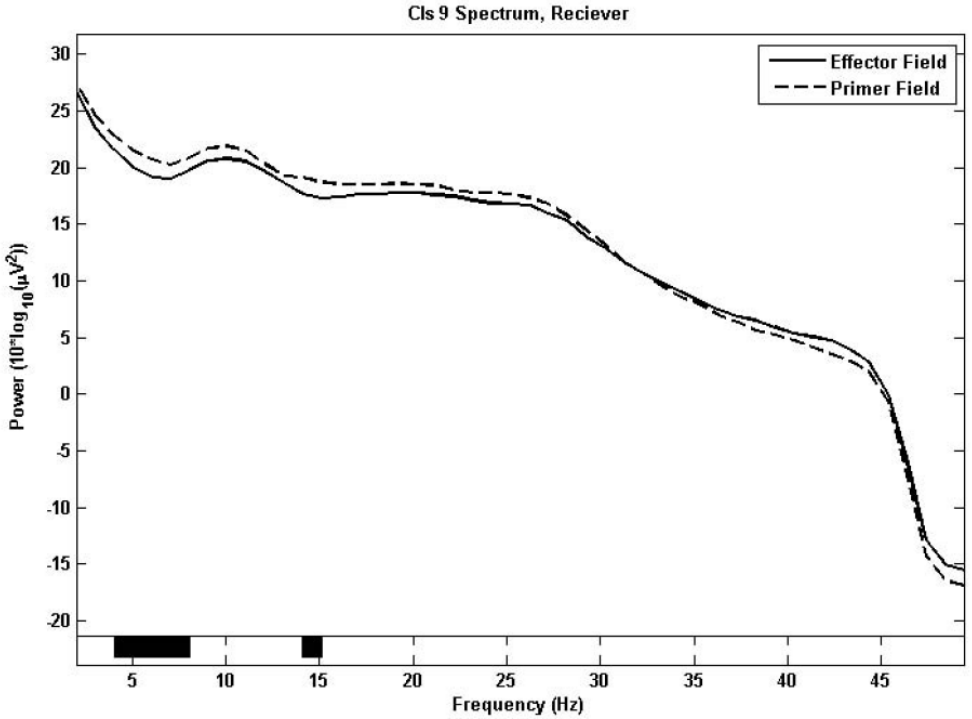

Figure 18. Power distributions over the frequency band of the EEG for the person serving as "the receiver" during the primer field (dotted line) and effector field (solid line). The black bars along the horizontal axis indicate the frequency intervals that differed significantly between the two conditions. Note the major difference in the theta (4- 7 Hz) band.

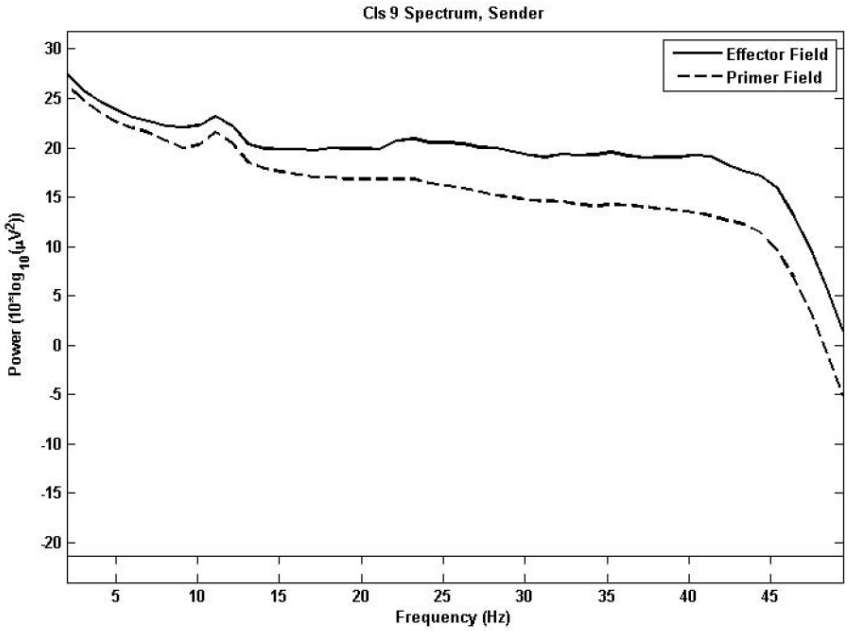

Figure 19. Power distributions over the frequency band of the EEG for the person serving as "the sender" during the primer field (dotted line) and effector field (solid line). There was no statistically significant difference.

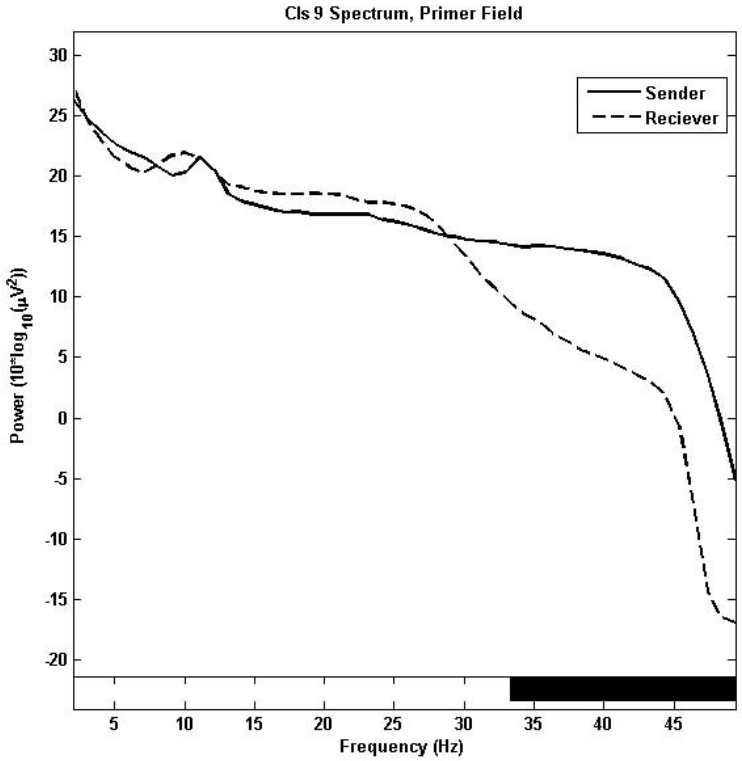

Figure 20. Power distributions over the frequency band during the primer field for the person serving as the sender and the receiver. The statistically significant effect was lower power in for the receiver within the gamma band (> 35 Hz).

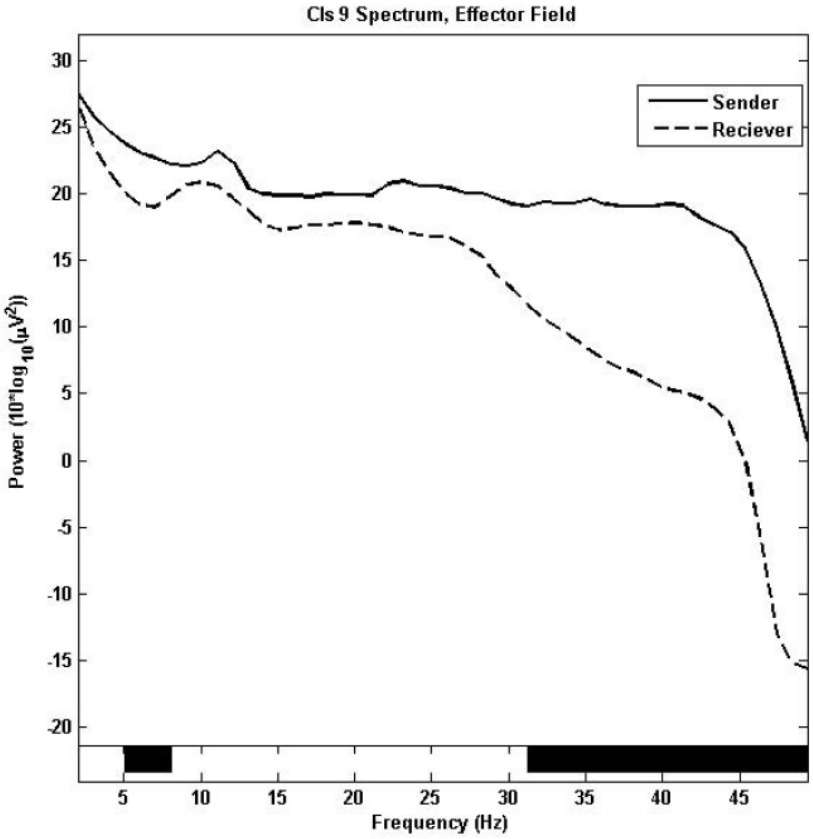

Figure 21. Power distribution across the frequency bands during the effector field for the persons serving as the sender or the receiver. The sender exhibited more power compared to the receiver within the theta band and well as in the gamma band.

The results supported the prediction. As shown in Table 6, the correlation between the scaled scores for the five pairs during the post baseline, after the excess correlation had been shown by QEEG profiles, was statistically significant for the scales of anger and vigour. The results are presented as Spearman rho coefficients instead of Pearson r values (although they were comparable) in order to reduce the potential effects from outliers. Compared to the pre-baseline when the correlations between the pairs' scores for anger and vigour were not statistically significant, the values for these two scales increased to 0.97 and -0.87 after the entanglement paradigm. The scores for the other four scales were not significantly correlated between the pairs separated by ~6,000 km.

Table 6. Spearman Rho correlations between each of the six scales from the Profile of Mood States (POMS) for the pairs (A and B) of people who shared the excess correlation magnetic field procedure during the pre- and post exposure conditions.

Scale	Pre (A-B)	Post (A-B)
Tension	-0.75	0.56
Depression	0.58	0.72
Anger	0.00	0.97**
Vigour	-0.32	-0.87*
Fatigue	-0.62	0.22
Confusion	0.08	0.40

p <.05; ** p <.01

Is the Superposition Isomorphic or Translational?

The excess correlation between separated brains for specific bands of cerebral activity and locations does not necessarily reveal how the information is being transformed or transposed. The simplest possibility is that the tonal pulse is transposed as an energetic pattern non-locally. That frequency or temporal pattern is the primary code by which sensory information from different modalities is integrated or translated into "the language of the brain" has been known for decades. For example the brilliant E. R. John (1967) in his seminal text *Mechanisms of Memory* had shown that the generalization of learning from one sensory context (auditory) to another (visual) could occur error-free if the two discriminant stimuli shared the same frequency. Recent principles of neuroscience indicate that the "line codes" for different sensory modalities are transformed to a more common code that allows intermodal integration. The locus for this transformation for intermodal confluence is within the parahippocampal gyrus (Gloor, 1997).

If the excess correlations between distal cerebrums operate in this manner then the 6.5 Hz tones presented to the sender should produce an increase in theta activity (4 to 7 Hz) within his or her brain. A complementary change in power within this theta band should also occur in the receiver's brain even though he or she was not exposed to the 6.5 Hz tone. If "entanglement" was present an increase in power within the 6.5 Hz range in the brain of the person receiving the tone should be coincident with a decrease in power with the other person who was not listening to the pulsed tone. In order to ensure there were no subject effects individuals in the A or B position alternated as senders (tone pulse) or receivers (non tone) during the various sequences of the experiment for the different types of baseline, primer, and effector field conditions.

Raw extractions (10 s increments) were performed for every instance of a tone presentation for each sequence of the experiment (i.e. Pre, Primer1, Primer2, Effector1, Effector2, and Post). Data were standardized by z-transformation and spectral analyzed. Data were coded to identify individuals receiving burst patterned tones or a primer tone followed by silence. Because the previous analyses had indicated the primary role of the right temporal lobe and the task was an auditory, only the power data from T4 and T6 were analyzed for the three, 1 Hz increments that included the 6.5 Hz tone pulse. They were 4-5 Hz, 5-6 Hz, and 7-8 Hz. As can be see in Figures 22 there were no statistically significant differences between the sender or the receiver condition for the 6 Hz-7 Hz band (the one corresponding to the pulse of the tone) over the T6 regions. A similar pattern was noted for T4. There were no significant differences for either the 5-6 Hz or 7-8 Hz increments for either region.

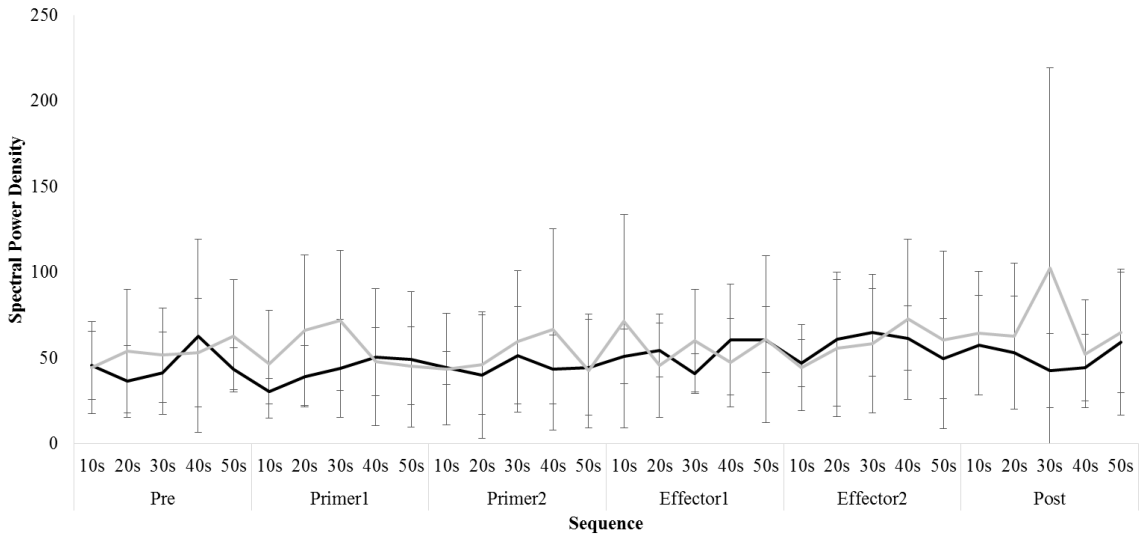

Figure 22. Spectral Power Densities within the 6 to 7 Hz range over T6 for senders (dark line) and receivers (light line). No significant differences were observed during the entanglement period.

However if the information was being mediated through a process strongly associated with consciousness then the changes would occur within the gamma band or the "40 Hz" band. To test this possibility spectral power densities (SPD) within the gamma or 30Hz to 40Hz band were averaged and loaded into SPSS. In addition to general increases in gamma-band SPDs (r^2= .87) over T6 for those receiving pulsed burst tones (M= 8.80, SE= .53) relative to those in silence (M= 2.60, SE= .15), if taken over the course of all tone presentations (n=30), a number of punctate features were apparent. The results are shown in Figure 23.

First, significant differences between sender (dark line; n=5) and receiver (light line; n=5) gamma activity over T6 could only be identified within Effector and Post-Field baseline sequences. The first of such instances was between 20-30

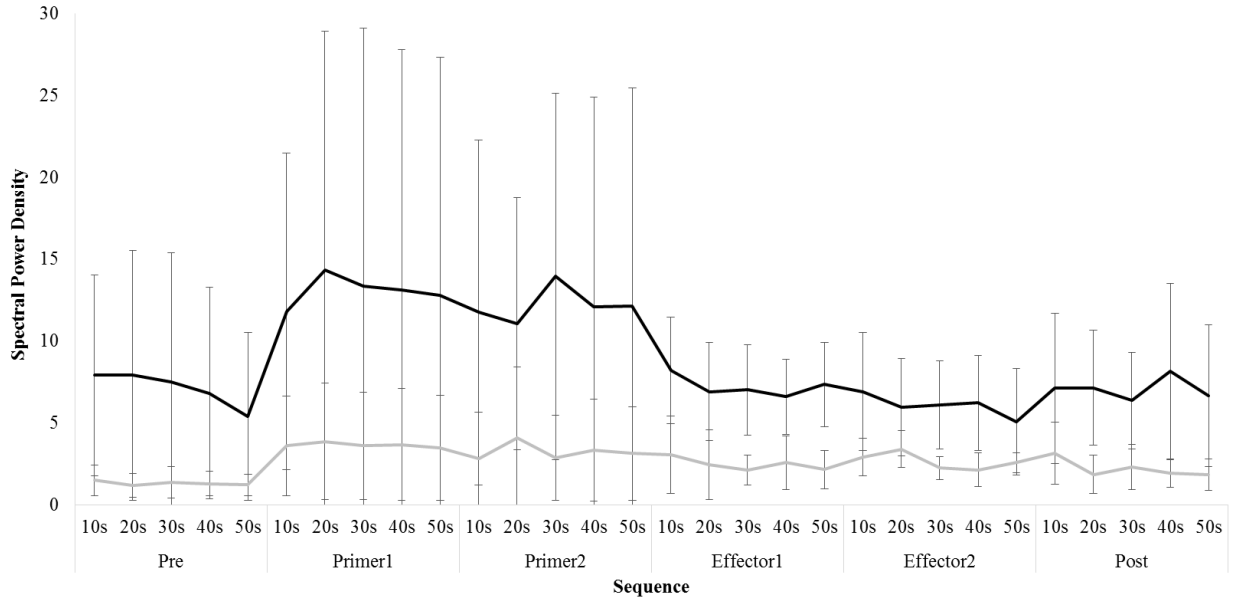

Figure 23. Mean 30-40Hz Spectral Power Densities (SPDs) and standard deviations over T6 for 10 second increments within tone presentations across sequences of the experiment.

seconds after the initiation of the burst tone pattern within the Effector 1 sequence, $t(4) = 5.53$, $p=.005$, $r^2= .86$. Differences persisted transiently within the Effector 1 sequence, re-emerging once again 20-30 seconds after the initiation of the burst tone pattern within the Effector 2 sequence, $t(4)= 3.21$, $p<.05$, $r^2= .72$. This pattern re-emerged for a third and final instance between 20-30 seconds after the initiation of the burst tone pattern within the Post-Field baseline sequence, $t(4)= 3.21$, $p<.05$, $r^2= .72$. In other words the discrepancies from chance occurred only during the effector field which has been associated with "excess correlation". That the effect was not likely to be spurious is strongly suggested by the absence of significant differences between senders and receivers for SPDs over T4 (see Figure 24), a more rostral region of the right hemisphere. T6 on the other hand is more directly correlated with activity changes within the right parahippocampal region.

The standard deviations were unusually high but might be expected normally because individuals often respond differentially to tonal inputs depending upon processing pathways, attention variations, and threshold sensitivities. The significant differences shown in effector field portions of Figure 23 were likely due decrease in variability of the gamma-band activity over T6 associated with the Effector sequences. Differences were not identified within Pre, Primer 1, or Primer 2 sequences ($p>.05$). As shown in Figure 25, this diminishment is conspicuous. The standard deviations of the SPD for the sender's profile decreased to that of the receiver's profile only during the effector field. If the metaphor that non-locality or excess correlation indicates that two loci behave as if they have been superimposed into the same space, then this type of convergence would be congruent.

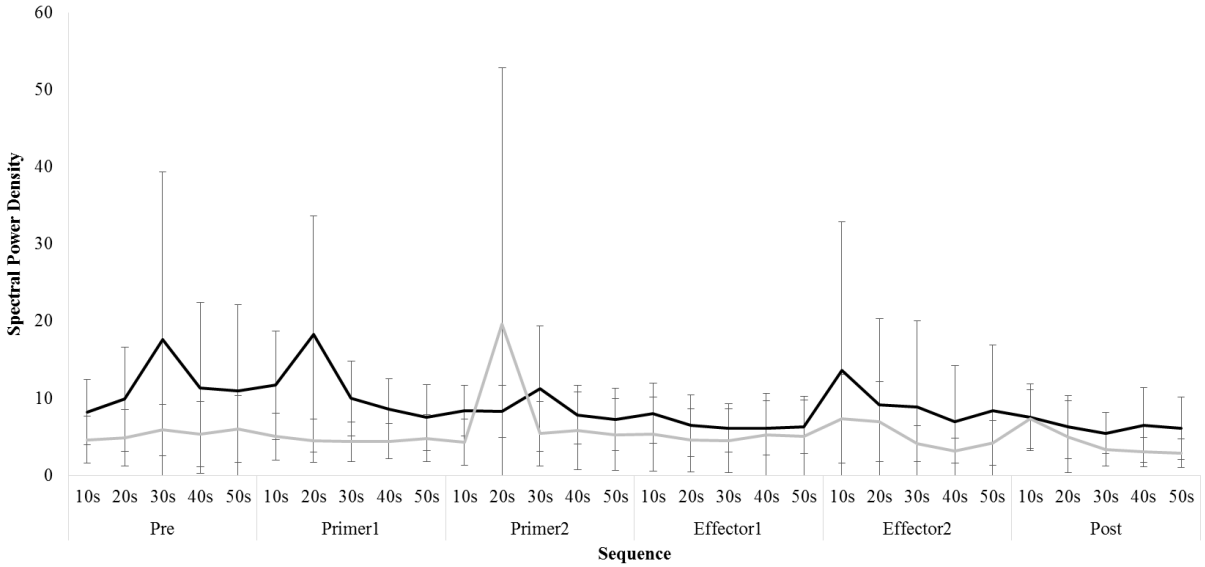

Figure 24. SPDs within the gamma or 30Hz-40Hz range over T4 for senders (dark line) and receivers (light line). No statistically significant differences were observed.

Precision Analyses With 250 Hz Sampling: Demonstration of Excess Correlation Parity

One of the typical indicators of the demonstration of entanglement between two objects in non-local settings is that the polarity of a property shared by the two components can change more or less simultaneously. If this were occurring between the two brains paired with the toroids then the presentation of the 6.5 Hz tone to one of the persons in the pair should be associated with an increased Spectral Power Density (SPD) around that frequency. On the other hand the receptive person, not listening to any sound, should show a diminished trough or "mirror" image of SPD around this frequency.

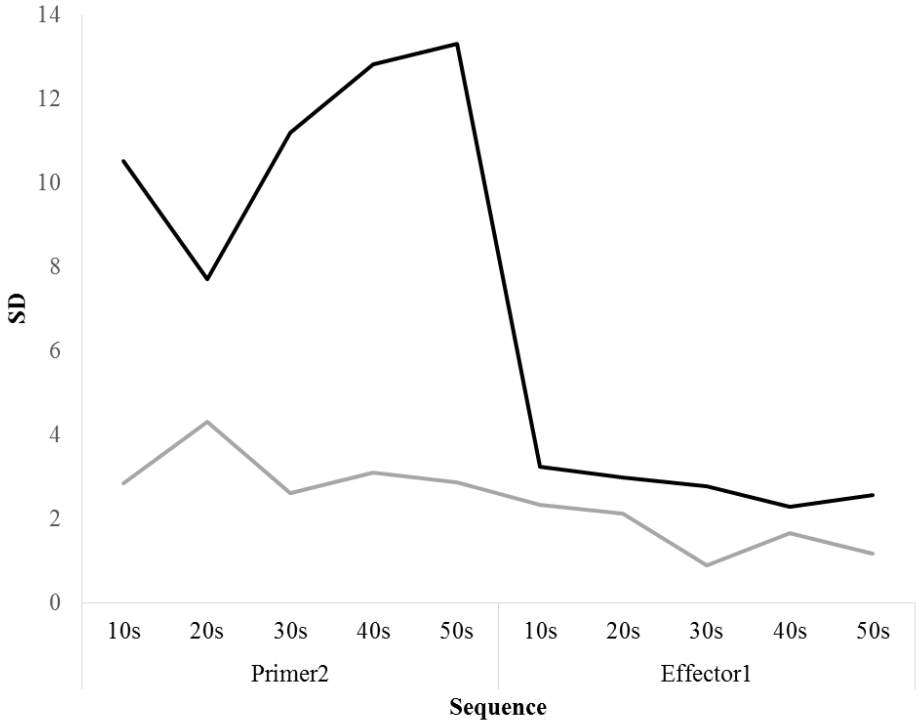

Figure 25. SDs of gamma-band SPDs at the point of transition between Primer 2 and Effector 1 sequence-associated tone presentations. The black line is the person in the pair listening to the pulsed tone; the grey line is the person in the pair receiving the continuous tone or silence.

To test this prediction the 2,500, 4 ms (250 Hz sampling rate) raw data from T6 from each of the individuals of the five pairs were obtained for successive intervals of 10 to 20 s, 20 to 30 s, 30 to 40 s and 40 to 50 s during the first and second 6.5 Hz presentations (to one of the two in each pair) during the effector field. During the second tone presentation the other person (the one who had been the "receiver") received the pulsed tone sequence. The data were then spectral analyzed by SPSS PC Spectra. We selected the increments of SPD between 4 and 9 Hz with the centroid being 6. 5 Hz (the pulse frequency) to demonstrate the effect it were present. The results were clear and present in each of the 5 pairs during the second pulsed tone presentations. Examples of two of the pairs are shown in Figures 26 and 27. These effects emerged between 20 and 40 s after the tonal pulses began.

As expected from normal neuroelectrophysiology, the subjects directly receiving the 6.5 Hz tone stimuli showed increased SPD around this frequency (blue dots). The other subject who was not listening to the tone displayed a diminishment of SPD within a trough around 6.5 Hz. Not all pairs showed these aesthetic, symmetrically distributed patterns but all showed the parity of response at this frequency. In other words the power spectral density over the caudal right temporal lobe showed the opposite effect between the "sender" and the "receiver" when a stimulus was presented to the sender but only when both brains were exposed to the effector fields.

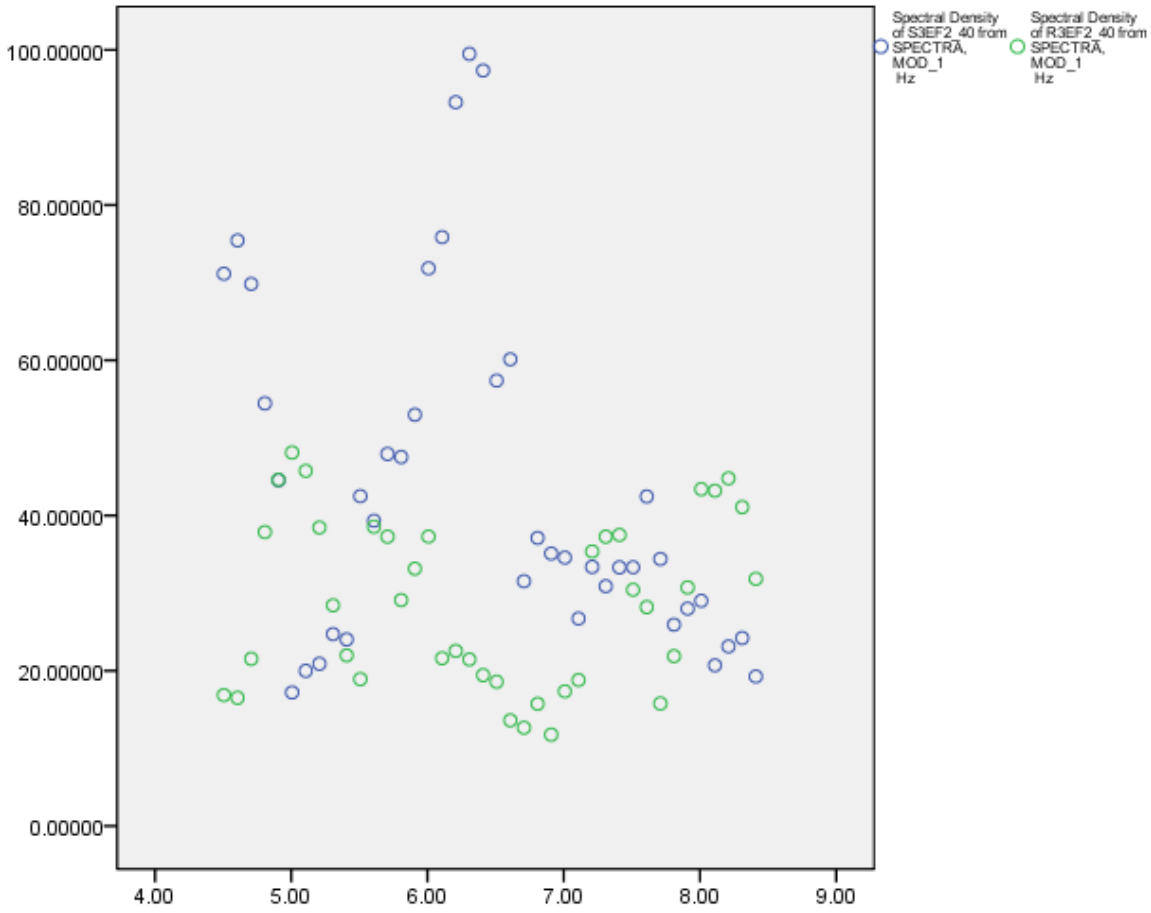

Figure 26. SPD (Spectral Power Density) for the amplitude shifts (vertical axis)from the raw QEEG voltages over T6 (right temporal lobe) between 4 and 9 Hz for the person hearing the 6.5 Hz tone (blue circles) and the person not hearing (green circles) the pulsed tones (Pair 3) when both shared the effector fields. Note the opposite direction around 6.5 Hz. This is only occurred between 40 and 50 s after the onset of the tone.

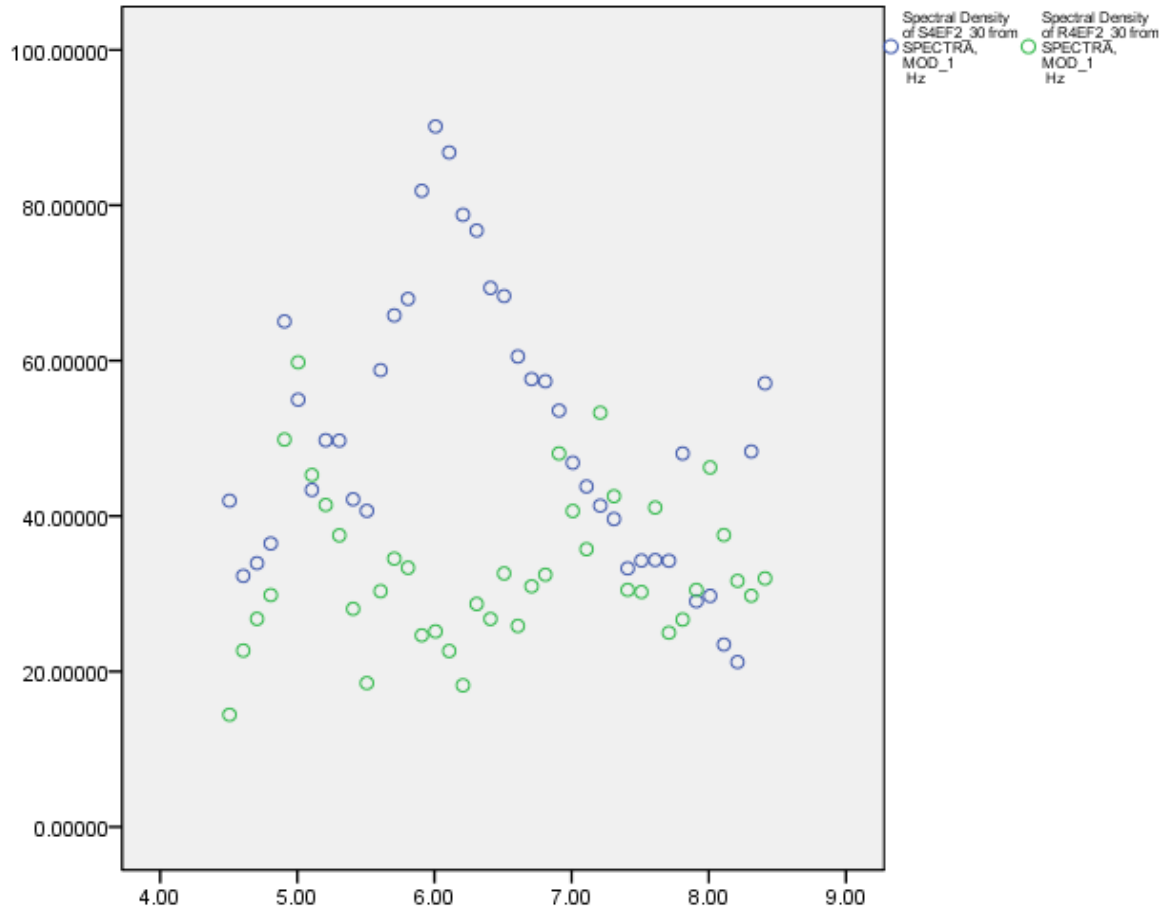

Figure 27. SPD (Spectral Power Density) for the amplitude shifts (vertical axis) from the raw QEEG voltages over T6 (right temporal lobe) between 4 and 9 Hz for the person hearing the 6.5 Hz tone (blue circles) and the person not hearing (green circles) the pulsed tones (Pair 4) when both shared the effector fields. Note the opposite direction around 6.5 Hz. This is only occurred between 30 and 40 s after the onset of the tone.

5. General Discussion

To our knowledge this is the first experiment that has demonstrated that sharing counterclockwise, rotating magnetic fields around the cephalic region resulted in shifts in quantitative brain parameters that are consistent with excess correlation or "entanglement" over such long distances. The predominance of the indicators of coherence in cerebral activity over the right hemispheres of paired participants, particularly their temporal lobes, is consistent with the inferences and indirect measurements reported by several experimenters for at least a century (Gurney et al, 1886; Harrington, 1995).

The right hemisphere's contribution to related "mystical" states has chemical correlates (Kurup and Kurup, 2003). The primary role of the right hemisphere in the production of

phenomena that suggest excess correlation has been a limiting feature for systematic exploration in the laboratory. After novel phenomena are verbally encoded following sometimes even a single presentation, subsequent presentation of another of the "same" stimulus is more proportionally processed by the left hemisphere that exhibits different properties and limitations. This may explain the frustrating history in this area of investigation whereby the first trial generates powerful indicators of excess correlation between individuals separated by non-traditional distances but subsequent trials manifest exponentially diminishing displays.

The probability that the shared coherences of right hemisphere activity between the pairs were artifacts of the circumcerebral magnetic fields is minimal. The specificity of the effects only during the effector field but not the primer field suggests the excess correlations of specific brain activities during the exposure to the effector field was not secondary to simply being exposed to these weak magnetic fields. In addition the effects were specific to the right hemisphere and two specific bands of power, the theta and gamma range, that are classically associated with consciousness and memory (Whitman et al, 2013; Henke et al, 1997) as well as complex, virtual maze navigation (Kahana et al, 1999). Finally, although the effects during the effector or excess correlation phase were displayed by all five pairs of subjects, there were distinct pair differences that would not be expected by electronic artifacts.

The decrease in coherence during the entanglement phase would be consistent with the more recent observations by Ecker et al (2010) who studied the recordings of multiple adjacent neurons in the primary visual cortex of awake macaques. Neurons with similar orientation tuning exhibited virtually no correlated variability. Ecker et al (2010) concluded that adjacent neurons shared only a few percent of their inputs or the activity was being activity decorrelated. Both conditions would be expected features of dense and multiple information processing. Highly correlated activity between neurons would suggest they all share the same (redundant) input. Lower correlations indicated that the pathways were processing at different rates which could be mediation of different information. If larger aggregates of neurons (such as that measured by QEEG activity) reflect a similar process, then the diminished coherence of theta power within the right temporal lobes represented by T4 only of the two subjects during the entanglement phase would be consistent with an exchange of information.

The predominance of the theta and gamma effects is important because this is a central mode by which the hippocampus through the entorhinal cortices within the parahippocampal gyrus interacts within the entire neocortical manifold. Consciousness and awareness involve an interaction between the inputs from the immediate sensory input and the comparison with representations of previous experiences, that is, memory (Bear, 1996). Electrophysiological measurements indicate that the theta fundamentals contain ripples of gamma frequency such that hippocampal information might be more congruent with the 40 Hz cerebral state (Buzaki, 2002).

When the specific isomorphic potential for entanglement was assessed by spectral analyses the person of the pair who received the 6.5 Hz pulse tones exhibited increased spectral power density over the right parahippocampal region where as the person of the pair who did not receive the tone displayed the opposite effect. This type of parity is quintessential entanglement (Aczel, 2002). However the effect was most evident for all five pairs during the second sound pulse presentations during the effector phase. The approximate time between the first and second

sound pulse presentations was 4 min. This suggests that a type of learning occurred within the pairs of subjects during the first presentation of the tonal pulses.

One interpretation of this interesting enhancement is that entanglement phenomena for this paradigm within the pairs of human brains we studied were mediated through memory-related processes. If this is valid, the conspicuous occurrence of right caudal temporal and presumably parahippocampal involvement indicates that "memory consolidation" is the process that has been entangled. A very similar idea was developed by Gurney et al (1886) during the late 19th century to explain their carefully collected "spontaneous" cases of excess correlation between pairs of people where entanglement was strongly probable. The human hippocampus is central to establishing associations (Henke, et al, 2007). For the "memories" to be represented within any single person's cerebral cortices approximately 10 to 20 min would be required for the dendritic spines to emerge into the spatial structure that is the memory. However permanent electrical changes can occur within portions of the hippocampus within 3 to 4 minutes after stimulus presentations.

Multiple experimental studies have demonstrated that only 1 s of a particular pattern of activation that elicits long term potentiation (LTP) is sufficient to initiate the processes that result in the formation of dendritic spines. In some temporal lobes maintained electrical stimulation can result in synaptic reorganization (Sutula et al, 1989). Because these spine matrices **are** the person's memories that contribute to "personality" alterations not coupled to classical sensory input such subtle entanglement manifestations could alter the patterns that are reconstructed as "personal (episodic) memories" during recall which often involves the right prefrontal region. Persistent deep temporal lobe stimulation could alter the person's behavioural patterns or "personality".

The multiple similarities between the temporal and electromagnetic properties of the human brain during the conditions associated with consciousness and the Schumann Resonances are not likely to be spurious. The prescient ideation and interdisciplinary applications of Nunez (1995) anticipated the significance of this convergence. The neurons within layer II of the entorhinal cortices within the parahippocampal lobe, the primary input to the hippocampus proper, display a rhythmic character of subthreshold oscillations of ~ 8 Hz (Alonso and Klink, 1993). The range is between 5.5 and 14.5 Hz. At the most typical membrane potential of -55 mV, the mean amplitude of the oscillation ranges between 0.5 and 9.7 mV (the mean is 2.6 mV). Even the times to traverse the respective spatial boundaries, in the order of 20 ms, are similar for bulk velocities of lighting and that of the rostral-caudal cerebral electromagnetic fields associated with consciousness. Nickolaenko and Hayakawa (2014) noted that satellite data at altitudes between 400 and 850 km have often measured up to 8 harmonics that would include the equivalents of the theta and gamma regions of cerebral activity.

The physical mechanisms by which the excess correlation occurred between two pairs of individuals whose cerebrums both shared similar toroidal magnetic fields might be reflected by the Lorenz Lemma. The required similarities of magnitudes of the magnetic and electric components of human cerebral cortical activity and the Schumann Resonances as well as their temporal properties exist. The Lemma's solution results in flux density that is within the range of photon emissions measured from the right but not the left temporal lobes in experimental settings

(Dotta et al, 2012). These emissions were associated with imaginative cognitive processes. Simplistically this suggests that the Schumann-human brain resonance, photon emissions, and the neurocognitive patterns associated with imagination display a persistent capacity for excess correlation. As stated by Vaziri et al (2002), "photons will for a long time remain the only means of quantum communication."

If spin-spin interactions are a major component of excess correlation involved with consciousness as suggested by Hu and Wu (2006a) then the earth itself may contribute to the condition for this "entanglement". Hunter et al (2013) described the earth as a polarized electron source that could mediate long-range spin-spin interactions. They found experimental evidence for possible long-range interactions spin polarize electrons and nucleons in laboratories and spin-polarized geoelectrons. These researchers established the boundary conditions for torsion gravity and the long-range spin-spin forces that could be associated with the virtual exchange of "bosons" or "unparticles".

The potential contributions of gravitational energies to the excess correlations we measured in the present experiments have been discussed by Rouleau and Persinger (2015) and Persinger and St-Pierre (2014). The rotational features of the toroidal pattern are superpositioned with those of the cerebral cortices and Schumann Resonances. In addition the diminishment of 1 to 5 nT in the geomagnetic field intensity along the east-west direction (primarily) when the toroids were activated would provide magnetic energies in the order of the mass equivalent of an electron. It may be relevant that the ratio of the earth's rotation velocity at the latitude in which the experiments were conducted divided by g (9.8 $m \cdot s^{-2}$) is within the range of 30 to 40 s. This was the time interval in which the strongest evidence of entanglement was manifested after the onset of the 6.5 Hs pulsing tones.

Appendix A

Instructional Script

[Verbatim to Participant]

Thank you for participating in this study exploring the synchronous brain activity of pairs of individuals separated by a distance. This means that during your participation in the study, at the very same time another individual located thousands of kilometers from you is also being exposed to the same paradigm. Your participation in this experiment will involve you sitting at rest, first with your eyes open to gather your resting baseline brain activity, and then with eyes closed for the remainder of the experiment (approx. 30min) until you will be asked to open your eyes again for your post-experiment baseline measure.

During the experiment you will periodically hear tones being played. These tones indicate it is time to rest and relax while keeping your eyes closed. You will also be cued verbally throughout the experiment to either send or receive white light. When verbally cued to "Send," imagine creating a ball or beam of light and sending it directly to the other participant in the study. It is not important that you know who this person is or what they look like, only that they are also engaged in the same experiment at a location thousands of kilometers from you.

During the "Send" condition you can imagine they are sitting in front of you as you imagine sending light. When verbally cued to "Receive," simply be open to receiving white light from the other participant. You can use visualization/imagination during this condition as well, by imagining the person is sitting across from you and sending you light as you receive it into yourself. Conditions of sending and receiving light will be separated by rest periods. Again, when you hear the tones played, that is your cue to stop sending/receiving and to simply rest. Please listen for the cues and respond appropriately (i.e. During Send/Receive do not stop until you are cued otherwise, either verbally or with the tones).

To review:

- At the start of the experiment, you will be cued to sit with "*Eyes open, gaze facing forward*"
- You will be cued to close your eyes: at this time you will simply relax
- You will hear tones played: this is your cue to relax with eyes closed
- You will hear my voice cuing you to SEND: imagine sending white light until cued
- You will hear my voice cuing you to RECEIVE: imagine receiving white light until cued
- At the end of the final send/receive condition, you will be cued to stop and rest with eyes closed.

Experimental Conditions, with Verbal and Audio Cues

#	Time (min)	Condition	Field	Verbal Cue	
				Local (A)	Non-Local (B)
1	0:00	Baseline EO-pre	NF	Eyes open, gaze facing forward	
2	3:00	Baseline EC-pre	NF	Eyes closed	
3	6:00	Rest	NF	*(burst tone)*	*(solid tone + silence)*
4	7:00	AB	NF	Send	Receive
5	9:00	BA	NF	Receive	Send
6	11:00	Rest	PF	*(solid tone + silence)*	*(burst tone)*
7	12:00	AB	PF	Send	Receive
8	14:00	BA	PF	Receive	Send
9	16:00	Rest	PF	*(burst tone)*	*(solid tone + silence)*
10	17:00	AB	EF	Send	Receive
11	19:00	BA	EF	Receive	Send
12	21:00	Rest	EF	*(solid tone + silence)*	*(burst tone)*
13	22:00	AB	EF	Send	Receive
14	24:00	BA	EF	Receive	Send
15	26:00	Rest	EF	*(burst tone)*	*(solid tone + silence)*
16	27:00	AB	EF	Send	Receive
17	29:00	BA	EF	Receive	Send
18	31:00	Rest	NF	*(solid tone + silence)*	*(burst tone)*
19	32:00	AB	NF	Send	Receive
20	34:00	BA	NF	Receive	Send

21	36:00	Baseline EC-post	NF	Please relax with eyes closed
22	39:00	Baseline EO-post	NF	Eyes open

Pre and post baseline conditions involved 3min each EO: eyes open, and EC: eyes closed. Rest periods (1min): passive send-receive conditions where participants were instructed to rest upon hearing the audio cue / tones. Intentional Send-Receive condition involved AB: the local participant (first to send) sends white light to the non-local participant, and BA: the non-local participant sends white light to the local participant. Field conditions included NF: no field, PF: primer field, and EF: effector field. Audio cues (i.e. tones, noted in italics) were either a burst tone pulsed at 6.5Hz for the passive sender condition during the Rest periods, or a solid (3sec) tone + silence for the passive receiver conditions also during the Rest periods.

Acknowledgements: The authors thank our colleagues abroad, Patrick Palucki in Berlin, Germany, and Dr. José Miguel Gaona in Madrid, Spain, for providing the quiet spaces required for data collection and facilitating participant recruitment. Without their support this study would not have been possible. We thank Professor Don Hill whose imagination, insights, and creativity serve as inspirations for all of us. This manuscript is dedicated to Dr. Linda S. St-Pierre who has bravely defended our academic freedom and has protected an environment that fosters bold ideas.

References

Aczel, A. D. (2002). Entanglement: the greatest mystery in physics. Raincoast: Vancouver.

Alonso, A. and Klink, R. (1993). Differential electroreponsiveness of stellate and pyramidal-like cells of medial entorhinal cortex layer II. Journal of Neurophysiology, 70, 128-143.

Bear, M. F. (1996). A synaptic basis for memory storage in the cerebral cortex. Proceedings of the National Academy of Sciences, 93, 13453-13459.

Bohr, N. (1958). Atomic physics and human knowledge. John Wiley and Sons: N.Y..

Burke, R. C., Gauthier, M. Y., Rouleau, N., & Persinger, M. A. (2013). Experimental demonstration of potential entanglement of brain activity over 300 km for pairs of subjects sharing the same circular rotating, angular accelerating Magnetic fields: verification by s_LORETA, QEEG measurements. Journal of Consciousness Exploration & Research, 4(1).

Buzsaki, G. (2002). Theta oscillations in the hippocampus. Neuron, 33, 325-340.

Caswell, J. M., Dotta, B. T. and Persinger, M. A. (2014). Cerebral biophoton emission as a potential factor in non-local human-machine interaction. NeuroQuantology, 12, 1-11.

Christian, H. J., Blakeslee, R. J., Boccippio, D. J., Boeck, W. L., Buechler, D. E., Driscoll, K. T., Goodman, S. J., Hall, J. M., Koshak, W. J., Mach, D. M. and Stewart, M. F. (2003). Global frequency and distribution of lightning as observed from space by the Optical Transient Detector. Journal of Geophysical Research, 108, doi: 10.1029/2002JD002347.

Collins, M. W. G. and Persinger, M. A. (2014). Enhanced power within the default mode network in normal subjects with elevated scores on an egocentric scale. The Open Neuroimaging Journal, 8, 5-10.

Dotta, B. T., Mulligan, B. P., Hunter, M. D. and Persinger, M. A. (2009). Evidence of macroscopic quantum entanglement during double quantitative electroencephalographic (QEEG) measurements of friends vs strangers. NeuroQuantology, 7, 548-551.

Dotta, B. T., Buckner, C. A., Lafrenie, R. M. and Persinger, M. A. (2011). Photon emissions from human brain and cell culture exposed to distally rotating magnetic fields shared by separate light-stimulated brains and cells. Brain Research, 388, 77-88.

Dotta, B. T. and Persinger, M. A. (2011). Temporal patterns of photon emissions can be stored and retrieved several days later from the "same space": experimental and quantitative evidence. NeuroQuantology, 9, 605-613.

Dotta, B. T. and Persinger, M. A. (2012). "Doubling of local photon emissions when two simultaneous, spatially separated chemilumiescent reactions share the same magnetic field configurations. Journal of Biophysical Chemistry, 3, 72-80.

Dotta, B. T., Saroka, K. S. and Persinger, M. A. (2012). Increased photon emission from the head while imaging light in the dark is correlated with changes in electroencephalographic power: Support for Bokkon's biophoton hypothesis. Neuroscience Letters, 513, 151-154.

Dotta, B. T., Koren, S. A. and Persinger, M. A. (2013a) Demonstration of entanglement of "pure" photon emissions at two locations that share specific configurations of magnetic fields: implications for translocation of consciousness. Journal of Consciousness Exploration & Research, 4, 25-34.

Dotta, B. T., Murugan, N. J., Karbowski, L. M. and Persinger, M. A. (2013b) Excessive correlated shifts in pH within distal solutions sharing phase-uncoupled angular accelerating magnetic fields: macro-entanglement and information transfer. International Journal of Physical Sciences, 8, 1783-1787.

Duane, T. D. & Behrendt, T. (1965). Extrasensory electrocephalographic induction between identical twins. Science, 150, 367.

Ecker, A. S., Berens, P., Keliris, G. A., Bethge, M., Logothetis, N. K. & Tolias, A. S. (2010) Decorrelated neuronal firing in cortical microcircuits. Science, 327, 584-486.

Eddington, A. (1981). Nature of the physical world. U. Mich. Press: Ann Arbor.

Edelman, G. M. (1989). The Remembered Present: a biological theory of consciousness. Basic Books: N.Y.

Fickler, R., Lapkiewicz, R., Plick, W. N., Krenn, M., Schaeff, C., Ramelow, S. and Zeilinger, A. (2012) Quantum entanglement of high angular momenta. Science, 338, 640-643.

Gloor, P. (1997). The temporal lobe and limbic system. Oxford University Press: N.Y.

Gurney, E., Myers, F. W. H. and Podmore, F. (1886). Phantasms of the living. Truebner: London.

Harrington, A. (1995). Unfinished business: models of laterality in the nineteenth century. In Davidson, R. J and Hugdahl, K. Brain asymmetry. MIT Press: Cambridge (Mass), pp. 3-28.

Henke, K., Buck, A., Weber, B. and Wieser, H. G. (1997). Human hippocampus establishes associations in memory. Hippocampus, 7, 249-256.

Hotta, M., Matsumoto, J. and Yusa, G. (2014). Quantum energy teleportation without limit of distance. Physical Review A, 89, 012311.

Houwelling, A. R. and Brecht, M. (2007) Behavioural report of a single neuron stimulation in somatosensory cortex. Nature, 451, doi: 10.1038/nature06447.

Hu, H. and Wu, M. (2006a). The essence and implications of quantum entanglement and the story of spin-mediated consciousness theory. NeuroQuantology, 1, 5-16.

Hu, H. and Wu, M. (2006b). Thinking outside the box II: The origin, implications and applications of gravity and its role in consciousness. NeuroQuantology, 4, 291-306.

Hu, H. and Wu, M. (2013). On the nature of quantum gravity and graviton. Journal of Consciousness Exploration & Research, 4, 1066-1089.

Hunter, L., Gordon, J., Peck, S., Ang, D. and Lin, J-F. (2013) Using the earth as a polarized electron source to search for long-range spin-spin interactions. Science, 339, 928-932.

Jin, X-M., Ren, J-G., Yang, B., Yi, Z-H., Zhou, F., et al. (2010). Experimental free-space quantum teleportation. Nature photonics, DOI: 10.1038, Nphoton.2010.87.

John, E. R. (1967). Mechanisms of Memory. Academic Press: N.Y.

Julsgaard, B., Kozheikin, A. and Polzik, E. S. (2001). Experimental long-lived entanglement of two macroscopic objects. Nature, 413, 400-403.

Kahana, M. J., Sekuler, R., Caplan, J. B., Kirschen, M. and Madsen, J. R. (1999). Human theta oscillations exhibit task dependence during virtual maze navigation. Nature, 399, 781-784.

Karbowski, L. M., Murugan, N. J. and Persinger, M. A. (2015). Experimentally-induced inhibition of growth in melanoma cell cultures separated by 2 kilometers when both share excess correlation magnetic fields: macroscopic evidence of free-space quantum teleportation? Journal of Signal and Information Processing, 6, 39-48.

Kawano, K., Yamamoto, M., Kokubo, H., Tanaka, M., Zhang, T., Parkhomtchouk, D. V., Kokado, T., Nakmura, H. and Soma, T. (2000). EEG alpha waves of a receiver in a remote action experiment. Journal of Interactional Society of Life Information Science, 18, 395-397.

Koenig, T., Prichep, L., Lehmann, D., Sosa, P. V., Braeker, E., Kleinlogel, H., Isenhart, R and John, E. R. (2001). Millisecond by millisecond, year by year: normative EEG microstates and developmental stages. NeuroImage, 16, 41-48.

Koren, S. A., Dotta. B. T. and Persinger, M. A. (2014). Experimental photon doubling as a possible local inference of the Hubble Parameter. The Open Astronomy Journal, 7, 1-6.

Kurup, R. K. and Kurup, P. A. (2003). Hypothalamic digoxin: hemispheric chemical dominance and spirituality. International Journal of Neuroscience, 113, 383-393.

Lehmann, D., Strik, W. K., Heneggler, B., Koeinig, T. and Koukku, M. (1998). Brain electric microstates and momentary conscious mind states as building blocks for spontaneous thinking. International Journal of of Psychophysiology, 29, 1-11.

Li, C. T., Poo, M-M. and Dan, Y. (2009). Burst spiking of a single cortical neuron modifies global brain state. Science, 324: 643-646.

Llinas, R. and Ribary, U. (1993). Coherent 40 Hz oscillation characterizes dream state in humans. Proceedings for the National Academy of Sciences, 90: 2078-2081.

Mach, E. and McCormack, T. J. (1988). The Science of Mechanics: A Critical and Historical Account of Its Development. Open Court Publishing Co. Chicago.

Makarec, K. and Persinger, M. A. (1990). Electroencephalographic validity of temporal lobe signs inventory in a normal population. Journal of Research in Personality, 24, 323-327.

Megidish, E., Halevy, A., Shacham, T., Dvir, T., Dovrat, L. and Eisenberg, H. S. (2013). Entanglement between photons that never existed. Physical Review Letters, 100, 210403 (2013).

Nickolaenko, A. and Hayakawa, M. (2014). Schumann Resonance for Tyros. Springer, Tokyo.

Nunez, P. L. (1995). Towards a physics of the neocortex. In Nunez, P. L. (ed). Neocortical dynamics and human EEG rhythms. Oxford: N.Y., pp. 68-130.

Pakkenberger, B. and Gundersen, H. J. G. (1997). Neocortical neuron numbers in humans: effects sex and age. The Journal of Comparative Neurology, 384, 312-320.

Pitkanen, M. J. (2012). Quantum mind in TGD universe. Journal of Nonlocality, 1.

Pitkanen, M. J. (2013). Persinger Group's recent experiments, spin network and TGD. Journal of Consciousness Exploration & Research, 4 (2).

Pitkanen, M. J. (2014). What is EEG made of? Journal of Consciousness Exploration & Research, 5(4).

Persinger, M. A. (2010). 10^{-20} Joules as a neuromolecular quantum in medicinal chemistry: an alternative approach to myriad molecular pathways. Current Medicinal Chemistry, 17, 3094-3098.

Persinger, M. A. (2012). Brain electromagnetic activity and lightning: potentially congruent scale-invariant quantitative properties. Frontiers in Integrative Neuroscience, 6, article 19.

Persinger, M. A. (2013a) Experimental evidence that Hubble's Parameter could be reflected in local physical and chemical reactions: support for Mach's Principle of Imminence of the Universe. International Letters of Chemistry, Physics, and Astronomy, 11, 86-92.

Persinger, M. A. (2013b). Billions of human brains immersed within a shared geomagnetic field: quantitative solutions and implications for future adaptations. The Open Biology Journal, 6, 8-13.

Persinger, M. A. (2015). Thixtotropic phenomena in water: quantitative indicators of Casimir-magnetic field transformations from vacuum oscillations (virtual particles). Entropy, 17, 6200-6212.

Persinger, M. A., Koren, S. A. and Tsang, E. W. (2003). Enhanced power within a specific band of theta activity in one person while another receives circumcerebral pulsed magnetic fields: a mechanism of influence at a distance? Perceptual and Motor Skills, 97, 877-894.

Persinger, M. A. and Koren, S. A. (2005). A response to Granqvist et al "Sensed presence and mystical experiences are predicted by suggestibility not by application of transcranial weak magnetic fields". Neuroscience Letters, 308, 346-347.

Persinger, M. A. and Koren, S. A. (2007). A theory of neurophysics and quantum neuroscience: implications for brain function and the limits of consciousness. International Journal of Neuroscience, 117, 157-175.

Persinger, M. A., Koren, S. A. and Lafreniere, G. F. (2008). A neuroquantologic approach to how human thought might affect the universe. NeuroQuantology, 6, 262-271.

Persinger, M. A. and Koren, S. A. (2013). Dimensional analyses of geometric products and the boundary conditions of the universe: implications for a quantitative value for the latency to display entanglement. The Open Astronomy Journal, 6, 10-13.

Persinger, M. A. and Koren, S. A. (2014). Evidence of a causal relationship between Mach's Principle and the quantitative latency for universal entanglement. International Letters of Chemistry, Physics and Astronomy, 15, 80-86.

Persinger, M. A. and St-Pierre, L. S. (2014). Is there a geomagnetic component involved with the determination of G? International Journal of Geosciences, 5, 450-452.

Persinger, M. A. and Saroka, K. S. (2015). Human quantitative electroencephalographic and Schumann Resonance exhibit real-time coherence of spectral power densities: implications for interactive information processing. Journal of Signal and Information Processing, 6, 153-164.

Persinger, M. A., Saroka, K. S., Lavallee, C. F., Booth, J. M., Hunter, M. D., Mulligan, B. P., Koren, S. A., Wu, H-P and Gang, N. (2010). Correlated cerebral events between physically and sensory isolated pairs of subjects exposed to yoked circumcerebral magnetic fields. Neuroscience Letters, 486, 231-234.

Persinger, M. A., Tsang, E. W., Booth, J. N. and Koren, S. A. (2008). Enhanced power within predicted narrow band theta activity during stimulation of another by circumcerebral weak magnetic fields after weekly spatial proximity: evidence for macroscopic quantum entanglement? NeuroQuantology, 6, 7-21.

Rouleau, N. and Dotta, B. T. (2014). Electromagnetic fields as structure-function zeitgebers in biological systems: environmental orchestration of morphogenesis and consciousness. Frontiers in Integrative Neurosciences, Vol. 8.

Rouleau, N., Carniello, T. N., & Persinger, M. A. (2014). Non-local pH shifts and shared changing angular velocity magnetic fields: Discrete energies and the importance of point durations. Journal of Biophysical Chemistry,5, 44-53.

Rouleau, N., & Persinger, M. (2015). Local electromagnetic fields exhibit temporally non-linear, east-west oriented 1-5 nT diminishments within a toroid: empirical measurement and quantitative solutions indicating a potential mechanism for excess correlation. Journal of Electromagnetic Analysis and Applications, 7, 19-30.

St-Pierre, L. S. and Persinger, M. A. (2006). Experimental facilitation of the sensed presence is predicted by specific patterns of magnetic fields not by suggestibility: re-analyses of 19 experiments. International Journal of Neuroscience, 116, 1-18.

Saroka, K. S. and Persinger, M. A. (2014). Quantitative evidence for direct effects between earth-ionosphere Schumann Resonances and human cerebral cortical activity. International Letters of Chemistry, Physics and Astronomy, 20, 166-194.

Scott, M. A. and Persinger, M. A. (2013). Cerebral activity and source profiles accompanying the process of non-locality. NeuroQuantology, 11, 378-390.

Standish, L. A., Johnson, L. C., Richards, T. & Kozak, L. (2003). Evidence of correlated functional MRI signals between distant human brains. Alternative Therapy and Health Medicine, 9, 122-128.

Standish, L. A., Kozak, L., Johnson, L. C. & Richards, T. (2004) Electroencephalographic evidence of correlated event-related signals between brains of spatially and sensory isolated human subjects. The Journal of Alternative and Complementary Medicine, 10, 307-314.

Sutula, T., Cascino, G., Cavazos, J., Parada, I. and Ramirez, L. (1989). Mossy fiber synaptic reorganization in the epileptic human temporal lobe. Annals of Neurology, 26, 321-330.

Tu, L-C.,, Luo, J. and Gilles, G. T. (2005). The mass of the photon. Reports on Progress in Physics, 8, 77-130.

Vaziri, A., Weihs, G., and Zeilinger, A. (2002). Experimental two-photon, three dimensional entanglement for quantum communication. Physical Review Letters, 89, 230401.

Whitman, J. C., Ward, L. M. and Woodward, T. S. (2013). Patterns of cortical oscillations organize neural activity into whole brain functional networks evident in fMRI BOLD signal. Frontiers in Human Neuroscience, Volume 7, Article 80.

Article

Potential Experimental Demonstration of the Entanglement Velocity of 10^{23} m·s^{-1} during Trans-Atlantic Excess Correlation of Paired Brain Activity

Nicolas Rouleau, Stanley A. Koren & Michael A. Persinger*

Neuroscience Research Group, Human Studies and Biomolecular Sciences Programs,
Laurentian University, Sudbury, Ontario, Canada P3E 2C6

ABSTRACT

Two separate approaches have suggested that the diffusivity parameter or diffusion velocity of ~10^{23} m·s^{-1} may be the quantitative value for the latency for displays of excess correlation or the consequences of entanglement. We have shown that pairs of individuals separated by 6,000 km but sharing toroidal magnetic fields with changing angular velocities displayed clear excess correlations in specific theta and gamma frequency power values over the right caudal hemispheres. The effect occurred only during the component of the exposure that has revealed excess correlations in photon and pH reactions separated by non-local distances. The predicted latency for the entanglement effects over distances of 6,000 km would be ~10^{-17} s while the time required for 1 orbit of an electron is ~10^{-16} s. Specific values indicated that between 10 and 30 s would be required before the entanglement would emerge within the domain of electronic matter. Quantitative measurements of the indicator of excess correlation in brain activity during the optimal interval of magnetic field configuration indicated the emergence occurred between 20 and 30 s after the effector field (but not the primer field) had been activated around the cerebrums of both subjects. The effect was clear for all 5 pairs of subjects. The results suggest but do not prove that the latency for entanglement may display a real time value coupled to the velocity of a diffusivity term derived from the relationship between four-dimensional geometry and the weighted products of Gravity and the mass, width and duration of the universe.

Keywords: entanglement velocity, 10^{23} m·s^{-1}, trans-Atlantic brain entanglement, circular magnetic fields; changing angular velocity; toroids.

1. Introduction

The concept of entanglement presumes that excess correlation between two events that have met specific conditions subsequent to a spatial-temporal contiguity can be displayed any time subsequent to this pairing at any distance. One perspective indicates that for this to occur there must be a pervasive process that permeates the universe such that distance between the two events or the time that has elapsed since their pairing does not determine the occurrence of the excess correlation (Vaziri, et al, 2002; Hotta, et al, 2014). The candidate for this permeating

*Corresponding author: Dr. M. A. Persinger, mpersinger@laurentian.ca

process that becomes apparent as a phenomenon when the entire set is considered, that is the entire universe and its total life time, has been related to the gravitational field potential connected through its quantized components such as the graviton. Hu and Wu's (2013, 2003) theory suggests that the entanglement became possible because the primordial events that lead to energy and matter were initially related by spin during pre-space-time. Their theory is a more quantitative extension of Mach's concept that moments of inertia relate all space to every single space.

The presumption has been that the latency for a response in particle A that has been entangled with particle B is instantaneous. This may be correct. However there may also be a component of the entanglement latency that is so small that it becomes negligible along distances that are much, much less than the length of the universe. While relating the fundamental geometries of a circle, because an action within a circle is infinite but bounded and accelerating, Persinger and Koren (2013,2014,2015) obtained the product of $2\pi r$, $4\pi r^2$, $4/3\pi r^3$ and $2\pi rf$ (time) which was $21.3\pi^4 r^7 f$. The dimensional solution was $m^7 s^{-1}$. The resulting aggregate of terms was solved by dimensional analyses for an equivalent form that was composed of the Gravitational constant (G), the mass of the universe (m), its duration (t), and its estimated width (d). The units for this solution was $[m^6 \cdot kg^{-2} \cdot s^{-4}] \cdot kg^2 \cdot m \cdot s^3$. The balanced solution was $G^2 \cdot m^2 \cdot d \cdot t^3$.

The solution for this diffusivity term ($m^7 \cdot s^{-1}$) when converted to velocity was about $2.8 \cdot 10^{23}$ m·s^{-1}. Persinger and Koren (2014) suggest that this diffusivity value might relate to the latency for entanglement effects to be manifested within the universe. For example across the extent of the entire universe about 7 to 8 min would be required. Between the earth and the sun about 10^{-12} s (the duration of the hydronium ion) would be required (DeCoursey, 2003). For the typical orbital heights for satellites the duration would be 10^{-16} s which is congruent with the values measured for drifts and drags in inertial time frames. Although the contemporary explanation for the inertial drag (Persinger and Koren, 2015) is based upon relativity approaches, this similarity would be also consistent with Mach's concept that the universe is connected by intrinsically shared moments of inertia.

A second approach (Persinger and Koren, 2014), converted the total energy in the universe based upon current estimates of mass to be about $2.2 \cdot 10^{69}$ J into equivalent magnetic field and electric field gradients ($V \cdot m^{-1}$) through the two relationships. The first is:

$$B=\sqrt{(E \cdot 2\mu \cdot m^{-3})} \quad (1)$$

where E is the energy, B is the magnetic field strength, μ it the magnetic permeability of a vacuum ($4\pi \cdot 10^{-7}$ N·A^{-2}) and m is the volume based upon a sphere with a diameter of $18 \cdot 10^{26}$ m for the final epoch. The solution is ~$1.4 \cdot 10^{-9}$ T. The second is:

$$V=\sqrt{(2 \cdot E \cdot \varepsilon^{-1})} \quad (2)$$

where V is the voltage and ε is the electric permittivity of a vacuum. The resulting value of $2.2 \cdot 10^{40}$ V when distributed over the current radius of $1.26 \cdot 10^{26}$ m, results in a voltage linear density of $1.8 \cdot 10^{14}$ V·m^{-1}. The ratio of this value to the magnetic field strength is ~$1.4 \cdot 10^{23}$ m·s^{-1}. This is the same order of magnitude as the value obtained from universal parameters.

Recently we completed an experiment where pairs of individuals each wearing a toroid through which specific changing angular velocity magnetic fields were delivered displayed excess correlation in theta and gamma patterns over the right caudal temporal regions. The two individuals in each of the pairs were separated by at least 6000 km. The onsets of the two fields were synchronized to the nearest 1 s. Measurement of the entanglement velocity would be very fast, that is in the order of 10^{-17} s if we assumed this distance as linear or slightly curvilinear from the earth's surface. In fact the latency would be less than that required to complete one orbit ($1.5 \cdot 10^{-16}$ s) in a Bohr atom.

However we reasoned, simplistically, that we could infer the validity of the entanglement velocity by assuming that between the time of the activation of the effective weak (1 to 5 nT) magnetic field and its manifestation within the entanglement phenomena measured by the shared power of quantitative EEG between the two people separated by at least 6,000 km would reflect the time required to exact superposition within the time frame in which local matter is defined. In other words, $1.5 \cdot 10^{-16}$ s divided by 10^{-17} s would suggest that between 10 and 20 s would be require before the entanglement effect was sufficiently manifested at the level of matter through electron orbits that define the human brain. At longer distances where the entanglement latency is equal to or greater than the time of a single electron orbit this lag to be manifested within matter would not occur. Here we present evidence to support this *a priori* prediction of this latency.

2. Method

The paradigm has been published in detail elsewhere (Scott et al, 2015). In summary five pairs of people served as subjects. The members of each pair were separated by ~6,000 km. Each pair of participants wore toroids around their heads. During the 42 min of the experiment weak magnetic fields (30 nT) were generated through the toroids with accelerating or decelerating velocities. The activation of the fields produced a 1 to 5 nT diminishment of the E-W component of the earth's magnetic field (Rouleau and Persinger, 2015).

During the exposures each person wore a standard 19 channel sensor QEEG cap that was connected to a Mitsar EEG-201. Measurements were sampled at 250 Hz. During the exposure eyes opened and eyes closed conditions data were collected when tones were presented or instructions were given to imagine "white light". During the experiment there were two types of field conditions. The first was the primer field. The second was the effector field. The primer pattern consisted of 7 all or none, 3 ms point potentials that were continuously looped, separated by incrementally longer inter-stimulus intervals that began with 20 ms and increased by 2 ms every pulse. This re-cycled back to 20 ms after the 7th pulse sequence. The 3 ms pulse was based upon the derivations by Persinger and Koren (2007) and empirical support by Koren et al (2014) that the time required for a proton to expand one Planck's Length given the contemporary Hubble Parameters would be about 3 ms.

The effector pattern involved the same all or none potentials. However the interstimulus interval between the points began with 20 ms and decreased by 2 ms for each pulse. The signals were generated from a laptop through Arduino circuits to the solenoids. The primary pattern

began 11 minutes after the QEEG data began to be recorded and was presented for 6 min. The effector pattern began and was presented for 840 s (14 min). This second effector pattern is when the excess correlation phenomena have been shown for shifts in pH and photon emissions. Reversal of the order of the fields does not produce evidence of excess correlations between the cerebral activities of the separated subjects. This specificity minimizes the likelihood that any coherent effects between subjects were because they are simply sharing the same rotating magnetic fields.

To test the potential accuracy of our prediction regarding the latency of response of the brain to the onset of entanglement as manifested through the effector field, we selected the power within the gamma band over the right caudal temporal lobe (T6). This region has shown the most consistent evidence for reliable inter-brain coherence that is consistent with entanglement. In the trans-Atlantic excess correlation reported by Scott et al (2015) this region was also the one in which multiple measures of coherence and intercalation over the 6,000 km was most evident. The T6 region often reflects right parahippocampal activity which was shown to be activated when Sean Harribance displayed evident of excess correlation with the brains of other people (Persinger and Saroka, 2012). This same region was most affected for experiments designed to examine potential gravitational-electromagnetic interactions (Persinger and Saroka, 2014).

3. Results

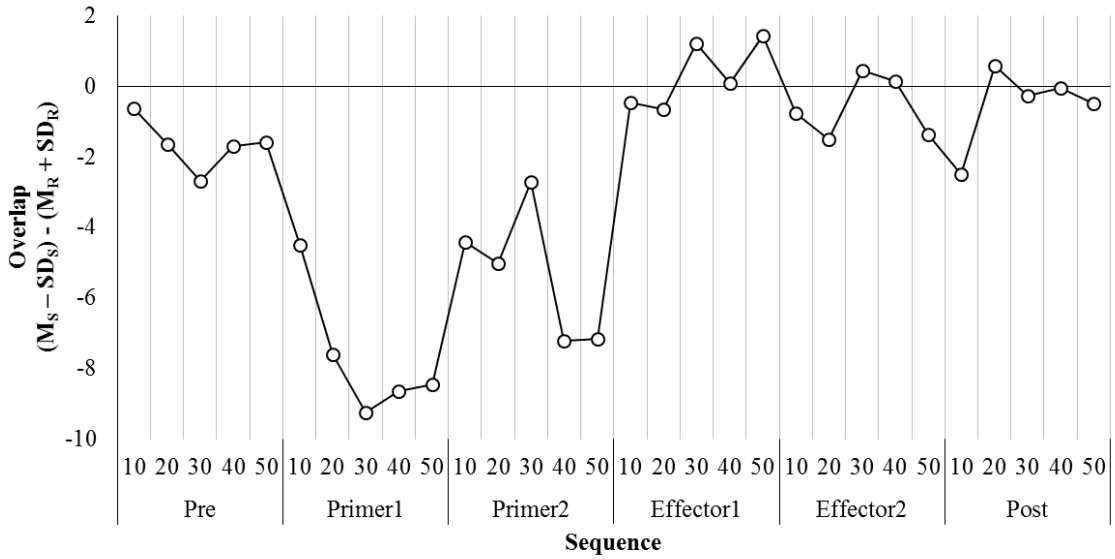

Figure 1. Overlap of error bars as displayed in the graph showing T6 gamma differences between senders and receivers (previous analysis for tone periods). Note the separation between the overlap occurs only during the effector fields (values above 0).

The results of the overlap between the power within the gamma region over T6 (the right temporal region that most reflects right parahippocampal activity) of the five pairs of individuals each separated by more than 6,000 km is shown in Figure 1. The negative values indicated that the power values for the gamma frequencies overlapped between the two individuals in the five

pairs. The values above 0 indicate no overlap. Only during the effector component of the field but not during the primer fields was there a significant separation of power. It first emerged between 20 and 30 s after the onset of the effector field. This is consistent with prediction.

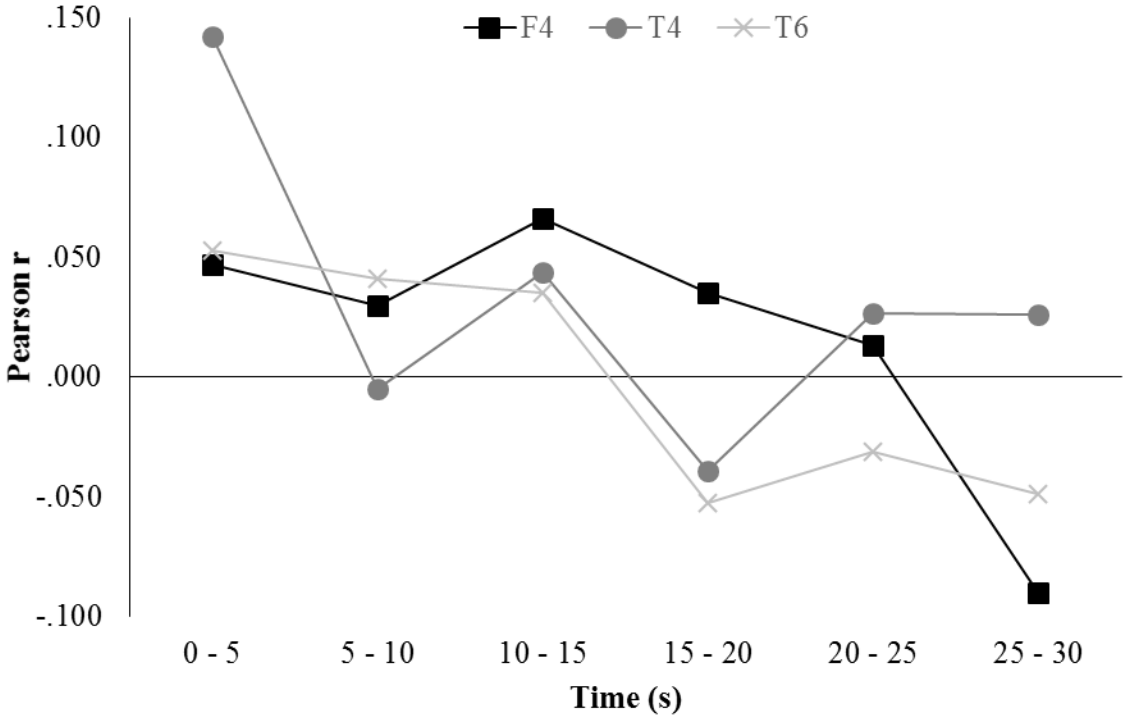

Figure 2. Inter-brain correlation of gamma power over the right frontal (F4; squares), right temporal anterior (T4; circles) and right temporal caudal (T6; crosses) over the 5 s blocks after the initiation of the entanglement (effector) field.

In order to discern the shift in polarity, which has been considered an indicator of the demonstration of entanglement, the correlations between the gamma power values over T6 for the pairs of brains were calculated for each of the 5 s increments after the effector field had been initiated. As shown in Figure 2 for F4, T4 and T6 (all right hemisphere) the significant reversal of correlations occurs between 15 to 20 s to 25 to 30 s after the initiation of the effector fields. Because of the sample sizes the differences between a correlation of r=0.05 and -0.05 are statistically significant.

4. Discussion

Several hundreds of years ago the velocity of light was considered to be instantaneous primarily because its quantity was beyond that discernable by contemporary instrumentation. A limiting value to the velocity of light was first realized when large spaces, those involved with the distances to Jupiter and its moons, were measured. Even as recent as the late 19th century some scientists assumed that the velocity of the action potential along the axon barrel, and hence "thought", was "instantaneous" or even the velocity of light. Direct measurement, improved

instrumentation and reasoning altered this perspective. A similar manifestation may be required for the latency for the manifestation of the entanglement.

If there is a specific latency for entangled phenomena to occur, or, once it has occurred to be manifested, then the mechanisms and processes that mediate these phenomena might require alternative interpretations. We (Persinger and Koren, 2013; 2014; 2015) have found that the velocity of about 10^{23} m·s^{-1} emerges from two separate approaches when universal values are involved. One was derived from finding the dimensional equivalence between the four dimensional geometry of a closed shape (the circle) and four universal parameters one of which was the Gravitational Constant. The second approach was the solution when the average potential gradient in the universe in V·m^{-1} was divided by the equivalent magnetic field strength during the final epoch when the total energy of the universe was converted into electric and magnetic forms.

If Mach's principle is correct then there should be local manifestations of this velocity. There is evidence for this possibility. The net change in voltage associated with an action potential the axon of a neuron is about $1.2 \cdot 10^{-1}$ V. When divided by the length of the Compton wavelength ($2.42 \cdot 10^{-12}$ m) the equivalent is $0.5 \cdot 10^{11}$ V·m^{-1}. When this value is divided by the typical functional magnetic field intensity from the cerebral cortices during cognition and the interface between axons which is about 0.5 pT (10^{-12} T) the velocity term is 10^{23} m·s^{-1}. This order of magnitude of magnetic field fluctuations is also displayed by the Schumann Resonance. It displays a fundamental resonance between 7 and 8 Hz with harmonics emerging every 6 Hz at approximately 13-14 Hz, 19-20 Hz, and 25-26 Hz until discernment by instrumentation becomes difficult around the 7th harmonic (Nickolaenko and Hayakawa, 2014).

Living systems are immersed within the Schumann Resonances. Resonance spectra indicate that the amplitude of the second harmonic around 14 Hz between 20 and 22 UT is about 3 pT·$\sqrt{\text{Hz}}^{-1}$ or about 10^{-11} T. If the typical vertical electric field values for the Schumann Resonance of ~10^{-3} V·m^{-1} were spread across the Compton wavelength of the proton ($1.32 \cdot 10^{-15}$ m), the velocity would be within the range of 10^{23} m·s^{-1}. This suggests that under certain conditions the entire Schumann spherical wave guide around the earth could display the capacity for the mediation of excess correlation or entanglement. More than 20 years ago Minakov et al (1993) showed mathematically that if gravitational fields were to interact with the electromagnetic phenomena, the most powerful amplification region would be the second global (f =14 Hz) harmonic of the Schumann Resonance.

The observation that substantial time, about 20 s, was required to display the evidence of entanglement may appear contradictory. If the diffusivity is in the order of 10^{23} m·s^{-1} then ~20 s would be sufficient for propagation over 10^{24} to 10^{25} m. Our assumption that ~20 s would be required for the very local property of this diffusivity to complete one Bohr orbit of an electron would reflect the latency to effect matter within a local space rather than the latency to traverse space. At distances where the diffusivity time is >10^{-16} s the manifestation within matter would be functionally instantaneous with the time required to complete one Bohr orbit. Perhaps this is one of the reasons why non-local and other entanglement effects are difficult to demonstrate when curvilinear distances are less than that of the circumference of the earth which is ~$4 \cdot 10^{7}$ m. At that distance the entanglement velocity would be in the order of 10^{-16} s.

The manifestation of this subtle effect within the right temporal region and presumably the right parahippocampal structure of the human brain may have quantum application. Burke and Persinger (2013) calculated convergent solutions that suggest the hippocampus could serve as a "singularity" for access to cosmological consciousness. The human hippocampus is effectively two, interlocking C-shaped structures that are geometrically congruous with a small spherical condenser wrapped and partially interdigitated by a larger spherical condenser. The shape is similar to a toroid with a gap which could allow discrete leakage of magnetic flux. This arrangement in non-brain circuits is strongly affected by polarization or phase vectors that can be matched within an order of magnitude of the geomagnetic scalar potential.

If it occurs in a similar manner within the human hippocampus then the structure could be an interface between shifts in phase of electromagnetic fields and the non-potential toroidal field of the geomagnetic matrix. This non-potential field corresponds to the types of vertical current densities coupled to the earth-ionosphere cavity. According to Schmidt quasi-normalization the magnitude of the dispersions for the internal field coefficients are between 1 and 6 nT (Winch et al, 2005). This is the diminishment produced by the toroids during the excess correlation between subjects in this study. Persinger and St-Pierre (2014) showed quantitatively that the variation in G was inversely correlated with the geomagnetic fluctuations in the order of 5 nT and that the energy available within a cerebral volume would be within the range of 10^{-14} J or the mass equivalent of an electron. Availability of universal current sources could be sufficient to affect the substrates that determine coherent brain activity once entanglement is manifested within the time frame that defines the electron orbit.

References

Burke, R. C. and Persinger, M. A. (2013). Convergent quantitative solutions indicating the human hippocampus as a singularity and access to cosmological consciousness. NeuroQuantology, 11, 1-7.

DeCoursey, T. E. (2003). Voltage-gated proton channels and other proton transfer pathways. Physiological Review, 83, 475-579.

Hotta, M., Matsumoto, J. and Yusa, G. (2014) Quantum energy teleportation without a limit of distance. Physical Review, 89, 012311.

Hu, H. and Wu, M. (2003). Spin as primordial self-referential process driving quantum mechanics, spacetime dynamics and consciousness. NeuroQuantology, 2, 41-49.

Hu, H. and Wu, M. (2013). On the natures of quantum gravity and graviton. Journal of Consciousness Exploration & Research, 4, 1066-1089.

Koren, S. A., Dotta, B. T. and Persinger, M. A. (2014). Experimental photon doubling as a possible local inference of the Hubble Parameter. The Open Astronomy Journal, 7, 1-6.

Megidish, E., Halevy, A., Schacham, T., Dvir, T., Dovarat, L. and Eisenberg, H. S. (2013) Entanglement between photons that never co-existed. Physical Review Letters, 110, 210403.

Minakov, A. A., Nikolaenko, A. P. and Rabinovich, L. M. (1992). Gravitational-to-electromagnetic wave conversion in electrostatic field of earth-ionosphere resonator. Radiofizika, 35, 488-497.

Nickolaenko, A. and Hayakawa, M. (2014) Schumann Resonance for Tyros: essential of global geomagnetic resonance in the earth-ionosphere cavity. Springer: Tokyo.

Persinger, M. A. and Koren, S. A. (2007). A theory of neurophysics and quantum neuroscience: implications for brain function and the limits of consciousness. International Journal of Neuroscience, 17, 157-175.

Persinger, M. A. and Koren, S. A. (2013). Dimensional analyses of geometric products and the boundary conditions of the universe: implications for a quantitative value for the latency to entanglement. The Open Astronomy Journal, 6, 10-13.

Persinger, M. A. and Koren, S. A. (2014). Evidence for a causal relationship between Mach's Principle and the quantitative latency for universal entanglement. International Letters of Chemistry, Physics and Astronomy, 15, 80-86.

Persinger, M. A. and Koren, S. A. (2015). Potential role of the entanglement velocity 10^{23} m·s^{-1} to accommodate recent measurements of large scale structures in the universe. International Letters of Chemistry, Physics and Astronomy, 23, 106-112.

Persinger, M. A. and St-Pierre, L. S. (2014). Is there a geomagnetic component involved with the determination of G? International Journal of Geosciences, 5, 450-452.

Persinger, M. A. and Saroka, K. S. (2012) Protracted parahippocampal activity associated with Sean Harribance. International Journal of Yoga, 5, 140-145.

Persinger, M. A. and Saroka, K. S. (2014). Quantitative support for the convergence of intrinsic energies from applied magnetic fields and "noise" fluctuations of Newton's Gravitational value within the human brain. International Letters of Chemistry, Physics and Astronomy, 19, 181-190.

Rouleau, N. and Persinger, M. A. (2015). Local electromagnetic fields exhibit temporally, non-linear, east-west oriented 1 to 5 nT diminishments within a toroid: empirical measurements and quantitative solutions indicating a potential mechanism for excess correlation. Journal of Electromagnetic Analysis and Applications, 7, 19-30.

Scott, M. A., Rouleau, N., Lehman, B., Tessaro, L., Juden-Kelly, L., Saroka, K. S. and Persinger, M. A. (2015) Experimental production of excess correlation across the Atlantic Ocean of right hemispheric theta-gamma power between five pairs of subjects sharing circumcerebral magnetic fields. Journal of Consciousness Exploration & Research, 6(9), 658-684.

Vaziri, A., Wiehs, G. and Zeilinger, A. (2002) Experimental two-photon, three dimensional entanglement for quantum communication. Physical Review Letters, 89, 240401-1.

Winch, D. E., Ivers, D. J., Turner, P. R. and Sterning, R. J. (2005). Geomagnetism and Schmidt quasi-normalization. Geophysical Journal International, 160, 487-504.

Article

Spectral Power Densities of the Fundamental Schumann Resonance Are Enhanced in Microtubule Preparations Exposed to Temporally Patterned Weak Magnetic Fields: Implications for Entanglement

Blake T. Dotta[1], David A. E. Vares[1,3] & Michael A. Persinger[*1,2,3]

Quantum Biology Laboratory
Behaviourial Neuroscience[1], Biomolecular Sciences[2], & Human Studies[3] Programs
Laurentian University, Sudbury, Ontario, Canada P3E 2C6

ABSTRACT

Preparations of microtubules (MT) from mouse melanoma cells emitted predictable photon counts when sampled 50 times per s (every 20 ms) that depended upon the numbers of these preparations. Counterbalanced serial 4 min exposures of the same MT to different temporally patterned magnetic fields with intensities between 3 and 10 μT did not alter the absolute photon emissions but shifted their spectral power densities (SPD). Compared to baseline (no field) 4 min periods there were conspicuous increases of power within the 7.7 to 7.8 Hz band during the 4 min exposures to patterned magnetic fields that facilitate long-term potentiation in neurons but not during exposures to a pattern associated with analgesia. *A priori* predictions of the shift in frequency (Δf) based upon the median mass of tubulin dimers, known numbers of unit charges per dimer, and the strength of the applied fields predicted a range between 0.11 and 0.14 Hz. SPD demonstrated two peaks at 7.74 Hz and 7.87 Hz or a Δf=0.13 Hz. The results indicate only 4 min exposures of microtubule preparations to specifically physiologically patterned magnetic fields associated with memory consolidation enhance the power of the numbers of photon emissions in a frequency band that is very similar to the fundamental Schumann Resonance.

Keywords: Tubulin, microtubules, photon emissions, weak magnetic field effects; spectral power density shifts.

1. Introduction

Consciousness in the universe and how it could be manifested in the brain has been the major thrust of Hameroff and Penrose's "Orch OR" theory [1]. They assume that neuronal microtubules are directly necessary for cognition and consciousness. Microtubules are important components of the cytoskeleton [2] that affect the location of organelles within the cell as well as intracellular transport [3]. If microtubules are critical for the emergence of consciousness and the implicit principle of superposition or potential for "excess correlation" between other microtubules independent of distance, they should exhibit photon emissions that respond to natural electromagnetic patterns. These patterns should reflect the frequency context in which living tissue exists upon this planet. We predicted that the spectral densities of photons emitted

*Corresponding author: Dr. M. A. Persinger, mpersinger@laurentian.ca

from preparations of microtubules in response to physiologically-patterned magnetic fields should exhibit coherence with the Schumann frequencies that permeate the earth-ionospheric cavity.

From a more integrated perspective, microtubules have been considered to be the most likely substrate for the "collapse of the wave function" to describe "consciousness" [1] and other complex phenomena such as "memory" and "excess correlations" [4]. The physical dimensions of microtubules exhibit interesting geometries that have been described by several researchers. For example Bras et al [5] indicated that the assembled microtubule exhibits approximately 13 protofilaments which compose a hollow tube whose maximum diameter is 24.6 ± 0.6 nm. The length extends in the micron range with a typical value between 1 and 2 μm. The subunits of the polymers are sequestered by weak non-covalent bonds which facilitate rapid assembly and disassembly [2,6,7]. These conditions of dynamic instability [6], in our experience, increase the probability that copious numbers of photons are emitted and could be detected by photomultiplier units. Rahnama et al [8] presented theoretical analyses that interactions between biophotons initiate fluctuations of microtubules between coherent and incoherent states. Dotta and his colleagues [9, 10] provided support for their hypothesis by measuring photon emissions in hyper-dark settings from both intact cells and microtubules preparations.

Alignment of macromolecular microtubules and related semi-rigid protein assemblies to applied static magnetic fields has been reported by several authors [11, 12]. The diamagnetic anisotropy of the dimeric subunits of tubulin in conjunction with the relative rigidity of the microtubules has been considered a major contribution to the phenomenon. As reiterated by Bras et al [5] diamagnetic anisotropy, that is the differential orientation of repelling effects from applied fields, originates from intrinsic properties of chemical bonds and particularly those that exhibit resonance structures such as peptide bonds. The effects are so small when static fields are applied that concentrated aggregates of microtubules must be exposed. Very strong magnetic fields that range from 8 T [13] to 17 T [14] were required to evoke discernable changes in diamagnetic anisotropy. We queried if there were other measurements by which much weaker magnetic fields could affect microtubule activities. One would expect the indicator of this activity to involve very small quantities of energy, such as that which might be associated with photons [15] within aqueous solutions [16]. Water, particularly Pollack [17] interfacial configurations adjacent to hydrophilic surfaces (exclusion zone water), has the capacity to transform disordered energy into coherent photons [18]. Appropriate frequency weak magnetic fields trapped within these coherent domains (~100 nm diameters) may contribute to this energy [19].

Ultraweak biophotons within the visible range are easily and reliably measured from non-malignant and cancer cells when they are removed from incubation [10, 20] and remain at room temperature. The irradiant flux densities are usually in the 10^{-12} to 10^{-11} $W \cdot m^{-2}$ or about 10 to 100 times greater than the background values for cosmic rays on the earth's surface. Emissions of photons have been measured from bacteria, cells, organs, and entire organisms for decades [21]. Spectral analyses indicate that one major interval for the spectral power densities (SPD) of the numbers of photon emissions from aggregate of cells occurs within the extremely low frequency range (1 to 100 Hz) and is correlated with their functional associations and conditions [9]. Cosic et al [22, 23] applied the Resonant Recognition Model to tubulin by substituting each

amino acid in the sequence with pseudopotential values and obtaining a spectral profile. She found peaks between 2.05 and 2.14 μm, 600 to 615 nm, and 440 to 470 nm. The latter is near the maximum sensitivity of our digital PMTs. That these frequencies relate to actual chemical sequences and pathways has been shown by Dotta et al [24].

Although changes in weak (nanoTesla) geomagnetic fields have been correlated with photon emissions [25], experimental elicitation of photons from cells by specific patterns of weak magnetic fields has only recently been reported. Dotta et al [26] tested a biophysical model of the cell plasma membrane by assuming the lateral diffusion of constituents within this "shell" produced a "membrane magnetic moment" which when interacting with a specific intensity, applied magnetic field would result in increased release of energies whose quantities were within the visible wavelength. The measurements strongly supported this hypothesis and indicated that photons are released from aggregates of cells when the appropriately temporally patterned and (weak) intensity magnetic fields are applied.

We designed experiments to test if the numbers of photons were quantitatively related to the numbers of microtubule preparations (MT) as inferred by measured medium only, a single dish, and a double dish of MT. Secondly we exposed the same single dish of MTs for intervals of 4 min to different physiologically patterned weak magnetic fields or baseline periods to discern if there were alterations in the SPD of the photon emissions. By employing a single dish of MTs at any given time as "its own control" and counterbalancing the presentation of the different patterned fields potential artifacts from handling would be minimal. Several of our unpublished studies had shown a specific enhancement of power of the flux density variations within the peaks that coincide with the Schumann Resonances whose fundamental frequency is about 7.8 Hz. Here we report that photons are related to the numbers of microtubule preparations and that the SPDs are enhanced at this frequency during sequential 4 min periods of specific (but not all) weak magnetic fields.

2. Materials and Methods

2.1 Microtubule Preparations and Exposure Parameters

Plates of ~10^6 B16-BL6 mouse melanoma cells were washed so that only microtubules (MTs) and the cell nuclei primarily remained in the dish [4]. Each standard plastic covered plate of microtubule preparations was then placed at room temperature on a table within 13 m^3 industrial acoustic chamber (also a Faraday Room) which was maintained as a hyperdark environment (<10^{-11} $W \cdot m^{-2}$). The plate was placed on top of the aperture of a digital PMT (Model DM0090C from SENS-TECH, LTD). The plate and the sensor for the PMT were positioned between two containers within which the solenoids were contained. A diagram of the experimental arrangement is shown in Figure 1. This is the same device that was employed to elicit the enhanced release of photons from intact melanoma cells when the appropriate intensity, predicted by modified magnetic moment equations for the entire cell, in previous experiments [26].

In the first series of experiments, to verify the sources of the photons were related to the numbers of MTs, a total of 6 plates containing medium only, 6 single plates of MTs and, 6 double plates (i.e., 12 plates) were place over the PMT shown in Figure 1 and measured for 4 min. We selected this time based upon the requirement for protracted presentations for appropriate temporal sensing by chemical reactions [27, 28]. All plates had been maintained in standard incubators at 37°C until they were placed in the chamber. There was no more than one experiment per week.

In the second series of experiments a single plate of MTs was exposed to a series of 4-min exposures to specific magnetic field patterns or no-field conditions. The order of presentation was counterbalanced. A total of 10 different dishes of MTs were measured. The magnetic fields were generated by transforming a series of numbers from 1 through 256 to -5 to +5 V where 127=0 V by computer software (©Complex; Professor Stanley Koren). This operation was completed by a custom-constructed digital-to-analogue converter that was connected to four pairs of solenoids arranged in a quasi-circle within the containers. The circuit was constructed so that at any given time only one pair (one in the left and one in the right container) was activated for 0.5 s. This value had been selected based upon previous optimal experimental results. Consequently one rotation around the four pairs required 2 s.

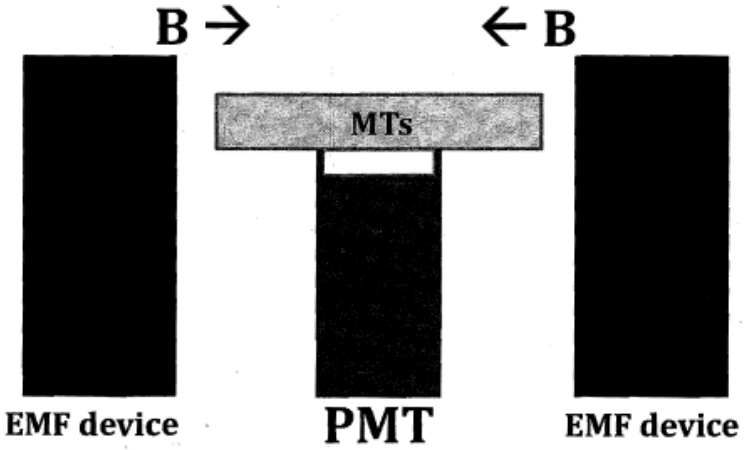

Figure 1. Diagram of the experimental arrangement indicating the placement of the plates of microtubule (MT) preparations over the aperture of the PMT and the placement of the EMF devices.

Three programmable patterns of magnetic fields were generated across the MTs. They are shown in Figure 2 and have been labeled: "Burstx", "Thomas", and "LTP". The Burstx, Thomas and LTP patterns were composed of 230, 849, and 225 points or columns of numbers, respectively, from which the voltages were determined. The point durations, which were programmable, for each of the three patterns was either 1 ms or 3 ms. Point duration is the time (in ms) each number (and hence voltage) is presented before moving to the next value. These values are similar to the binding constants of about 1.5 ms reported by Pilla et al [29] for Ca^{++}/CaM-dependent myosin phosphorylation during nonequilibrium phases. The intensities of the magnetic fields within the area of the dish as measured by power meters were between 3 and 10 μT. In addition to the experimental demonstrations that such weak fields supply relevant energies to molecular targets within cells, the traditional kT "constraint" argument against the

effects of such weak fields has been refuted on the bases of its applicability to systems near thermal equilibrium, which biological systems are not [30].

The Burstx pattern was a crude digital representation of an amygdaloid neuron during an "epileptic discharge" from a human patient while the "Thomas" pattern was a more symmetrical decelerating frequency-modulated magnetic field derived from communication-like signals [31, 32]. The third pattern was the magnetic equivalent of the pattern that when applied as an electric current to hippocampal slices [33] results in long-term potentiation which is considered to the primarily biophysical-chemical substrate for representation of information (memory) within brain space. Each of these patterns has been associated with robust and significant changes in behaviors at the level of the organism that reflect the predicted function which have included analgesia and altered learning and memory [34,35].

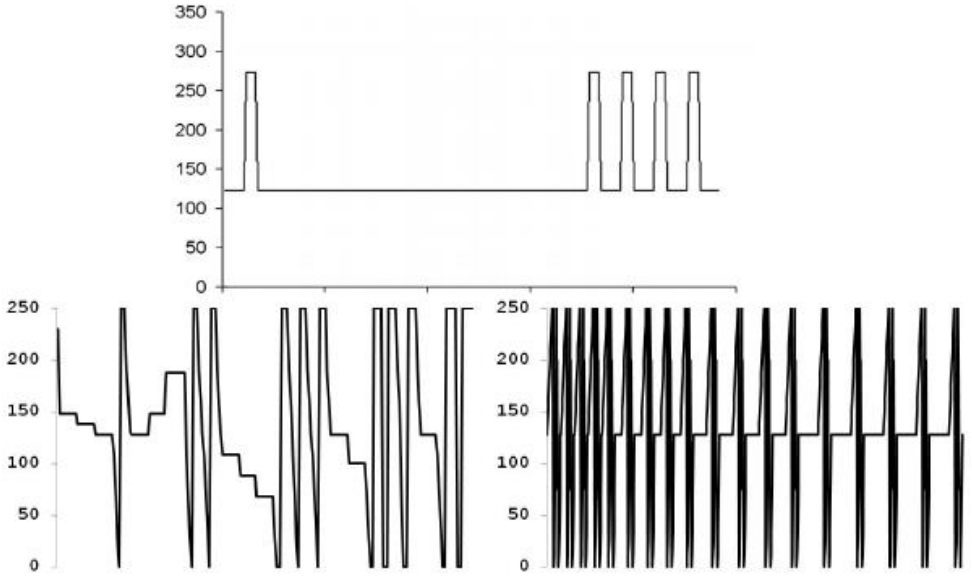

Figure 2. The temporal shape of the three patterns employed in the present study that affected the Spectral Power Density of the photon emissions from microtubule preparations. Top is "LTP", bottom left is the "BurstX" pattern and the bottom right is the "Thomas" pulse. The vertical axis refers to the numbers associated with voltage (-5 to +5 V) while the horizontal axis reflects the order of the points whose durations were either 1 ms or 3 ms.

2.3. Measurement and Analysis Procedures

During the 4 min increments successive exposures to various patterns of magnetic fields or no field intervals, the numbers of photons emitted from the MTs were measured once every 20 ms (50 Hz) which was the upper limit for the collection software of the equipment. The monitoring equipment for the PMT as well as the computer that initiated the different magnetic field patterns were outside of the exposure chamber whose double doors were closed. Consequently once the experiment with a given dish of MTs began there was no human presence or disturbance within the exposure area containing the MTs. The data were then loaded into SPSS 16 programs and analyzed for total photon counts per second for each 4 min interval. In addition, spectral analyses were completed for each 4 min (240 s) segment in order to discern

Spectral Power Densities (SPD). In previous experiments we had found that although the absolute numbers of photons may not increase with some types of patterned magnetic fields there was a robust shift in the amplitude distributions of the photon emissions during the exposures.

3. Results and Discussion

In order to ensure that the photon counts were directly related to the presence of the MTs, the raw measures per 20 ms were obtained for plates containing only medium but no MTs, one plate of MTs or two (stacked) plates of MTs. The results for one experiment are shown in Figure 3. It is important to emphasize that these values are means and standard deviations. This indicates that effectively there was no overlap within 3 standard deviations between the photon values from the no MT (medium only) plates and the two plate photon emissions. There were about twice the numbers of photons emitted from one plate of MTs compared to the medium only and four times this number for two stacked plates of MTs. This specific ratio strongly suggests the photon counts were a function of the numbers of MTs. The increase of 2 counts per 20 ms is equivalent to about 100 counts per s from the preparation. Given the aperture of the PMT is 1 cm^2 and assuming the maximum sensitivity of the PMT (400 nm), the energy equivalent would be about 10^{-12} W m^{-2} per plate. Figure 4 shows the results of all experiments (24 plates of MT) transformed to z-scores because different batches of MTs exhibited different baseline photon counts. The general MT number-dependent relationship is clearly obvious.

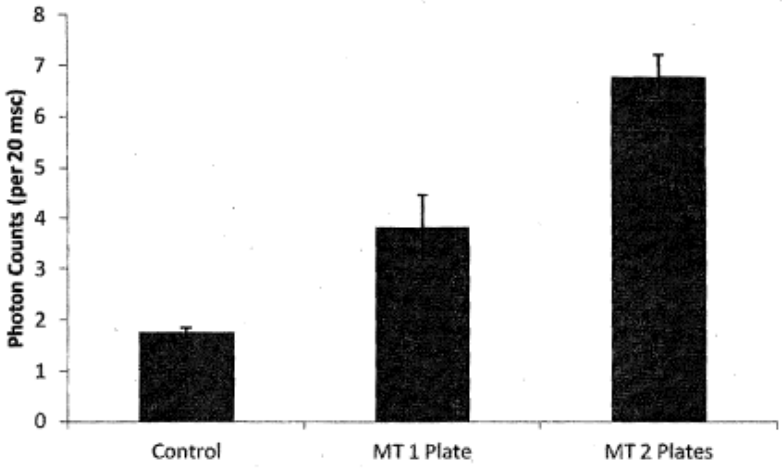

Figure 3. Example of the numbers of photon counts per 20 ms (limits of sampling rate) from plates containing medium only, a single plate containing microtubule preparations and two stacked plates of MTs. Vertical bars indicate SDs.

However there were no significant differences in the numbers of photons per second from single plates of MTs when they were exposed for 4 min each to either the sham condition (no field), Thomas configuration, LTP, or Burst patterns (grand mean=3.2 photons per 20 ms; SD=1.6). The results of the SPD analyses were very clear. The clearest difference over the 0.1 Hz Δf

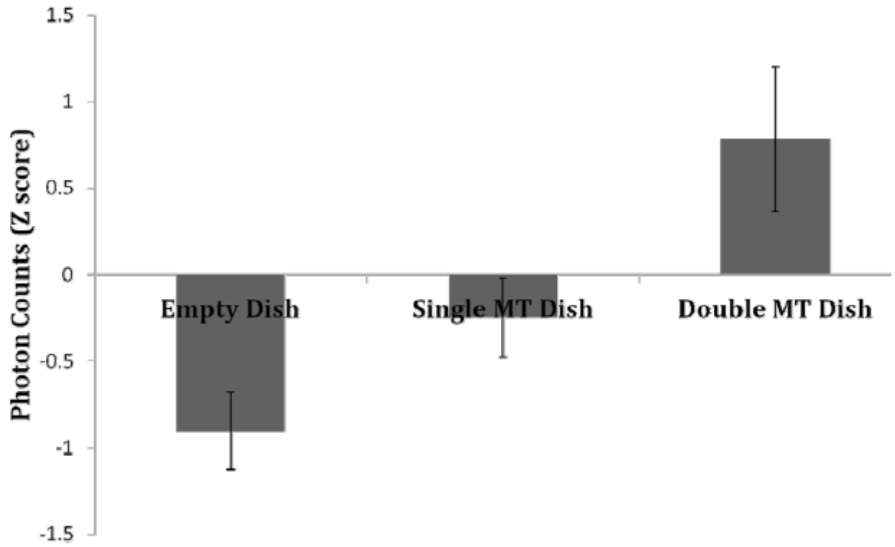

Figure 4. Standardized (z) scores for the numbers of photon counts per second from dishes containing only medium (no MT), a single dish of MTs, and two (superimposed) dishes of MTs for all experiments.

between the minimal and 25 Hz (the Nyquist limit is ½ of 50 Hz) value occurred within the 7.7 to 7.8 Hz interval. The results are shown in Figure 5. During the LTP and Thomas pattern exposures the MTs displayed greater SPD within this frequency interval than during either the Burstx or no field intervals. In other words there was a shift of the amplitude variations of the temporal distributions in the photon emissions during these 4 min of field exposures rather than alterations in the numbers of photons.

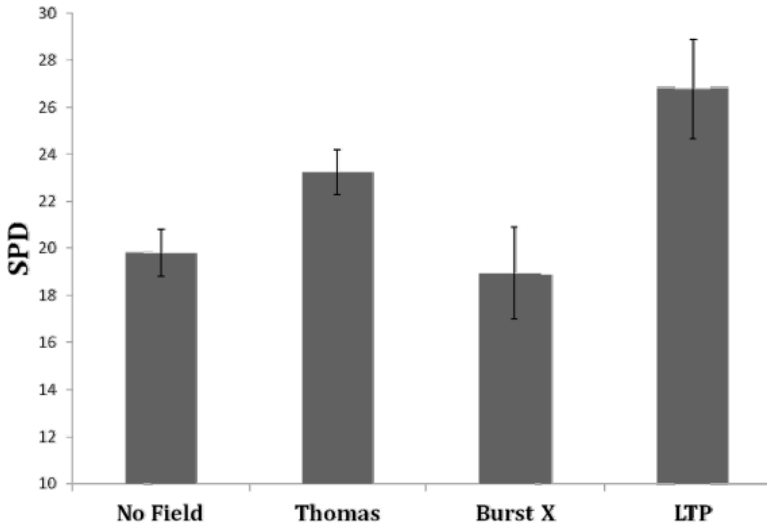

Figure 5. Spectral Power Densities (SPD) of photon emissions within the 7.7. to 7.8 Hz interval from microtubule preparations as a function of the no field and three field conditions. Vertical bars indicate standard deviations.

The 7.7 to 7.8 Hz band is the same as the fundamental for the Schumann Resonance which is generated within the spherical waveguide between the earth's surface and the ionosphere. Our local Schumann Resonance measurement station (compliments of Professor Kevin S. Saroka) as well as a major station in Italy (the data from which our measurements are highly correlated) indicates a comparable peak frequency [36]. We reasoned that if the application of the magnetic field shifted the SPD towards the 7.7 to 7.8 Hz band there should be a bimodal distribution or "split spectra" that would be directly and quantitatively calculable from the intensity of the applied field. This "double peak" might be considered analogous to the Zeeman split found in many spectra. That the Schumann fundamental displays intermittent split spectra of about 0.4 Hz in response to various geomagnetic events has been measured several times [37].

The general relationship between charge, mass and strength of the magnetic field according to dimensional analysis is $q \cdot kg^{-1} \cdot B$, resulting in Hz, where q is unit charge, kg is the mass, and B is the applied field. Assuming the median mass of a tubulin dimer is 55 kD with each monomer carrying 10 unit charges [38], the resulting frequency would be $32 \cdot 10^{-19}$ A·s divided by $9.13 \cdot 10^{-23}$ kg multiplied by the median root mean square for the intensity range (3 to 10 μT) of ~between 3 and $4 \cdot 10^{-6}$ T, or, between 0.11 and and 0.14 Hz. To test this prediction with the data the SPD were analyzed by SPSS according to the maximum Δt associated with the sample number (12,000, i.e., 50 per s, 60 s per min for 4 min) was 25 ms or 0.04 Hz.

The enhanced SPDs within the 7.7 to 7.8 Hz band when the Thomas and LPT were presented reflected this potential. Consequently we combined the data for these two conditions and compared them to periods where there no field conditions. As can be seen in Figure 6, the MTs exposed to either the LTP or Thomas pattern displayed the strongest difference in SPD compared to the sham field exposed MTs in two peaks, 7.74 Hz and 7.87 Hz, which was separated by 0.13 Hz. This difference is within the range of the predicted shift in frequency. The results are shown in Figure 6. The difference was statistically significant ($p < 0.05$)**.** When the two field conditions were analyzed separately they both displayed this double peak but the split did not reach statistical significance. The Burstx pattern did not display this effect. In fact at 7.74 Hz the SPD did not differ from that of the sham field conditions.

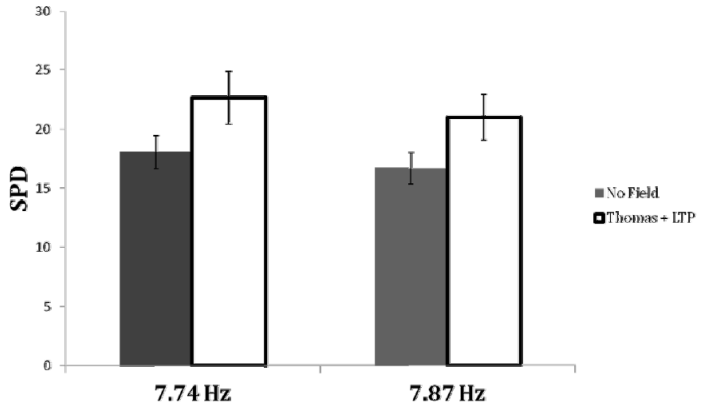

Figure 6. Peaks in the SPD of photon emission from MTs exposed to the two classes of fields demonstrating the potential "split spectrum" around the Schumann fundamental.

Additional analyses indicated that the MTs during the intervals when the Burstx pattern was presented displayed a statistically significant *diminishment* of SPD compared to no field intervals at around 20.5 Hz. This is congruent with the third harmonic of the Schumann Resonance. Exposures to the other two magnetic field patterns did not show this effect.

Considering the significance of photon emissions for intra- and intercellular communication, the reliable productions of these packets of energy from microtubules would be expected. As indicated by Alberts et al [2] microtubules can form noncovalent polymers and some tubulin subunits are enzymes that catalyze the hydrolysis of triphosphates which are often GTP (T-form) filament structures which can expand and GDP (D-form) structures that more rigorously restrict expansion. This rapid interconversion between a shrinking and growing state when there is a relatively homogenous concentration of free subunits produces a dynamic instability. We suggest that this condition would allow weak, appropriately patterned magnetic fields to shift the distribution of the energy from photon emissions within a specific ELF range.

That similarity in the maximum increase in SPD that occurred within a narrow band of 7.7 to 7.8 Hz and the fundamental Schumann resonance that is generated between the earth's surface and ionosphere [37] may be coincidence. The intensity of this magnetic field is about 2 pT which appears to be remarkably small. However the Schumann Resonance has been present since abiogenesis [39] and may have influenced the subtle structural evolution and interactions within proteins in general. The Schumann Resonance and its harmonics are due to global lightning discharges which occur between 40 and 100 times per s. Miller and his colleagues [40] had shown the electrical discharges within preCambrian atmospheric gases produced more than a dozen different amino acids.

The novel observation of a "split" of the SPD around the Schumann fundamental in microtubule preparations that had been exposed to the patterned fields that are known to affect "memory" (the representation of experience) may not be anomalous. Spectral analysis of the quantitative electroencephalogram of human brain activity reveals the recondite presence of Schumann harmonics as well as a bimodal peak [37]. Tanashi [41] while pursuing previous research of a 0.2 to 0.4 Hz spacing in the first mode of Schumann peaks also noted three peaks between 7.1, 7.85 and 8.5 Hz. These occurred within the earth's magnetic field which is about a factor of 10 stronger than the experimental fields employed in this study. The presence of a reliable resonance split in the preparations of microtubules that was enhanced by the appropriately patterned magnetic field might suggest an occluded property in the amplitude variation of photon emissions that reflects the evolutionary history of these fundamental structural proteins.

The shift in spectral power frequencies rather than the elevation of energy or power has significant thermodynamic implications for higher functions such as consciousness. A useful metaphor might be that a defective radio (that delivers static) and a functional radio (that delivers salient information) use the same power. The precision of the frequency might be critical. Harmony [42] who assessed quantitative electroencephalographic activity during different tasks found increased 7.8 Hz power in children that diminished during adulthood. Lisi et al [43] found that human keratinocytes exposed to 7 Hz, ~9 μT magnetic fields for one hour twice daily

displayed altered shapes and actin distributions. Altered microtubule organizations, which can be disrupted by psychotropic drugs such as lysergic acid diethylamide (LSD), may be involved with some forms of psychosis [44]. It may be relevant that the isotype of beta-tubulin III, found almost exclusively in neurons, increases tumor aggressiveness.

4. Conclusion

The dynamics of the microtubule and its constituent tubulin dimers during periods of adaptation to a disrupted environment are associated with increased photon emissions. Spectral analyses of the photon emissions from plates of MT preparations within standard media in a Faraday room exhibited weak but significant, reliable peaks of SPD around 7.7 to 7.8 Hz. Exposures for only 4 min to 3 to 10 μT temporally patterned magnetic fields that are associated with the physiological substrates of "learning and memory" enhanced the magnitude of the SPD of photon emissions from MT. There was also a split in the spectra, not observed during the no field conditions, that was predicted by the gross quantitative relationship between the strength of the applied magnetic field, the estimated numbers of unit charges per dimer, and the aggregate's mass. As noted in previous experiments applications of the appropriate, temporally patterned magnetic fields to MTs do not affect the total photon emissions but shift the distributions of the amplitudes power spectra during the brief interval of exposure. If intracellular information is contained within shifting temporal patterns of energy but not the absolute shift in energy within dynamic systems then weak magnetic fields might affect the function of cells through microtubules.

Acknowledgements: We thank Dr. Carly Buckner for preparation of the MTs and Dr. Robert Lafrenie for his patience and contributions. Special thanks to Dr. W. E. Bosarge, Jr., CEO, Capital Technologies, Inc. for his support of innovative ideas.

References

1. S. Hameroff and R. Penrose, "Consciousness in the universe: A review of the 'Orch OR' theory," *Physics of Life Reviews,* Vol. 11, pp. 39-78, 2014.
2. M. Bizzarri, A. Pasqualato, A. Cucina and V. Pasta, "Physical forces and non linear dynamics mould fractal shape. Quantitative morphological parameters and cell phenotype," *Histology and Histopathology,* Vol. 28, pp. 155-174, 2013.
3. B. Alberts, A. Johnson, J. Lewis, M. Raff, K. Robets and P. Walter, *Molecular Biology of the Cell*, Garland Science (4th edition), 2002
4. M. Ostovari, A. Alipour and A. Mehdizadeh, "Entanglement between biophotons and tubulins in the brain: implications for memory storage and information processing," *NeuroQuantology*, Vol. 12, 350-355, 2014.
5. W. Bras, J. Torbet, G. P. Diakum, G. L.J. A. Rikken and J. F. Diaz, "The diamagnetic susceptibility of the tubulin dimer," *Journal of Biophysics*, Vol. 2014, 5 pages, 2014 Article ID 985082.
6. M. Cifra, J. Pokorny, D. Havelka and O. Kucera, "Electric field generated by axial longitudinal vibration modes of microtubule," *BioSystems*, Vol. 100, pp. 122-131, 2010.
7. J. Pokorny, "Excitation of vibrations in microtubules in living cells," *Bioelectrochemistry*, Vol. 63, pp. 321-326, 2004.

8. M. Rahnama, J. A. Tusynski, I. Bokkon, M. Cifra, P. Sardar and V. Salari, "Emission of mitochondrial biophotons and their effect on electrical activity of membrane via microtubules," *Journal of Integrative Neuroscience*, Vol. 10, 65-88, 2011.
9. B. T. Dotta, D. E A. Vares, C. A. Buckner, R. M. Lafrenie and M. A. Persinger, "Magnetic field configurations corresponding to electric field patterns that evoke long-term potentiation shift power spectra of light emissions from microtubules from non-neural cells," *Open Journal of Biophysics*, Vol. 4, pp. 112-118, 2014.
10. B. T. Dotta, C. A. Buckner, D. Cameron, R. F. Lafrenie and M. A. Persinger, "Biophoton emission form cell cultures: biochemical evidence for the plasma membrane as the primary source," *General Physiology and Biophysics*, Vol. 30, pp. 301-309, 2011.
11. W. Bras, G. P. Diakun, J. F. Diaz et al., "The susceptibility of pure tubulin to high magnetic fields: a magnetic birefringence and X-ray fiber diffraction study," *Biophysical Journal*, Vol. 74, pp. 1509-1521, 1988.
12 U. Raviv, D. J. Needleman, K. K. Ewert, and C. R. Safinya, "Hierarchical bionanotubules formed by the self assembly of microtubules with cationic membranes or polypeptides," *Journal of Applied Crystallography*, Vol. 40, pp. s83-s87, 2007.
13. P. M. Vassilev, R. T. Dronzine, M. P. Vassileva and G. A. Georgiev, "Parallel arrays of microtubules formed in electric and magnetic fields," *Bioscience Reports*, Vol. 2, pp. 1025-1029, 1982.
14. P. Rub and G. Maret, "New 18-T resistive magnet with radial bores," *IEEE Transactions on Magnetics*, Vol. 30, pp. 2158-2161, 1994.
15. L. M. Karbowski and M. A. Persinger, "Variable viscosity of water as the controlling factor in energetic quantities that control living systems," *International Letters of Chemistry, Physics and Astronomy*, Vol. 40, pp. 1-9, 2015.
16. N. J. Murugan, B. T. Dotta, L. M. Karbowski, and M. A. Persinger, "Conspicuous bursts of photon emissions in malignant cell cultures following injections of morphine: implications for cancer treatment", *International Journal of Current Research*, Vol. 6, pp. 10588-10592, 2014.
17. G. H. Pollack, X. Figueroa, and Q. Zhao, "Molecules, water, and radiant energy: new clues for the origin of life," *International Journal of Molecular Sciences*. Vol 10, pp. 1419-1429, 2009.
18. H. J. Niggli, "Ultraweak electromagnetic wavelength radiation as biophotonic signals to regulate life processes," *Electrical and Electronic Systems*, Vol 3 (2)m 1000126.
19. E. Del Giudice and G. Preparata, "Coherent dynamics in water as a possible explanation of biological membranes formation," *Journal of Biological Physics*, Vol. 20, pp. 105-116, 1994.
20. B. T. Dotta, C. A. Buckner, R. M. Lafrenie and M. A. Persinger, "Photon emissions from human brain and cell culture exposed to rotating magnetic fields shared by separate light-stimulated brains and cells," *Brain Research*, Vol 388, pp. 77-88, 2011.
21. F-A. Popp, "Photon storage in biological system," *Electromagnetic Information*, Urban and Schwarzenberg, 1979, pp. 123-149.
22. I. Cosic, "Macromolecular bioactivity: is it resonant interaction between macromolecules? Theory and applications," *IEEE Transactions on Biomedical Engineering*, Vol. 41, pp. 1101-1114, 1994.
23. I. Cosic, K. Lazar and D. Cosic, "Prediction of tubulin resonant frequencies using the resonant recognition model (RRM)," *IEEE Transactions on NanoBioscience*, 10.1109/TBN.2104.2354841, 2014.
24. B. T. Dotta, N. J. Murugan, L. M. Karbowski, R. M. Lafrenie and M. A. Persinger, "Shifting wavelengths of ultraweak photon emissions from dying melanoma cells: their chemical enhancement and blocking are predicted by Cosic's theory of resonant recognition model for molecules," *Naturwissenschaften*, Vol. 101, 87-94, 2014.
25. L. Yu. Berzhanskaya, O. Yu. Beloplotova and V. N. Berzhansky, "Electromagnetic field effect on luminescent bacteria," *IEEE Transactions on Magnetics*, Vol. 31, pp. 4274-4275, 1995.

26. B. T. Dotta, R. M. Lafrenie, L. M. Karbowski and M. A. Persinger, "Photon emission from melanoma cells during brief stimulation by patterned magnetic fields: is the source coupled to rotational diffusion within the membrane?," *General Physiology and Biophysics*, Vol. 33, pp. 63-73, 2014.
27. T. A. Litovitz, M. Penafiel, D. Krause, D. Zhang, and J. M. Mullins, "The role of temporal sensing in bioelectromagnetic effects," *Bioelectromagnetics* Vol. 18, pp. 388-395, 1997.
28. T. A. Litovitz, D. Krause, C. J. Montrose, and J. M. Mullins, "Temporally incoherent magnetic fields mitigate the response of biological systems to temporally coherent magnetic fields," *Bioelectromagnetics*, Vol. 15, pp. 399-409, 1994.
29. A. A. Pilla, D. J. Muesham, M. S. Markov and B. F. Sisken, "EMF signals and ion/ligand binding kinetics: prediction of bioeffective waveform parameters," *Bioelectrochemistry and Bioenergetics*, Vol. 48, pp. 27-34, 1999.
30. M. Cifra, J. Z. Fields and A. Farhadi, "Electromagnetic cellular interactions," *Progress in Biophysics and Molecular Biology*, Vol. 105, pp. 223-246, 2011.
31. M. A. Persinger, "Neurobehavioral effects of brief exposures to weak intensity, complex magnetic fields within experimental and clinical settings," in M. J. McLean, S. Engstrom and R. R. Holocomb (eds), *Magnetotherapy: Potential Therapeutic and Adverse Effects*. TGF Press, 2003, pp. 89-118.
32. A. W. Thomas, M. Kavaliers, F. S. Prato and K-P. Ossenkopp, "Antinoceptive effects of pulsed magnetic field in the land snail, *Cepaea nemoralis*, *Neuroscience Letters,* Vol. 222, pp. 107-110, 1997.
33. G. M. Rose, D. M. Diamond, P. Pang and T. V. Dunwiddie, "Primed burst potentiation: lasting synaptic plasticity invoked by physiologically patterned stimulation. In H. L. Hass (ed), *Synaptic Plasticity in the Hippocampus*, Springer-Verlag, 1988, pp. 96-98.
34. L. J. Martin, S. A. Koren and M. A. Persinger, "Thermal analgesic effects from weak, complex magnetic fields and pharmacological interactions," *Pharmacology, Biochemistry and Behavior* Vol. 78, pp. 217-227, 2004.
35. Q. H. Mach and M. A. Persinger, "Behavioral changes with brief exposures to weak magnetic fields patterned to stimulate long-term potentiation," *Brain Research*, Vol. 1261, pp. 45-53, 2009.
36. K. S. Saroka and M. A. Persinger, "Quantitative evidence for direct effects between earth-ionosphere Schumann Resonances and human cerebral cortical activity," *International Letters of Chemistry, Physics and Astronomy* Vol. 20(2) pp. 166-194, 2014.
37. A. Nickolaenko and M Hayakawa, *Schumann Resonance for Tyros*: *Essentials of Global Electromagnetic Resonance in the Earth-Ionospheric Cavity*, Springer, 2014.
38. J. A. Tuszynski, W. Malinski, E. J. Carpenter, T. Luchko, J. T. Huzil and R. F. Ludena, "Tubulin electrostatic and isotype specific drug binding," *Canadian Journal of Physiology*, Vol. 86, pp. 635-640, 2008.
39. F. E. Graf and E. R. Cole, "Precambrian ELF and abiogenesis," in M. A. Persinger (ed) *ELF and VLF Electromagnetic Field Effects*, Plenum Press, 1974, pp. 243-273.
40. A. P. Johnson, H. J. Cleaves, J. P. Dworkin, D. P. Glavin, A. Lazcano and J. L. Bada, "The Miller volcanic spark discharge experiment," *Science*, Vol. 322, pp. 404, 2008.
41. S. Tanahshi, "Detection of line splitting of Schumann resonances from ordinal data," *Journal of Atmospheric and Terrestrial Physics*, Vol. 38, pp. 135-142, 1976.
42. T. Harmony, "The functional significance of delta oscillations in cognitive processing," *Frontiers in Integrative Neuroscience*, Vol. 7, Dec, 2013, Article 83.
43. A. Lisi, A. Foletti, M. Ledda, F. De Carlo, L. Giuilani, E. D'Emilia, and S. Grimaldi, "Resonance as a tool to transfer information to living systems: the effect of 7 Hz calcium ion energy resonance on human epithelial cells (HaCaT) differentiation," *PIERS Proceedings,* Cambridge, U.SA., July 2-6, 2008.
44. G. Benitez-King, G. Ramirez-Rodriguez, and L. Ortiz-Lopez, "Altered microtubule associated proteins in schizophrenia," *NeuroQuantology*, Vol. 5, pp. 58-61, 2007.

Article

Demonstration of Excess Correlation in Non-Local Random Number Generators Sharing Circular, Changing Angular Velocity Magnetic Fields

Lyndon M. Juden-Kelly[1,2], Blake T. Dotta[1,3], David A. E. Vares[1,2] & Michael A. Persinger[1,2,3*]

Neuroscience Research Group[1], Human Studies[2] and Biomolecular Sciences[3] Programs, Laurentian University, Sudbury, Ontario, Canada P3E 2C6

ABSTRACT

To test if temporally-coupled diametric shifts in parity could be demonstrated for non-local distances between "random" events generated by electron tunnelling-based circuits, two REG (Random Event Generators) were each exposed within a circular array of solenoids separated by 10 m. Each circular array generated a patterned rotating magnetic field that has previously produced transient excess correlation and entanglement in photon reactions and alterations in pH in spring water. During a 30 min interval the REGs were exposed first to an accelerating group velocity embedded with a diminishing frequency/phase-modulated field (the primer) followed by a decelerating group velocity embedded with an increasing frequency/phase-modulated magnetic field (the effector). Only after exposures for about 4 min to the second (effector) condition that is known to manifest the effects of entanglement did the random numbers deviate significantly and by more than one standard deviation in an opposite direction to each other. The estimated increments of energy were between 10^{-21} and 10^{-20} J which is within the range of the energy derived from the universe's total force per Planck's voxel distributed over the distance of the hydrogen wavelength. These results indicate that excess correlation can be generated within "random", quantum electronic processes whose spatial domains are similar to neuronal synapses at the macro-level by appropriate applications of weak, microTesla level, magnetic fields.

Keywords: Entanglement, random event generators, circular rotating magnetic fields, excess correlations.

1. Introduction

Entanglement, frequently studied since the term was first introduced by Erwin Schrodinger (Aczel, 2002), is still considered a mystery with respect to mechanism and explanation. Traditionally excess correlation between two particles representative of entanglement has been restricted to photons or to clusters of photons (Vaziri et al, 2002). Considering the intricate relationship between photons as quanta of energy and shifts in electron

*Corresponding author: Dr. M. A. Persinger, mpersinger@laurentian.ca

shells, one would expect that phenomena that involve the movement of electrons across specific geometries, such as p-n junctions, might also exhibit this capacity.

Many REGs (Random Event Generators) employ these mechanisms in order to discern if proximal stimuli can affect "random distributions" of 0, 1 outcomes. If the electron tunnelling processes associated with REG operations that produce 0, 1 series of numbers are similar to that of parity in paired, entangled photons, then there should be an elementary test of this manifestation of excess correlation. If the two (REG) systems are "entangled" then a deviation in one direction of "randomicity" exhibited by one REG should occur co-temporally with a deviation in the other direction of randomicity in the coupled second REG. He we present experimental evidence for this effect.

The operational essence of entanglement that leads to excess correlations is that two loci share specific physical parameters in space-time. The two loci then respond as if they occupy the identical space-time field. One interpretation is that superposition has resulted in a virtual juxtaposition and transposition of the two loci's axes. The concept is an extension of Mach's principle which suggested that all particles in the universe are relatable by their (angular) momentum or their moments of inertia. As a result every particle in the universe is affected by all other particles in the universe. The movement of an electromagnetic field around a circle is a special condition because of the angular velocity and its implicit constant "acceleration".

When a packet of particles are moving through space time there are two components. The first is the group velocity; the second is the phase velocity of the particles within the group. If the two are equal then there are no interference or bifringence patterns. Tu et al (2005) has strongly suggested that if these packets of particles are photons and there is a discrepancy between the group and phase velocity then a non-zero mass emerges for the photons. One of the consequences is the emergence of a third direction of the photon. The other directly applicable consequence is that the product of the upper limit of the rest mass of a photon ($\sim 2 \cdot 10^{-52}$ kg), the entanglement velocity (Persinger and Koren, 2013) of $2.8 \cdot 10^{23}$ $m \cdot s^{-1}$, and the velocity of light in a vacuum ($3 \cdot 10^{8}$ $m \cdot s^{-1}$) is $\sim 1.7 \cdot 10^{-20}$ J.

The 10^{-20} J is a value that emerges when the total force within the universe is divided by the sum of Planck's voxels that comprise its volume and the force is then applied across the wavelength of the neutral hydrogen line (Persinger, 2015). This is the quantum associated with a single action potential of an axon as well as the energy from the force between potassium ions that contribute to the resting membrane potential of the plasma cell membrane. It is also within the range of the increment of energy known to be associated at the fundamental level with the electron tunnelling within the type of p-n junctions within the REGs. The convergences would be consistent with the conditions required for phenomena that exhibit properties of entanglement.

Dotta and Persinger (2012) applied this concept to an experimental setting whereby pulsing magnetic fields generated through optocoupler systems to circular arrays of 8 pairs of solenoids were uncoupled with respect to phase and group velocity. The group velocity which was the changing angular velocity as the magnetic field rotated around the circular arrays of solenoids and the phase velocity, defined as the shifting frequency and phase modulation of the complex pattern that composed the magnetic field, differed. When two bioluminescent reactions were placed in the center of each of the two circular arrays separated by 10 m a doubling of

photon emission (as if the two loci had been superimposed) occurred if they were first exposed to an accelerating group velocity embedded with a decreasing phase velocity and then to a decreasing group velocity embedded with an increasing phase velocity. These were called the primer and effector fields, respectively. Reversal of the presentations of the sequence, coupled phase-group velocity fields, or no changing angular velocity, did not produce the "doubling" of photons.

The effect was also observed in spring water within which diametrically opposite shifts occurred in pH within the two distant spaces surrounded by the rings of solenoids. In a series of 24 experiments; inverse shifts in pH were noted in two quantities of spring water separated by 10 meters that shared rotating magnetic fields with changing angular velocities when one solution was injected with proton donors (weak acetic acid). It was also found that the associated fixed amount of energy of 10^{-20} J 10^{-21} J per molecule from the coordinated fields in the two loci was related to the change in numbers of H^+ within these volumes and predicted the time required to produce the maximum shift in pH (Dotta et al., 2013).

Excess correlation is not exclusive to pH shifts in water but also applies to electron spins and gases (Ahn et al., 2000; Fickler et al., 2012; Hoffman et al., 2012; Julsaarg et al., 2001). Excess correlation has been found up to 300 km between pairs of brains that shared circularly rotating magnetic fields from a different technology where the fields were generated through cerebral toroids driven by Ardueno circuits maintained by laptop computers. Discrete changes in QEEG (quantitative electroencephalographic) power within the cerebral space of a non-local subject was experimentally demonstrated when the pair were exposed to specific configurations of circular magnetic fields with changing angular velocities that dissociated the phase and group components. These non-local discrete changes in power occurred when the local participant was exposed to sound pulses but not light flash frequencies (Burke et al., 2013).

The signal to noise ratio and inferences of manifestation within excess correlations with regard to human cerebrums seems to be heightened when the pairs of individuals have had proximal space-time relations from previous relations. When 'pairs' of individuals were separated by 75 m, ~50% of the variance of the "simultaneous" electroencephalographic power was shared between the pairs of brains. Positive correlations were found within the alpha and gamma bands within the temporal and frontal lobes. However the alpha and theta bands were found to be negatively correlated for pairs of people who had a protracted history of interaction (Dotta et al., 2009). This would be consistent with a more macro-entanglement of the frequent observation that if the parity of one entangled photon is changed the other changes in the opposite direction.

2. Theory and Presumed Operation of the RNG

The RNG (Random Number Generator) or REG (Random Event Generator) device was purchased from Psyleron Inc. (hardware ID: RGZD750) and is designed to generate random numbers based on quantum principles. As described Psyleron's technicians and by Vares and Persinger (2013), two environmentally shielded, Fairchild NPN Epitaxial 0.048mg Silicon Transistors (BCX70K), under a reversed biased current employed heavily doped electrons to

quantum tunnel across a classical channel barrier. The authors assume the proprietary distance of the gap junction barrier is of the order of the industry about 1 μm with a functional width of similar magnitude. Following the Heisenberg Uncertainty Principle, the probability of an electron randomly occurring on the opposite side of the gap junction channel barrier, translates into a varying voltage level.

The varying voltage (white noise) generated by quantum tunnelling electrons is sampled from a reverse-biased 'Field Effect Transistor' (FET). The unpredictably 'high' and 'low' voltages are due to more or less electrons tunnelling across the barrier (gap junction), with a spectrum +/- 1dB, from 50Hz to 20kHz. A 1 kHz cut-off attenuates frequencies, followed by filtering, transistor signal amplification and clipping to produce a rectangular wave. Gated sampling at an approximate constant 1-kHz rate yields a regularly spaced sequence of random bits. To eliminate environmental biases, the two streams from both chips undergo Boolean Exclusive-OR logic gate operation procedures, whereby: [(1 XOR 1 = 0), (1 XOR 0 = 1), (0 XOR 1 = 1), and (0 XOR 0 = 0)] respectively. Further, the entire circuit is shielded by an outer aluminum enclosure, as well as with an inner perm alloy mu-metal which isolates both electrical and magnetic effects from inside and outside the REG device. In short, the Psyleron REG is a professional, non-classical coin flipper with data accessed by computer via USB port.

Leo Esaki (1958) noted that the current in the reverse diode might only be carried by internal field emission. The barrier breakdown occurs at less than the threshold voltage for electron-hole pair production, and so an avalanche should be excluded. Due to the extensive shielding and calibration testing of the Psyleron REG-1 device, classical physical interactions can be ruled out as the source of deviation from statistical randomness. The velocity of an incident tunnelling electron wave packet becomes infinite inside a zero-time space barrier. With wave number *k* imaginary, the duration of time for the incident electron wave packet to tunnelling across the potential barrier approaches zero. We have assumed, based upon the diffusivity velocity calculated by Persinger and Koren (2013), that the value is very fast but non-zero. If the manifestation of entanglement velocity is $2.8 \cdot 10^{23}$ $m \cdot s^{-1}$, the time required to traverse p-n junction of ~1 μm would be $0.3 \cdot 10^{-29}$ s. This tunnelling phase change is a special solution of the Schrodinger wave function:

$$\psi_{\mathrm{I}}(x,t) = e^{-\frac{iEt}{\hbar}} \left[A_{\mathrm{I}} e^{\frac{ipx}{\hbar}} + B_{\mathrm{I}} e^{-\frac{ipx}{\hbar}} \right] \quad (1)$$

where; particle momentum $p = (\sqrt{2mE})$, A_I and B_I are Eigen functions of the momentum operators for the incident and reflected propagations of the particle in each region. During tunnelling in the barrier region (II), the corresponding wave function solution $[(\psi]_{II})$ undergoes absorption. Although the energy of the instantaneously tunnelled electron remains consistent, the probability amplitude is no longer the simple addition of oscillating functions, but combinations of exponential ones (Hartman, 1962). There exists the quantum wave function state possibility of a transition of electrons from the valence band, into quantum states of like energy in the conduction band. Quantum tunnelling is therefore known as the finite probability, as determined by the ratio of coefficients of the special Schrodinger equation, of finding instantaneous particles at the instantaneous inflection points between discrete regions.

The phase change solutions to the special Schrodinger equations violate Einstein causality for signal transmissions through a vacuum. For: ($W^2 = c^2p^2$) where: W = (energy), and

p = (momentum), the instantaneous tunnelling electron is faster than the speed of light. However when the entanglement velocity is assumed and the traversal time is $0.3 \cdot 10^{-29}$ s, the equivalent frequency is $3.3 \cdot 10^{29}$ Hz and hence the energy of the wave packet would be the multiplication by Planck's constant ($6.626 \cdot 10^{-34}$ J·s) or ~$22 \cdot 10^{-5}$ J. When divided by the rest mass ($9.1 \cdot 10^{-31}$ kg) of 10^{10} electrons ($9.1 \cdot 10^{-21}$ kg), the estimated numbers involved with the expected density of silicon molecules on each surface between the barriers, the remaining value is $2.4 \cdot 10^{16}$ $m^2 \cdot s^{-2}$ or $1.6 \cdot 10^8$ $m \cdot s^{-1}$. This is very convergent with the velocity of light. Hence if the tunnelling duration is assumed to be a non-zero value which is the entanglement velocity the resulting energy values for a specific aggregate of electron masses moving coherently resolves as the velocity of light in that domain. This functional equivalence between the photonic property and the aggregate of electrons that displays one wave function for the whole system (Ψ) and not separate waves for each particle also suggests that the electron tunnelling *process* might be entangled experimentally.

Considering the fluctuations are quantum in nature, literature investigation revealed a laboratory device that measures quantum vacuum fluctuations (Symul et. al., 2011). A laser is split, and two homodyne photodetectors measure the difference. Electronic noise was filtered to reveal inherent vacuum fluctuation measures which were then sourced to create quantum random numbers. Modern measuring techniques use a charge coupled device (CCD) to measure vacuum fluctuations, a review of their structure, and that semiconductors are light sensitive, indicate a similar p-n junction as the RNG device. The baseline means per second for one of these devices that operated continually for one month was 99.9945. The standard deviation was 0.1228 and the minimum and maximum was 99.6606 to 100.3397.

3. Methods

A total of 9 trials were complete over a 25 day period. The experimental procedure involved two Random Event Generators (REG's) and two custom-constructed "Octopus" devices (Dotta and Persinger, 2012) each composed of circular arrays of 8 pairs of solenoids and located in two remote locations within the Consciousness lab at Laurentian University. The first location, designated as "local" was an industrial acoustic chamber. The second location was another room approximately 10 m away. The designation for this experiment was arbitrary because there was no stimulation or experimental manipulation in one locus to discern the inverse response in the other locus. We assumed the opposing polarity would occur "spontaneously" due to the nature of entanglement. The object of the experiment was to discern the fluctuation in putatively "random" processes from the level of quantum operations across p-n junction tunnelling and to measure the change when the consequences of entanglement had occurred. The REG devices were placed in the center of the array solenoids as shown in Figure 1.

The Experimental REG 'Entanglement' procedure was identical to the procedure employed by Dotta and Persinger (2012) to produce the "doubling" of photon emissions from chemiluminescent reactions when both reactions were exposed to the same circularly, rotating magnetic fields. In their study the entanglement occurred during the second (effector) pattern after the presentation of a specific (primer) pattern had been presented. The field strength within the center of the ring of solenoids, where the Psyleron sensors were placed, was ~1 uT.

The sequence of presentations employed in the present study which was identical to the Dotta and Persinger (2012) sequence included nine 2 minute conditions spaced by 1 minute intervals which commenced in the following order: Baseline 1 (BL1), Baseline 2 (BL2), Thomas 1 (T1), Thomas 2 (T2), Burst-X 1 (B1), Burst-X 2 (B2), Burst-X 3 (B3), Baseline 3 (BL3), Baseline 4 (BL4). These terms refer to the names attributed to the pattern of the field generated by the computer that was delivered sequentially to each solenoid.

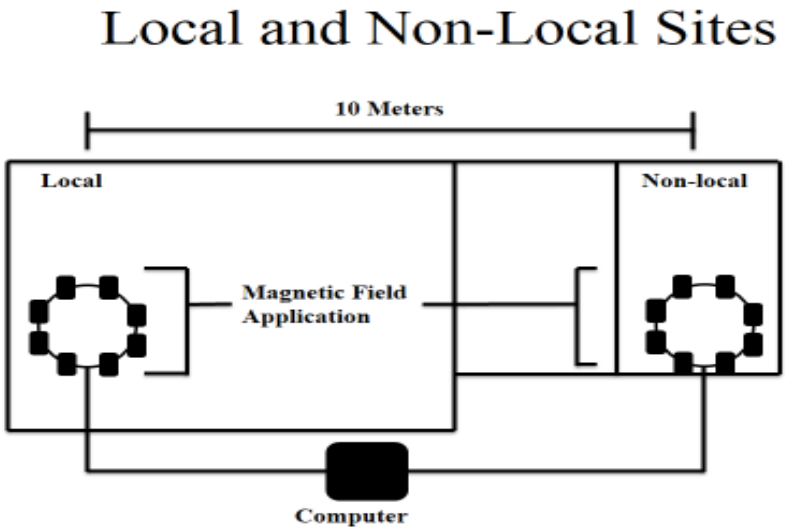

Figure 1. Diagram of the experimental arrangement. The two circular arrays of pairs of solenoids are indicated by the rings. The rate of rotation (counterclockwise from the top) and the accelerating or decelerating phase patterns were generated by the programmable software from the computer. Each REG was placed within the center of one of the coils. The location of each REG was counterbalanced over the 9 trials.

The Thomas pattern was a decelerating frequency or "phase" modulated pattern composed of 839 points. The shape has been published elsewhere Dotta and Persinger (2012). The Burst-X pattern was an accelerating frequency or phase modulated pattern composed of 230 points. The designation number (suffix) refers to the partitioning of the time for analyses in order to discern consistency of any effect as well as their potential transience.

All point durations that composed the patterns were 1 ms. This duration was based upon the calculation by Persinger and Koren (2007) for the hypothetical time, derived from Hubble's Parameter, for an electron to expand one Planck's Length. This meant that the value between 0 and 256 from the column of numbers from which the patterns were generated were converted into a value between -5 V and +5 V (127 = 0 V) for 1 ms (plus the port time) from the IBM 286 computer. The Thomas pattern was generated through the pairs of solenoids in each of the 8 positions as they were activated with an accelerating angular velocity. The duration of the field in the first solenoid was 20 ms and was decreased by 2 ms for each successive solenoid in the ring until the final duration in the 8^{th} solenoid was 6 ms. We described this the primer field where the uncoupled group and phase velocity resulted in an increasing group velocity (the rotating speed) and a decreasing phase velocity.

The Burst-x pattern produced a temporally opposing effect. It was generated within each solenoid, starting with 20 ms, but increased in duration by 2 ms until by the 8th solenoid the duration was 34 ms. We described this field as the effector field, where the display of "excess correlation" is clearly evident. During this condition the "group velocity" was decreasing while the phase velocity was increasing. We reasoned that if a discrete shift in space and the energy within it mediated the effects of "excess correlation" in this paradigm, any deviation from random variation in the REG outputs should occur during this phase. The REG's were synchronized through stop watches which ran continuously throughout the experiment after being synchronized. All field conditions had 1,1 delay between points and point duration presentations. Several variables were collected from each REG in each condition including; Overall Z-score, Mean, Standard Deviation, Max/Min Z-score value and min/max z-scores.

4. Results

The results were clear and conspicuous. As shown in Figure 2, the means and standard deviations for the two random numbers clustered around the average of 100. There was no statistically significant differences between the local and non-local sites except for the period during the *middle* of the burst-x (2) field which is the effector field where excess correlations have been observed for luminescent and pH reactions in previous experiments. This would be about 4 min after the "entanglement" field began. As predicted by "entanglement" principles, the shift in the random number generation was significantly in the opposite direction (no overlap of standard deviations) during this interval. The effect was maintained for about 4 min and was not evident in the third burst-x segment.

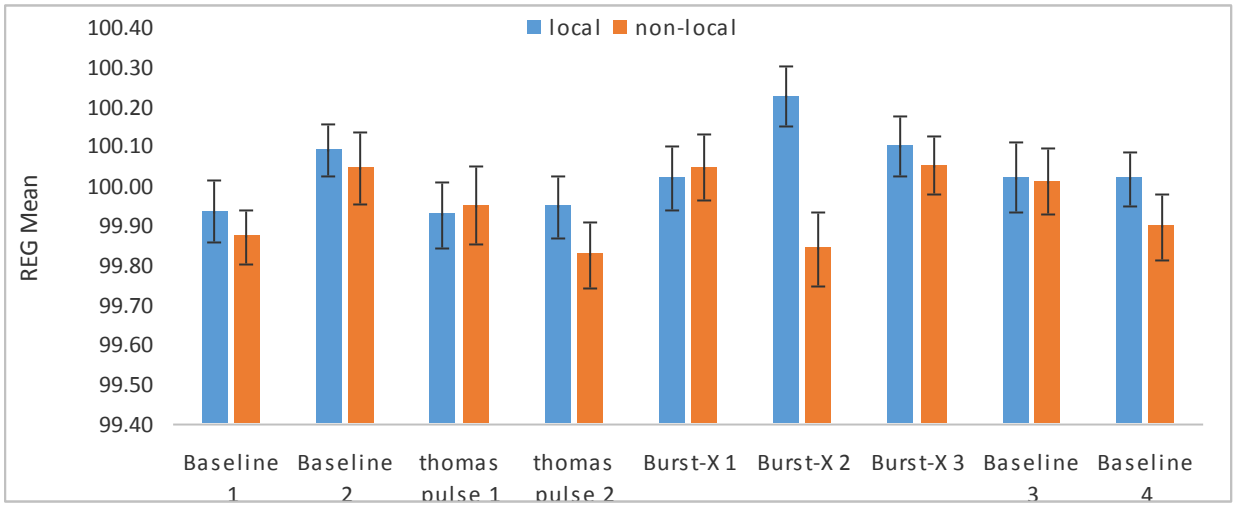

Figure 2. Means and standard deviations for the average numbers of 0s and 1s generated by the two REG in the local (chamber) and non-local room (10 m away) over the various baseline and magnetic field configuration presentations. The local designation was an arbitrary reference. The Thomas pulse is now called the primer pulse while the burst-x pattern is called the effector pulse within which entanglement is usually manifested. The effect was transient but powerful in the center of the entanglement interval (Burst-X2). Vertical bars are standard errors of the mean (SEM).

5. Discussion

The consequence of entanglement (Aczel, 2002) is that two particles are "connected" such that when one of the pairs changes an indicator of polarity, the other member of the pair responds in the opposite direction. This could be considered a higher order manifestation of Newton's Third Law where ever force (action) displays an equal and opposite force (reaction). Such entanglement, which has been considered central for quantum communication (Vaziri, et al, 2002) is assumed to be restricted to photons. In the present study photonic-energies cannot be excluded because electron tunnelling and the p-n junctions associated with this process involves energies that could facilitate photon involvement. Caswell et al (2014) had shown experimentally that cerebral biophotons could be the potential mediator for non-local human-machine interactions. It may be relevant that the product of the rest mass of a photon (~$2 \cdot 10^{-52}$ kg) the entanglement velocity ($2.8 \cdot 10^{23}$ m·s^{-1}) and the velocity of light ($3 \cdot 10^{8}$ m·s^{-1}) is $1.7 \cdot 10^{-20}$ J which is well within the energy associated with each action potential.

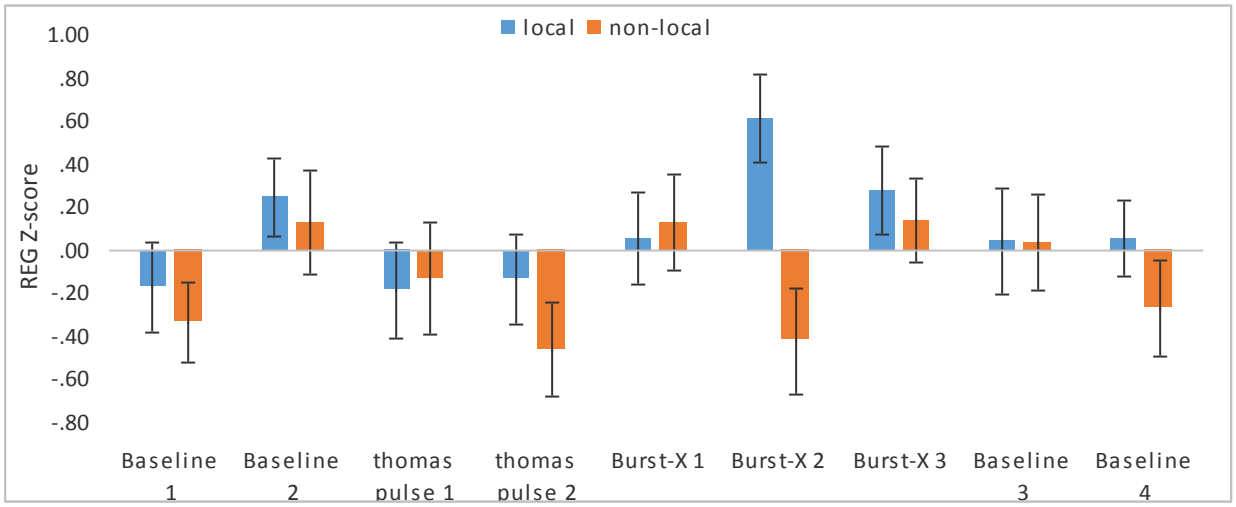

Figure 3. Means and standard deviations for the z-scores of the average numbers of 0s and 1s generated by the two REG in the local (chamber) and non-local (room 10 m away) over the various baseline and magnetic field configuration presentations. The local was an arbitrary reference. The Thomas pulse is now called the primer pulse while the burst-x pattern is called the effector pulse within which entanglement is usually manifested. Note the difference is equivalent to 1 standard deviation. Vertical bars are SEMs.

In the present study there were no human interactions directly within the entanglement processes although we obviously observed the REG and were within their proximity before and after the experiments in order to organize the equipment. Within the portion of the circularly generated fields that have been associated with excess correlations in pH and bioluminescent experiments the parity of the shift from centrality of these "random variations" was clearly apparent. Consequently the probability is very low that the effect was simply an induction artefact from the applied 1 μT magnetic fields. If these spurious inductions had occurred the deviations from random average would have been evident during the primacy field presentations and as well as during the entire interval of the effector fields. This effect did not occur.

Instead the manifestation of what we have interpreted as the consequence of the entanglement was the "excess correlation" that occurred during the second 4 min increment of the effector field presentation. During that interval there were marked and statistically significant deviations from random fluctuations of 0,1 events through the electron tunnelling through the p-n junctions in both loci. However the deviation was in the *opposite* directions as would be predicted from the consequences of an entanglement-like process. The standardized diametric displacement during this period was equivalent to about 1 standard deviation (Figure 3). This deviation is between 5 to 8 times more than the typical variation displayed by these instruments when operating continually without experimental manipulation for a month.

If two electrons as waves within the two circular arrays that generated this specific pattern of magnetic field sequences were entangled then their mass equivalents ($9.1 \cdot 10^{-31}$ kg) applied across the width of the p-n junction (0.1 μm, 10^{-7}) and multiplied by the velocity light ($3 \cdot 10^{8}$ m·s^{-1}) and the frequency of the universal hydrogen line ($1.42 \cdot 10^{9}$ s^{-1}) results in ~$3.8 \cdot 10^{-20}$ J. If the functional length of the p-n junction was 20 nm, more typical of the width between neuronal plasma cell membranes, the value would be $7.6 \cdot 10^{-21}$ J. The median value would be within the 10^{-20} J range which has been shown to emerge from fundamental universal forces (Persinger, 2015). If the functional width was ~1 μm the wavelength would be within the visible range.

The energy source for this excess correlation should be related to that available from the circularly generated magnetic fields. The central field strength was about 1.5 μT. Consequently the square of this value divided by $2.5 \cdot 10^{-6}$ N·A^{-1} (twice the value of the magnetic permeability in vacuum) multiplied by the volume (assuming a width of 10^{-12} m^2 and a functional separation of 10^{-8} m) of 10^{-20} m^3 would be 10^{-26} J. However at least 4 min ($2.4 \cdot 10^{2}$ s) was required for the effect to be displayed. The cumulative energy would have been $2.4 \cdot 10^{-24}$ J. The equivalent frequency, obtained by dividing by Planck's constant of ($6.626 \cdot 10^{-34}$ J·s) is about $3.6 \cdot 10^{9}$ Hz. Considering the range of the actual volume in the p-n junction associated with the tunnelling this value is well within the range of the energy sufficient to be equivalent to the neutral hydrogen line that was required to converge with the 10^{-20} J universal unit.

References

Aczel, A. D. (2002). Entanglement: the greatest mystery in physics. Raincoast Books: Vancouver.

Ahn, J., Weinacht, T.C., Bucksbaum, P.H., (2000). Information storage and retrieval through quantum phase. Science 287:462-466.

Burke, R.C., Gauthier, M.Y., Rouleau, N., Persinger, M.A., (2013). Experimental demonstration of potential entanglement of brain activity over 300 km for pairs of subjects sharing the same circular rotating, angular accelerating magnetic fields: verification by s_LORETA, QEEG measurements. Journal of Consciousness & Exploration Research, 4,:35-44.

Caswell, J. M., Dotta, B. T. and Persinger, M. A. (2014). Cerebral biophoton emission as a potential factor in non-local human-machine interaction. NeuroQuantology, 12: 1-11.

Dotta, B.T., Mulligan, B.P., Hunter, M.D., Persinger, M.A., (2009). Evidence of macroscopic quantum entanglement during double quantitative electroencephalographic measurements of friends vs strangers. NeuroQuantology, 7: 548-551.

Dotta, B.T., Murugan, N.J., Karbowski, L.M., Persinger, M.A., (2013). Excessive correlated shifts in pH within distal solutions sharing phase-uncoupled angular accelerating magnetic fields: Macro-entanglement and information transfer. International Journal of Physical Sciences, 8: 1783-1787.

Dotta, B. T. and Persinger, M. A. (2012). "Doubling" of local photon emissions when two simultaneously, spatially separated, chemiluminescent reactions share the same magnetic field configurations. Journal of Biophysical Chemistry, 3, 72-80.

Eskai, L. (1958). New phenomenon in narrow Germanium P-N junction. Physics Review, 10: 603.

Fickler, R., Lapkiewicz, R., Plick, W.N., Krenn, M., Schaeff, C., Ramelow, S., Zeilinger, A., (2012). Quantum entanglement of high angular momenta. Science. 338:640-644.

Hartman, T. (1962). Tunnelling of a wave packet. Journal of Applied Physics. 33, 3427-33.

Hoffman, J., Krug, M., Ortegel, N., Gerard, L., Weber, M., Rosenfield, W., Weinfurter, H., (2012). Heralded entanglement between widely separated atoms. Science. 337:72-75.

Julsgaard, B., Kozhekin, A., Polzik, E.S., (2001). Experimental long-lived entanglement of two macroscopic objects. Nature. 413: 400-403.

Persinger, M. A. and Koren, S. A. (2013). Dimensional analyse of geometric products and boundary conditions of the universe: implications for a quantitative value for the latency to display entanglement. The Open Astronomy Journal, 6:10-13.

Persinger, M. A. (2015). Thixotropic phenomena in water: quantitative indicators of Casimir-magnetic transformations from vacuum oscillations (virtual particles). Entropy, 17, 6200-6212.

Persinger, M. A. and Koren, S. A. (2007). A theory of neurophysics and quantum neuroscience: implications for brain function and the limits of consciousness. International Journal of Neuroscience, 117, 157-175.

Symul, T., Assad, S. M., & Lam, P. K. (2011). Real time demonstration of high bitrate quantum random number generation with coherent laser light. Applied Physics Letters, 98: 231103-231103.

Tu, L.-C., Luo, J. and Gilles, G. T. (2005). The mass of the photon. Reports on Progress in Physics, 68, 77-130.

Vares, D. E., & Persinger, M. (2013). Predicting Quantum Random Events from Background Photon Density Two Days Previously: Implications for Virtual-to-Matter Determinism and Changing the Future. *Journal of Nonlocality*, *2*(2).

Vaziri, A., Weihs, G. and Zeilinger, A. (2002). Experimental two-photon, three-dimensional entanglement for quantum communication. Physical Review Letter, 89, 240401.

Article

Quantitative Support for Water as the Conduit of Interaction for Universal Entanglement

Trevor N. Carniello[1,3], David A. E. Vares[1,2] & Michael A. Persinger[1,2,3*]

Neuroscience Research Group, Human Studies and Biomolecular Sciences Programs,
Laurentian University, Sudbury, Ontario, Canada P3E 2C6

ABSTRACT

Quantification, supplementing experimental results, suggests a convergence associating the physical properties of water as mediating the relationship between the entire observable set (Universe) and the underlying constituents which construct the entire set (Planck scale). Furthermore, these convergences may necessitate the appropriate parameters required for the initial synthesis of biogenic material facilitating the ultimate genesis of biology. The marked overlap between the energetic equivalents, magnetic field interactions and resulting electric field dynamics associated with the ultrastructural organization of water allows for the possible interaction of an entanglement-type process which is inherently linked to the microscopic (Planck scale) and macroscopic (Universal set) organization of the entire observable set.

Keywords: Entanglement, Universe, water, conduit, biology, Planck scale.

1. Introduction

Water has been described as "the solvent of Life". Water reflects the basic properties of universal particles. For example the ratio of the magnetic moment of a proton ($1.41 \cdot 10^{-26}$ A·m^2) and the unit charge ($1.6 \cdot 10^{-19}$ A·s) is a diffusivity value $0.88 \cdot 10^{-7}$ m^2·s^{-1}. When multiplied by the viscosity of water ($8.94 \cdot 10^{-4}$ kg·m^{-1} ·s^{-1}) at living temperatures there is a force of $7.87 \cdot 10^{-11}$ kg·m·s^{-2}. When this force is applied across the distance of two O-H bonds ($1.92 \cdot 10^{-10}$ m) the energy is $1.5 \cdot 10^{-20}$ J (Karbowski and Persinger, 2015; Persinger, 2015a). This is not only the energy associated with the movements of protons but is also the solution for the average force from the entire universe at Planck's Length when distributed across the most common distance (wavelength) in the universe: the hydrogen line.

For example with a mass of ~10^{52} kg, a distance (width) of ~10^{26} m and the squared frequency of the vacuum oscillations (10^{86} s^{-2}), the functional force of the universe is 10^{164} N (Persinger, 2015a). If the universe exhibits a net volume of 10^{78} m^3 and the smallest volume is a Planck's voxel (10^{-105} m^3), there are 10^{183} Planck's voxels within the universal volume. This means there is 10^{-19} N per Planck's voxel and when distributed over the 10 cm hydrogen wavelength, the energy is 10^{-20} J. Thus the intrinsic energy within the universe at vacuum

*Corresponding author: Dr. M. A. Persinger, mpersinger@laurentian.ca

fluctuation level is congruent with the energy that is produced by the physical nature of the elements that compose the water molecule.

2. Basic Properties of Water

If altering the structure of a given medium can change its electrodynamic properties so too should altering the nature of water. Zheng and colleagues (2006) examined the exclusion zone (a given structural arrangement) of water corresponding to the alignment of molecules along a boundary. Results suggest that the extent of the exclusion zone extended beyond 200 um to 1 mm depending on the material which served as an interface. Most notably, non-zero potentials could be detected between 120 and (-) 160 mV and which were altered by the addition of various chloride salts. The addition of any salt to a solvent changes the solvation state (degree of interaction of water molecules in order to reduce the net charge distribution in the medium) of the molecules resulting in the ultimate change in structure.

Further alterations in the physical properties of water reflecting changes in its electrical characteristics were presented by Teschke et al (2001). Here, measures of the relative permittivity of bulk and interfacial water were conducted and suggest that the permittivity of bulk water decreased from 79 to 3.8 at the level of the interface (within 10 nm of the surface) between water and a mica surface. Relative permittivity is a measure of the potential for a medium to generate electric field flux. The greater the relative measure of permittivity, the greater the resistance for the formation of an electric field. Conversely, a low relative permittivity increases the net potential to generate an electrical field of flux within a medium.

Although not directly related to the electrical properties of water, changes in viscosity at an interface can infer structural arrangements and electrodynamic changes. Goertz et al (2007) measured the viscosity of nanometer thick water films corresponding to interfacial water with effective alterations in viscosity approaching 10^6 times greater than bulk water. Alterations of the interacting media to a non-polar surface resulted in the absence of the enhancement of viscosity. Viscosity ($kg \cdot m^{-1} \cdot s^{-1}$) is related to electric field strength ($kg \cdot m \cdot A^{-1} \cdot s^{-3}$) by way of magnetic diffusivity ($m^2 \cdot s^{-1}$) and the inverse of charge $(As)^{-1}$. If both the number of charges and the magnetic diffusivity remain constant, any change in the magnitude of viscosity would result in a proportional change in the electrical field strength of water.

The interface between water and the membrane (a polar molecule) undergoes rotation, flipping and precession. Such dynamics, particularly when quantized angular orbital momentum is involved (Fickler et al, 2012), sets the conditions for entanglement or excess correlations of particles (or photons) differing by markedly high quantum numbers separated by significant distances. The resultant effect on the generated electric field would also respond to the dynamic nature of the membrane and in turn become itself dynamic or time-varying.

The physical characteristics of the hydronium dynamics were investigated by Lobaugh and Voth (1996) who measured the activation energy of the proton transfer to H_3O^+ was approximately 0.51 kcal/mol or 0.9 k_bT which varied according to the geometric assemblage of the solvent. A charge in the concentration of available H_3O^+ invariably changes the dynamics of

the system and should be reflected in the structural organization of the solvent. The latter structural re-organization in the presence of excess protons was investigated by Lobaugh and Voth (1996) which revealed a smaller O-O separation which approximates 0.25 nm and allows for the flipping of a proton between the pairs in a Grötthus mechanism. These inter-molecular O-O distances corroborate the findings of Tuckerman et al (1995) who also demonstrated that the temporal duration of the hydration shell associated with the hydronium ion complex remains intact (structured) for a duration of 2-3 picoseconds.

In order to maintain an equilibrium state, hydronium ions undergo a neutralization reaction with its diametric opposition, the hydroxide ion. Its time constants should also reflect the same temporal duration as the generation of the hydronium ion itself. Mathematical verification was completed by Hassanali et al (2011) on the recombination of H_3O^+ and OH^- suggesting that the neutralization reaction involved a collective compression of oxygen along the water wire corresponding to a time of 0.5 picoseconds and involved the simultaneous movement of 3 protons. The proposed movement along the water wire, although occurring over a relatively short duration, should express a relatively short distance of action. Hassanali et al (2011) found that within a distance of 0.6 nm the hydrogen wires coordinating the movement of protons enhance the diffusion constant whilst outside this limit, diffusion constants are best modeled according to bulk water parameters.

If water demonstrates properties of changing electric fields then it should also be affected by magnetic fields and thus can be modeled by Maxwell's relationships. Yamashita et al (2003) examined that the application of 60 Hz AC magnetic fields (~100 mG) and DC magnetic fields (~1000 G). They demonstrated slow to large fluctuations in pH deviations and deviations on oxidation reduction potentials of 60 mV. Gang et al (2012) exposed samples of spring water to 0.16 T static magnetic fields. Measures suggestive of increases viscosity maximized after 5.9 hours, 7.4 hours and 8.6 hours corresponding to volumes of 25, 50 and 100 cc samples respectively. Water exposed to high intensity (14 T) magnetic fields intensities demonstrated a measurable change in peak wavelengths by 1 - 3 nm (Iwaska and Ueno, 1998).

Application of 1 uT intensity, physiologically patterned electromagnetic fields which were applied to water in the dark for 18 days displayed a reliable 10 nm shift in peak fluorescence of water (Murugan et al, 2015). Still weaker fields (Rouleau et al, 2014) within the 30 nT range rotating around toroids within which spring water was placed exhibited non-local effects. When two quantities of spring water each contained within toroids that shared specific patterned magnetic fields were exposed to this procedure for a critical duration, the induction of a proton shift (increased acidity) in one volume was associated with a decreased acidity in the other untouched volume of water. These volumes were separated by 1 m. However these changes have been noted over several km.

If water, or at least the microstructural organization of water serves as a conduit between the manifestation of complex biological organizations and the necessary energetic equivalents driving the processes responsible for the changes within organisms (manifested as behaviour) then the properties of water should demonstrate a convergence upon the physical parameters of the entire set of observable variables (the Universe) and the fundamental units which comprise the entire set (Planck scale). The synthesis of dynamism and materialism should be inherently

linked to a fundamental organization of the Universe which reflects fundamental physical properties of the whole.

3. Casimir and Electromagnetic Interactions

When two parallel, non-conducting plates are brought into proximity of each other, such that the separation between the plates is magnitudinally less than the surface area of the plates, a negative force is generated between the plates (Plunien et al, 1986). The resultant force that is generated has been coined the Casimir force and reflects the possibility of transforming virtual particles into real particles in the presence of a magnetic field. The force generated through a Casimir-type effect is modeled by the equation:

$$F_c = \frac{-\hbar c \pi^2}{720 a^3} A \quad (1)$$

where ħ is reduced Planck's constant ($1.05 \cdot 10^{-34}$ kg·m^2·s^{-1}), a is the separation between the plates (meters) and A is the surface of the plates (m^2).

If we set the resultant Casimir force in the order of bond strengths (10^{-12} kg·m·s^{-2}) and if the distance between the parallel plates is set to the distance between adjacent oxygen atoms in a solution containing excess protons (2.5 Ā or $2.5 \cdot 10^{-10}$m) the surface area required to generate forces in the order of bonds would be $3.62 \cdot 10^{-14}$m^2. The resultant surface area is in the order of the annulus surrounding a 1 um axon. Taking the square root of the calculated surface area results in a linear equivalent distance of 190 nm, which is well within the distances occupied by the exclusion zone of water. If one treats the resultant linear equivalent of 190 nm as a wavelength of light, energy can be calculated using equation:

$$E = h\frac{c}{\lambda} \quad (2)$$

where E is the energy in Joules (kg·m^2·s^{-2}), h is Planck's constant ($6.626 \cdot 10^{-34}$ kg·m^2·s^{-1}), c is the speed of light ($3.0 \cdot 10^8$ m·s^{-1}) and λ is the wavelength of light in meters.

The resultant energy would be in the order of $1.05 \cdot 10^{-18}$ kg·m^2·s^{-2}. The temporal equivalent of this wavelength can be approached using equation:

$$t = \frac{d}{v} \quad (3)$$

where t is the time (seconds), d is the distance (meters) and v is the velocity (m·s^{-1}). Assuming that the distance displaced is a wavelength of light in the order of 190 nm, the relative speed of travel would be the speed of light ($3.0 \cdot 10^8$m·s^{-1}) resulting in a temporal component in the order of $6.33 \cdot 10^{-16}$ seconds. The calculated temporal duration of $6.33 \cdot 10^{-16}$ seconds is within the limits of error for the duration of rotation of a Bohr electron and is complimented by the duration of time it takes light, at c, to traverse the thickness of a cell membrane.

Finally, given that the spatial extent of a molecule of oxygen is approximately $3.0 \cdot 10^{-10}$ m, $6.3 \cdot 10^{2}$ molecules would be required to accommodate a distance of 190 nm. This latter organization is reflective of 10-20 clusters of water (40-50 molecule aggregates at varying temperatures) (Pan et al, 2004). If water is the necessary conduit for the underlying processes that pre-determine the ultimate geometric organization of the organism then values reflective of the inherent electric field generated by a single molecule should converge upon Universal constraints. This property could be considered a condition for excess correlation or entanglement. The energy of a water molecule, contingent upon the generation of the hydronium complex, is ~ $2.0 \cdot 10^{-20}$ Joules (Persinger, 2010, Persinger, 2014). The electric field strength can be dimensionally approached as the quotient of energy and the electrical dipole moment of water as expressed by:

$$E = \frac{\mathrm{J}}{p} \tag{4}$$

where E is the electric field ($kg \cdot m \cdot A^{-1} \cdot s^{-3}$), J is the energy in Joules ($kg \cdot m^{2} \cdot s^{-2}$) and p is the electric dipole moment (Asm).

The electric dipole moment of water is 1.85 Debye ($6.17 \cdot 10^{-30}$ Asm) and the energy associated with a water molecule is $2.0 \cdot 10^{-20}$ J. This produces an electric field strength in the order of $3.2 \cdot 10^{9}$ $kg \cdot m \cdot A^{-1} \cdot s^{-3}$. To relate the intensity of the electric field to the intensity of a magnetic field (B) measured in Tesla ($kg \cdot A^{-1} s^{-2}$) a division by a speed is required. To isolate a speed necessary to equate the inherent electric fields strength of water to the intergalactic magnetic field we can use the relationship:

$$v = \frac{E}{B} \tag{5}$$

where E is the electric field strength, B is the intensity of the magnetic field and v is velocity ($m \cdot s^{-1}$). Thus for the lower limit of the intensity of the intergalactic magnetic field (10^{-15}T), and the electric field strength of $3.2 \cdot 10^{9}$ $kg \cdot m \cdot A^{-1} \cdot s^{-3}$, the speed in the order of ~10^{24} to 10^{23} $m \cdot s^{-1}$. This is similar to the theoretical limit of the entanglement velocity (Persinger and Koren, 2013).

The magnetic field strength squared can be dimensionally approached by the relationship:

$$B^{2} = \frac{\sigma}{\varepsilon} \tag{6}$$

where B is the intensity of the magnetic field, σ is the density of the material ($kg \cdot m^{-3}$) and ε is the relative permittivity of the material ($A^{2} s^{4} \cdot kg^{-1} m^{-3}$). For water the density of the material is 10^{3} $kg \cdot m^{-3}$ and the relative permittivity along the interfacial surface is $3.363 \cdot 10^{-11}$ $A^{2} s^{4} \cdot kg^{-1} m^{-3}$. The squared magnetic field strength would be in the order of $2.97 \cdot 10^{13}$ T^{2}. However, the energy stored within the magnetic field can be described by the relationship:

$$E = \frac{\mathrm{B}^{2}}{2 * \mu} v \tag{7}$$

where E is the energy of the magnetic field, B is the intensity of the magnetic field, μ is the permeability of free space ($1.26 \cdot 10^{-6}$ $kg \cdot m \cdot A^{-2} s^{-2}$) and v is the volume ($m^{3}$). Assuming that the

resultant magnetic field strength squared of $2.97 \cdot 10^{13}$ T^2, had an energy equivalent of $2.0 \cdot 10^{-20}$ J, the resultant volume that is required to equate the two would be in the order of $1.69 \cdot 10^{-39}$ m^3. Usually volumes are not considered to describe the relationship between electron wavelength and classic radius. However assuming a general cylindrical quantum tube of the type considered by Planck's earlier visions, the product of the square of the Compton wavelength of an electron and the classic particle radius would be within this volumetric range.

4. Gravitational Considerations

Similarly, the gravitational potential energy can be calculated using the equation:

$$E_g = G\frac{m^2}{r} \tag{8}$$

where E_g is the gravitational potential energy in Joules, G is the gravitational constant ($6.67 \cdot 10^{-11}$ $m^3 \cdot kg^{-1}s^{-2}$), m is mass (kg) and r is the separation between the masses. Setting Equation (7) equal to (8) and isolating for a given separation between water molecules in order to accommodate the equivalence the relationship is Equation (9):

$$r = \frac{2\mu * G * m^2}{B^2 * V} \tag{9}$$

Thus the separation between water molecules in the exclusion zone provided that each has a mass of $3.0 \cdot 10^{-26}$ kg and there are approximately $6.3 \cdot 10^2$ molecules that occupy the exclusion zone, the distance must be $1.15 \cdot 10^{-36}$ m or within the error of a Planck's length ($1.616 \cdot 10^{-35}$ m). If the possibility that two water molecules approach the limit of separation in the order of Planck's length is considered, the resultant energy associated with two non-conducting surfaces can be approached using a Casimir phenomenon and can be calculated using the equation:

$$E_c = \frac{-\hbar c \pi^2}{720 a^3} A \tag{10}$$

where "a" is the separation between the plates, A is the surface area of the plates, c is the speed of light and ħ is reduced Planck's constant. Continuing with the hypothesis that two water molecules approach the limit of separation of a Planck's length, then the surface of the plates would be in the order of the linear extent of water at a surface which is in the order of 10^{-12} m^2 and the separation between the molecules would be $1.15 \cdot 10^{-36}$ m. The calculated resultant Casimir energy would be in the order of 10^{69} J, reflecting the total energy stored within the Universe (Persinger, 2013; 2014; 2015).

Further support for the convergence of water as a mediator for the transition from Universal operational parameters and the potential for the generation of the organism would be contingent upon homogeneity with the photon and the graviton. One can calculate the change in magnetic moment of an object operating in a magnetic field with Equation 11.

$$\Delta m = \frac{e^2 r^2}{4me} B \tag{11}$$

where Δm is the change in magnetic moment ($kg \cdot A^{-1}s^{-2}$), e is the charge of the electron ($1.6 \cdot 10^{-19}$ As), r is the circumference of the water molecule ($1.57 \cdot 10^{-9}$), m_e is the mass of the electron ($9.11 \cdot 10^{-31}$ kg) and B is the applied magnetic field.

Dimensionally analyzing Equation 11 ultimately results in a magnetic moment (Am^2) which can be further digested as the aggregate of Joule divide by Tesla. In this instance in order to accommodate energy we would simply have to modify Equation 11 producing Equation 12:

$$E = \frac{e^2 r^2}{4m_e} B^2 \tag{12}$$

where E is the energy obtained in Joules and all other parameters are consistent with Equation 11.

Inputs all variables except for a value for B result in an approximate value of $1.74 \cdot 10^{-26}$ $A^2s^2m^2 \cdot kg^{-1}$. Setting an external field to a measure of 1 T would demonstrate a change in magnetic moment of water in the order of $1.74 \cdot 10^{-26} Am^2$ or effectively the difference in magnetic moment between the spin magnetic moment of the electron and the orbital magnetic moment of the electron. An applied magnetic field in the order of 10^{-13} T, or the intensity of the intergalactic magnetic field, becomes significant. In this instance the net energy that would result from Equation 12 would be in the order of 10^{-52} Joules. This may be an inherently small amount of energy however if we consider the mass equivalent of this energy at rest (when c is set to 1) then the mass, as derived by the Einstein-Eddington equation (13) would be in the order of 10^{-52} kg or the upper limit of the rest mass of the photon (Tu et al, 2005, Luo et al, 2003):

$$E = mc^2 \tag{13}$$

The application of weak intensity magnetic fields in the order of 3.0 nT (those values that were utilized in the excess correlation experiments) the resultant energy (calculated from Equation 12) would be in the order of 10^{-44} Joules. Again the mass equivalent of this energy, as calculated using the Einstein-Eddington equation (13) would isolate a mass in the order of 10^{-60} to 10^{-61} kg. This range of mass is well within the order of magnitude of the graviton (Gershtein et al, 1997; Novello and Neves, 2002; Goldhaber and Nieto, 1974; Goldhaber and Nieto, 2010). Another parameter that can be extracted from the approach offered here is a temporal component of water operating in a nT strength field. Given that the energy obtained from the change in magnetic moment of water in 3.0 nT field is in the order of 10^{-43} to 10^{-44} J a frequency can be calculated:

$$f = \frac{E}{h} \tag{14}$$

where *f* is the frequency (s^{-1}), E is the energy in Joules ($kg \cdot m^2 \cdot s^{-2}$) and h is Planck's constant ($6.626 \cdot 10^{-34}$ $kgm^2 \cdot s^{-1}$)

For a mean value of $5.0 \cdot 10^{-43}$ Joules for water in a 3.0 nT field, the resultant frequency would be $7.55 \cdot 10^{-10}$ s^{-1}. The inverse of a frequency would be a time, thus the temporal equivalent of $7.55 \cdot 10^{-10}$ s^{-1} would be $1.325 \cdot 10^{9}$ seconds. This duration is within the order of the approximate

lifetime of a human being. However it is also representative of processes whose durations exist over time frames more typically found within much larger spatial increments.

5. The Exclusion Zone

There is a specific physical nature of the exclusion zone of interfacial water compared to bulk water. It is suggested that a net increase in the viscosity of the exclusion zone occurs such that the increase can be as high as ~10^6 times larger than the viscosity of water. The general linear expansion of the exclusion suggests a relative mean occupancy in the order of 100 um. Given that that the molecular diameter of a water molecule is 3.0^{-10} m, the total amount of water molecules that would occupy the linear equivalent of 100 um would be approximately $3.3 \cdot 10^5$ molecules.

The bond strength of water is in the order of 10^{-12} N ($kgm \cdot s^{-2}$) the net force is calculated as the product of the force of a single bond and the total available molecules and would approach 10^{-6} to 10^{-7} N. The upper limit of force is 10^{-6} N. Viscosity is the quotient of the force by a diffusion constant:

$$\eta = \frac{F}{\upsilon} \tag{15}$$

where F is force ($kg \cdot m \cdot s^{-2}$), υ is the diffusion constant ($m^2 \cdot s^{-1}$) and η is viscosity ($kg \cdot m^{-1} s^{-1}$).

If the force is in the order of 10^{-6} N and the diffusion mobility constant of water is taken to be in the order of $3.6 \cdot 10^{-7}$ $m^2 \cdot s^{-1}$, the viscosity would be in the order of 10^1. Comparatively, given the lower limit of force across the exclusion zone to be in the order of 10^{-7} N, and substituting the diffusion constant for that of water ($8.65 \cdot 10^{-9} m^2 \cdot s^{-1}$) the magnitude of the viscosity would approach 10^2 $kg \cdot m^{-1} s^{-1}$. Given that the viscosity of bulk water is $8.94 \cdot 10^{-4}$ $kg \cdot m^{-1} s^{-1}$, these calculated values would be 10^5 to 10^6 times greater and reflects what Goertz et al (2007) found in their experiments.

An energy equivalent of 10^{-7} N requires that this force be applied over a distance. Provided that the force of the linear equivalent of the exclusion extends the length of the exclusion zone (10^{-4} m) the resultant energy would be in the order of 10^{-11} Joules. One can isolate a magnetic field strength associated with the energy of the magnetic field using the equation 16:

$$B = \sqrt{\frac{E * 2\mu}{v}} \tag{16}$$

where B is the intensity of the magnetic field ($kg \cdot A^{-1} s^{-2}$), E is the energy in Joules, u is the permeability of free space and v is the volume. If we assume that the volume of water is consistent with the volumes used in experiments (25 cc) through which excess correlation was demonstrated then the strength of the magnetic field would be in the order of 10^{-6} Tesla. This value is the same order of magnitude that was shown to produce excess correlation in other experimental paradigms involving non-toroid equipment but where the circular changing angular velocities were produced (Dotta et al, 2013).

6. Photon-Graviton Entanglement in Water

The background radiant flux density of photons is in the order of $2 \cdot 10^{-12} W \cdot m^{-2}$ ($kg \cdot s^{-3}$) the convergence upon the level of water should be evident. If we assume that the flux density is related to the magnetic equivalence it can be equated such that:

$$B = \Phi \cdot I \cdot f \quad (17)$$

where B is the magnetic field, I is the current (A) f is frequency, and Φ is radiant flux density ($kg \cdot s^{-3}$). Assuming that the effective intensity of an incident magnetic field is $\sim 10^{-9}$ T, to homogenize the structure of water to hybridize with background parameters of the Universe, then the aggregate of current and frequency would represent a current per unit time ($A \cdot s^{-1}$). The necessary value to equate a magnetic field strength of 1 nT and background radiant flux density of 10^{-12} $kg \cdot s^{-3}$ would be in the order of $2\text{-}3 \cdot 10^{-3}$ $A \cdot s^{-1}$ (Persinger, 2015b).

The Universe is composed of $1.58 \cdot 10^{79}$ particles or Eddington's Number. If each particle had a charge equivalent of $1.6 \cdot 10^{-19}$ As, the resultant net Universal charge would be $2.53 \cdot 10^{60}$ As (Persinger, 2015b). The quotient of the net Universal charge and the current of 2 to $3 \cdot 10^{-3}$ $A \cdot s^{-1}$ resulting frequency squared approximately $1.14 \cdot 10^{-63} s^{-2}$. This is $3.37 \cdot 10^{-32}$ s^{-1}. An energy equivalent of this latter frequency can be calculated by multiplying by Planck's constant ($6.626 \cdot 10^{-34}$ $kgm^2 \cdot s^{-1}$) and would be $2.24 \cdot 10^{-65}$ Joules. The rest mass equivalent (when c is set to 1) of an energy of $2.24 \cdot 10^{-65}$ Joules would be $2.24 \cdot 10^{-65}$ kg, or the upper limit of the rest mass of the graviton (Gershtein et al, 1997; Novello and Neves, 2002; Goldhaber and Nieto, 1974; Goldhaber and Nieto, 2010). The product of the mass of $2.24 \cdot 10^{-65}$ kg and the square of the entanglement velocity (10^{23} $m \cdot s^{-1}$) the resultant energy would be in the order of 10^{-18} to 10^{-19} Joules converging on the approximate energy within wavelengths in the low 100 nm range. According to Clary (1999) excitation with 122 nm "causes electrons in the ground "X" electronic state to jump to antibonding orbitals labelled "B". Although this model has been applied to explain the dissociation of water molecules into H^+ and OH^-, the emergence of a B+X state would set the conditions for entanglement.

If Mach's principle of the Eminence of the Universe (Mach, 1887) is valid then the convergence upon 2 to $3 \cdot 10^{-3}$ $A \cdot s^{-1}$ should also converge on the properties of water. Dimensionally, the inherent current per unit time can be calculated by the product of conductivity, electric field strength and a diffusion parameter and is represented in equation 18:

$$\frac{I}{t} = \sigma \cdot E \cdot \upsilon \quad (18)$$

where I/t is current per unit time ($A \cdot s^{-1}$), σ is the conductivity ($A^2 s^3 \cdot kg^{-1} m^{-3}$), E is the electric field ($kg \cdot m \cdot A^{-1} s^{-3}$) and υ is diffusion ($m^2 \cdot s^{-1}$).

Provided that the current is in the order of 2 to $3 \cdot 10^{-3}$ $A \cdot s^{-1}$, the average conductivity of water is $1.75 \cdot 10^{-4}$ $A^2 s^3 \cdot kg^{-1} m^{-3}$. The inherent electric field of a given water molecule is $3.2 \cdot 10^9$ $kg \cdot m \cdot A^{-1} s^{-3}$, the resultant diffusion constant would be $4.46 \cdot 10^{-9} m^2 \cdot s^{-1}$. This is within the error of the diffusion constant of water (Bett and Cappi, 1965). This suggests that the convergence between light, magnetic fields and the graviton is reflected or mediated by the simple diffusion of water over a given temporal span. The persistence of the homogeneity of physical parameters

converging at the level of water consistently reflects the possibility that water may act as a conduit to facilitate the conditions leading to excess correlations and entanglement.

References

Bett, K.E., Cappi, J.B. (1965). Effect of pressure on the viscosity of water. *Nature* 207**:** 620-621.

Clary, D. C. (1999). Interfering with water. *Science*, 285: 1218-1219.

Dotta, B. T., Murugan, N. J., Karbowski, L. M., & Persinger, M. A. (2013). Excessive correlated shifts in pH within distal solutions sharing phase-uncoupled angular accelerating magnetic fields: Macro-entanglement and information transfer. *International Journal of Physical Sciences*, *8*(36), 1783-1787.

Fickler, R., Lapiewicz, R., Plick, W. N., Krenn, M., Schaeff, C., Ramelow, S. and Zeilinger, A. (2012). Science, 338: 640-644.
Gang, N., St-Pierre, L. S., & Persinger, M. A. (2012). Water dynamics following treatment by one hour 0.16 tesla static magnetic fields depend on exposure. *Water*, 3: 122-131.

Gershtein, S. S., Logunov, A. A., & Mestvirishvili, M. A. (1997). The upper limit on the graviton mass. *arXiv preprint hep-th/9711147*.

Goertz, M. P., Houston, J. E., & Zhu, X. Y. (2007). Hydrophilicity and the viscosity of interfacial water. *Langmuir*, 23: 5491-5497.

Goldhaber, A. S., & Nieto, M. M. (1974). Mass of the graviton. *Physical Review D*, *9*: 1119.

Goldhaber, A. S., & Nieto, M. M. (2010). Photon and graviton mass limits. *Reviews of Modern Physics*, *82*: 939.

Hassanali, A., Prakash, M. K., Eshet, H., & Parrinello, M. (2011). On the recombination of hydronium and hydroxide ions in water. *Proceedings of the National Academy of Sciences*, 108: 20410-20415.

Iwasaka, M., & Ueno, S. (1998). Structure of water molecules under 14 T magnetic field. *Journal of Applied Physics*, 83: 6459-6461.

Karbowski, L. M. and Persinger, M. A. (2015). Variable viscosity of water as the controlling factor in energetic quantities that control living systems: physicochemical and astronomical interactions. *International Letters of Chemistry, Physics and Astronomy*, 4: 1-9.

Lobaugh, J., & Voth, G. A. (1996). The quantum dynamics of an excess proton in water. *The Journal of Chemical Physics*, 104: 2056-2069.

Luo, J., Tu, L. C., Hu, Z. K., & Luan, E. J. (2003). New experimental limit on the photon rest mass with a rotating torsion balance. *Physical Review Letters*, 90: 081801.

Mach, E. (1887). Mach's Principle. *Mach's archive, Deutches Museum, Munich*.

Murugan, N. J., Karbowski, L. M., Lafrenie, R. M., & Persinger, M. A. (2015). Maintained exposure to spring water but not double distilled water in darkness and thixotropic conditions to weak (~ 1 μT)

temporally patterned magnetic fields shift photon spectroscopic wavelengths: effects of different shielding materials. *Journal of Biophysical Chemistry*, 6: 14.

Novello, M., & Neves, R. P. (2002). The mass of the graviton and the cosmological constant. *arXiv preprint gr-qc/0210058*.

Pan J, Lorenzen LH, Carrillo F, Wu H, Zhou M, Wang ZY (2004). Clustered water and bio-signal networks. *Cybernetics and Intelligent Systems, 2004 IEEE Conference*, 2: 902-907.

Persinger, M. A. (2010). 10-20 Joules as a neuromolecular quantum in medicinal chemistry: an alternative approach to myriad molecular pathways?. *Current Medicinal Chemistry*, 17: 3094-3098.

Persinger, M. A. (2013). Support for Eddington's Number and his approach to astronomy: recent developments in the physics and chemistry of the human brain. *International Letters of Chemistry, Physics and Astronomy*, 8: 8-19.

Persinger, M. A. (2014). Astronomical, chemical, and biological implications of 10^{-20} Joules as a fundamental quantum unit of information for neurofunction. *Archives of Neuroscience*, 1(3).

Persinger, M. A. (2014). Discrepancies between predicted and observed intergalactic magnetic field strengths from the universe's total energy: is it contained within submatter spatial geometry?. *International Letters of Chemistry, Physics and Astronomy*, 11, 18-23.

Persinger, M. A. (2015a). Thixotropic phenomena in water: quantitative indicators of Casimir-Magnetic transformations from vacuum oscillations (virtual particles*). Entropy*, 17: 6200-6212.

Persinger, M. A. (2015b). The graviton: an emergent solution from the equivalence of universal magnetic field intensity and radiant flux density. Journal of Advances of Physics, 10: 2811-2815.

Persinger, M. A., & Koren, S. A. (2013). Dimensional analyses of geometric products and the boundary conditions of the universe: implications for a quantitative value for the latency to display entanglement. *Open Astronomy Journal*, 6:10-13.

Plunien, G., Müller, B., & Greiner, W. (1986). The Casimir effect. *Physics Reports*, 134: 87-193.

Rouleau, N., Carniello, T. N., & Persinger, M. A. (2014). Non-local pH shifts and shared changing angular velocity magnetic fields: Discrete energies and the importance of point durations. *Journal of Biophysical Chemistry*, *2014*.

Teschke, O., Ceotto, G., & De Souza, E. F. (2001). Interfacial water dielectric-permittivity-profile measurements using atomic force microscopy. *Physical Review E*, 64: 011605.

Tu, L. C., Luo, J., & Gillies, G. T. (2005). The mass of the photon. *Reports on Progress in Physics*, 68: 77.

Tuckerman, M., Laasonen, K., Sprik, M., & Parrinello, M. (1995). Abinitio molecular dynamics simulation of the solvation and transport of hydronium and hydroxyl ions in water. *The Journal of Chemical Physics*, 103: 150-161.

Yamashita, M., Duffield, C., & Tiller, W. A. (2003). Direct current magnetic field and electromagnetic field effects on the pH and oxidation-reduction potential equilibration rates of water. 1. Purified water. *Langmuir*, 19: 6851-6856.

Zheng, J. M., Chin, W. C., Khijniak, E., & Pollack, G. H. (2006). Surfaces and interfacial water: evidence that hydrophilic surfaces have long-range impact. *Advances in Colloid and Interface Science*, 127: 19-27.

News

Transatlantic Excess Brain Correlations Are Experimentally Produced by Persinger's Group

Huping Hu* & Maoxin Wu

ABSTRACT

Michael A. Persinger and his reasearh team at Laurentian University, Canada, have achieved new breakthroughs which are published in this Focus Issue. These new results include the experimental production of execess brain correations across the Atlantic Ocean as measured by QEEG. If independently confirmed, these results represent important progress in the fields of biological quantum entanglement, consciousness research and parapsychology.

Keywords: Transatlantic, excess brain correlations, rotating magnetic field, QEEG, biological quantum entanglement.

Michael A. Persinger

Michael A. Persinger at Laurentian University, Canada, has been a pioneer in the field of experimental studies of mystical experiences and is known together with his research team for the "God Helmet" [1]. Persinger's group has also made important discoveries in the fields of biological quantum entanglement and consciousness studies [2-6]. Now, they have achieved new breakthroughs which are published in this Focus Issue [7-9]. These new results include the experimental production of execess brain correations across the Atlantic Ocean as measured by QEEG [7]. If independently confirmed, these results represent important progress in the fields of biological quantum entanglement, consciousness research and parapsychology.

For examples of contributions made by other researchers in these and/or related fields, please see references 10-31.

Correspondence: Huping Hu, Ph.D., J.D., QuantumDream Inc., P. O. Box 267, Stony Brook,, NY 11790. E-mail: editor@prespacetime.com

Experimental Production of Excess Correlation across the Atlantic Ocean of Right Hemispheric Theta-Gamma Power between Subject Pairs Sharing Circumcerebral Rotating Magnetic Fields

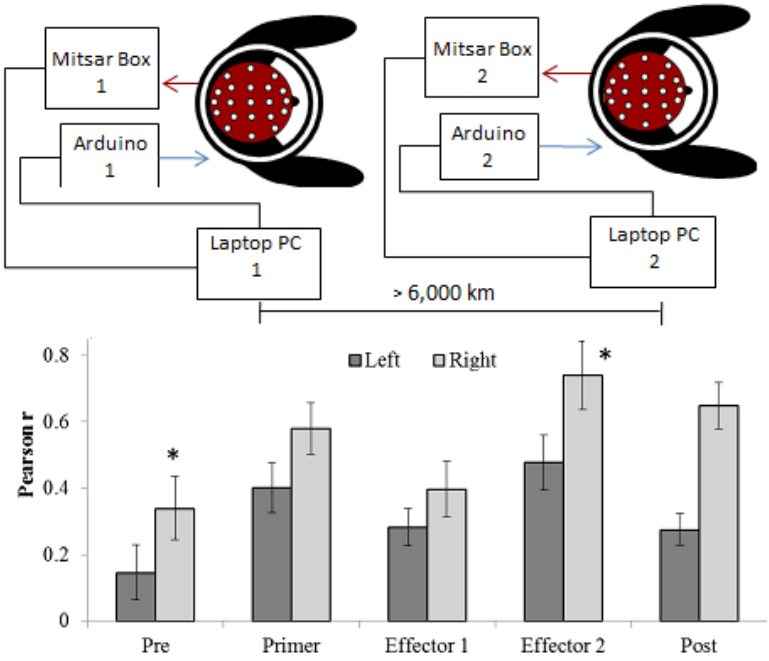

According to Persinger's research team [7], this experiment was completed during the summer of 2015. In the experiment, 5 pairs of volunteers separated by more than 6,000 km wore identical cerebral toroids which produce patterns of phase shifting, 30 nT magnetic fields and were exposed to the sequences that produced excess correlation in chemiluminescent reactions and shifts in pH [7].

They found that, in comparison to the various baselines and control procedures, enhanced power between the right hemispheres of pairs of participants occurred during the interval documented to produce excess correlation [7]. Their specific analyses indicate that only coherence within the theta band of the right temporal lobes of the pairs was diminished. Further, their sequential block analyses reveal that the paired brains' responses to pulsed tones at 6.5 Hz occurred within the 30-40 Hz band over the caudal temporal lobes during the exposures to an effector field. Their primary independent component analyses verified these results [7].

Further, they found that, during the 6.5 Hz pulsed tones, there was a peak in the spectral power density at that frequency over the right temporal lobe of the person listening but a trough in the spectral power density over this region for the person who was not. The research team found that even subjective experiences, as measured by the Profile of Mood States, indicated significantly increased excess correlation for scales by which increased anger and decreased vigour are inferred.

Therefore, This experiment, if independently confirmed, has the potential for creating a technology that can generate reliable excess correlation of brain activity (and potentially consciousness and specific experiences) between two people separated by thousands of kilometers [7].

Enhancement of Spectral Power Densities in Microtubule Preparations Exposed to Temporally Patterned Weak Magnetic Fields

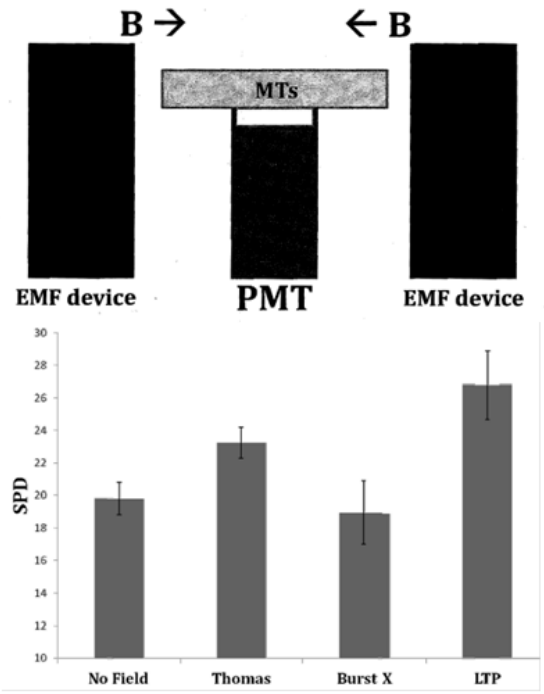

In the second experiment, Persinger and his research team exposed microtubule ("MT") preparations to temporally patterned weak magnetic fields and studied the spectral power densities ("SPD") of the photon emissions from the said MT preparations [8].

According to the authors [8], the dynamics of the MT and its constituent tubulin dimers during periods of adaptation to a disrupted environment are associated with increased photon emissions. Through spectral analyses of the photon emissions from plates of MT preparations within standard media in a Faraday room, they found that the emitted photons exhibited weak but significant and reliable peaks of SPD around 7.7 to 7.8 Hz. They further found that only exposures for 4 min to 3 to 10 μT temporally patterned magnetic fields (that, they state, are associated with the physiological substrates of "learning and memory") enhanced the magnitude of the SPD of photon emissions from MT.

They also noted that, as in their previous experiments, applications of the appropriate, temporally patterned magnetic fields to MTs do not affect the total photon emissions but shift the distributions of the amplitudes power spectra during the brief interval of exposure.

Thus, Persinger and his team suggest that, if intracellular information is contained within shifting temporal patterns of energy but not the absolute shift in energy within dynamic systems, then weak magnetic fields might affect the function of cells through microtubules [8].

Demonstration of Excess Correlation in Random Number Generators at Two Locations Sharing Specific Patterns of Magnetic Fields

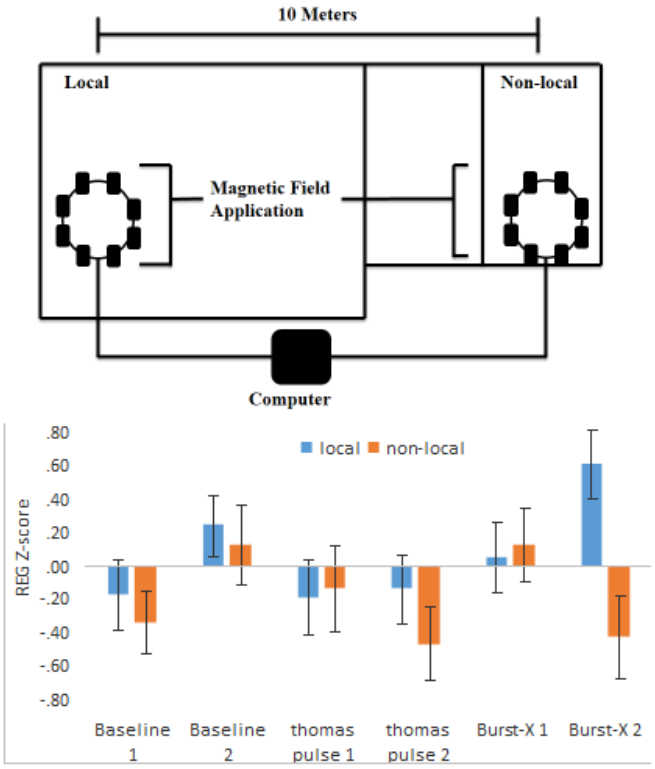

In the third experiment, Persinger and his research team tested whether temporally-coupled diametric shifts in parity could be demonstrated between two Random Event Generators ("REGs") located at two locations and exposed to patterned magnetic field in a circular array of solenoids separated by 10 m [9].

According to the authors [9], each circular array generated a patterned rotating magnetic field that has previously produced transient excess correlation and entanglement in photon reactions and alterations in pH in spring water. During a 30 min interval, the REGs were exposed first to an accelerating group velocity embedded with a diminishing frequency/phase-modulated field (the primer) followed by a decelerating group velocity embedded with an increasing frequency/phase-modulated magnetic field (the effector) [9].

They found that only after exposures for about 4 min to the second (effector) condition that is known to manifest the effects of entanglement did the random numbers deviate significantly and by more than one standard deviation in an opposite direction to each other [9]. Therefore, these results indicate that excess correlation can be generated within "random" quantum electronic processes whose spatial domains are similar to neuronal synapses at the macro-level by appropriate applications of weak, microTesla level, magnetic fields [9].

References

1. Persinger, M. A., Vectorial cerebral hemisphericity as differential sources for the sensed presence, mystical experiences and religious conversions. Psychological Reports, 1993; 76: 915-930.

2. Persinger, M.A., Koren, S.A. & Tsang, E.W. Enhanced power within a specific band of theta activity in one person while another receives circumcerebral pulsed magnetic fields: a mechanism for cognitive influence at a distance? Perceptual and Motor Skills, 2003; 97: 877-894.

3. Persinger, MA, Tsang, EW, Booth, JN and Koren, SA, Enhanced power within a predicted narrow band of theta activity during stimulation of another by circumcerebral weak magnetic fields after weekly spatial proximity: evidence for macroscopic entanglement? NeuroQuantology 2008; 6(1): 7-21.

4. Persinger, M. A., Dotta, B. T., Saroka, K. S., & Scott, M. A., Congruence of energies for cerebral photon emissions, quantitative EEG activities and ~5 nT changes in the proximal geomagnetic field support spin-based hypothesis of consciousness. Journal of Consciousness Exploration & Research, 2013; 4(1): 1-24.

5. Dotta, B. T., Koren, S. A. & Persinger, M. A., Demonstration of entanglement of "pure" photon emissions at two locations that share specific configurations of magnetic fields: implications for translocation of consciousness. Journal of Consciousness Exploration & Research, 2013; 4(1): 25-34.

6. Burke, R. C., Gauthier, M. Y., Rouleaum,N. & Persinger, M. A., Experimental demonstration of potential entanglement of brain activity over 300 Km for pairs of subjects sharing the same circular rotating, angular accelerating Magnetic fields: verification by s_LORETA, QEEG measurements. Journal of Consciousness Exploration & Research, 2013; 4(1): 35-44.

7. Scott, M. A., Rouleau, N., Lehman, B. S., Tessaro, W. E., Juden-Kelly, L. M., Saroka, K. S. & Persinger, M. A., Experimental Production of Excess Correlation across the Atlantic Ocean of Right Hemispheric Theta-Gamma Power between Subject Pairs Sharing Circumcerebral Rotating Magnetic Fields (Part I & II), *Journal of Consciousness Exploration & Research*, 6(9): pp. 658-707.

8. Dotta, B. T., Vares, D. A. E., & Persinger, M. A., Spectral Power Densities of the Fundamental Schumann Resonance Are Enhanced in Microtubule Preparations Exposed to Temporally Patterned Weak Magnetic Fields: Implications for Entanglement, *Journal of Consciousness Exploration & Research*, 6(9): pp. 716-727.

9. Juden-Kelly, L. M., Dotta, B. T., Vares, D. A. E. & Persinger, M. A., Demonstration of Excess Correlation in Non-Local Random Number Generators Sharing Circular, Changing Angular Velocity Magnetic Fields, *Journal of Consciousness Exploration & Research*, 6(9): pp. 728-737.

10. Grinberg-Zylberbaum, J. & Ramos, J., Patterns of interhemispheric correlation during human communication. International Journal of Neuroscience, 1987; 36: 41–53.

11. Davenas E, Beauvais F, Amara J, et al. Human basophil degranulation triggered by very dilute antiserum against IgE, Nature, 1988; 333 (6176): 816–8.

12. Reid, B. L. On the nature of growth and new growth based on experiments designed to reveal a structure and function for laboratory space. Medical Hypotheses, 1989; 29: 105-127.

13. Gariaev, P.P., et. al., Holographic Associative Memory of Biological Systems, Proceedings SPIE, Optical Memory and Neural Networks, 1991; 1621: 280- 291.

14. Josephson, B.D., Pallikari-Viras, F., Biological utilisation of quantum nonlocality, Foundations of Physics, 1991, 21: 197-207.

15. Stapp, H. P., Mind Matter and Quantum Mechanics, 1993, Springer-Verlag, Berlin.

16. Pizzi, R, Fantasia, A, Gelain, F and Rosetti, D, Vdscovi, A. Nonlocal correlations between separated neural networks. Quantum Information and Computation II. Proceedings of SPIE 2004; 5436: 107.

17. Achterberg, J. et. al., Evidence for correlations between distant intentionality and brain function in recipients: A functional magnetic resonance imaging analysis. J. Altertaive & Complimentary Med., 2005; 11 (6): 965–971.

18. Wackermanna,J, Seiterb,C, Keibel,H and Walach, H, Correlations between brain electrical activities of two spatially separated human subjects, Neuroscience Letters 2003; 336(1): 60–64.

19. Wackermann, J., Dyadic correlations between brain functional states: present facts and future perspectives. Mind and Matter, 2004; 2(1): 105–122.

20. Standish, L, Johnson, L, Kozak, L and Richards, T, EEG evidence of correlated event related signals between the brains of spatially and sensorily isolated human subjects. J. Alter. Compl. Med. 2004; 10, 307.

21. Emoto, M., The Hidden Messages in Water, 2005, Atria.

22. Radin, D., Entangled Minds: Extrasensory Experiences in a Quantum Reality, 2006, Paraview Pocket Books.

23. Hu, H. & Wu, M., Thinking outside the box: the essence and implications of quantum entanglement. NeuroQuantology, 2006; 4: 5-16.

24. Hu, H. & Wu, M., Photon induced non-local effect of general anesthetics on the brain. NeuroQuantology, 2006; 4: 17-31. Also see Progress in Physics, 2006; v3: 20-26.

25. Hu, H. & Wu, M., Evidence of non-local physical, chemical and biological effects supports quantum brain. NeuroQuantology, 2006; 4: 291-306. Also see Progress in Physics 2007; v2: 17-24.

26. Desbrandes, R., Gent, D. V., Intercontinental quantum liaisons between entangled electrons in ion traps of thermoluminescent crystals. arXiv:quant-ph/0611109.

37. Tiller, W. A., Psychoenergetic Science, 2007, Pavior.

28. Sheldrake, R., Morphic Resonance: The Nature of Formative Causation, 2009, Park Street Press.

29. Jahn, R. G., Dunne, B. J., Margins of Reality: The Role of Consciousness in the Physical World, 2009, ICRL Press.

30. Montagnier, L et al., DNA waves and water, 2010; arXiv:1012.5166.

31. Hu, H. & Wu, M., New nonlocal biological effect: a preliminary research. NeuroQuantology, 2012; 10(3): 462-467.